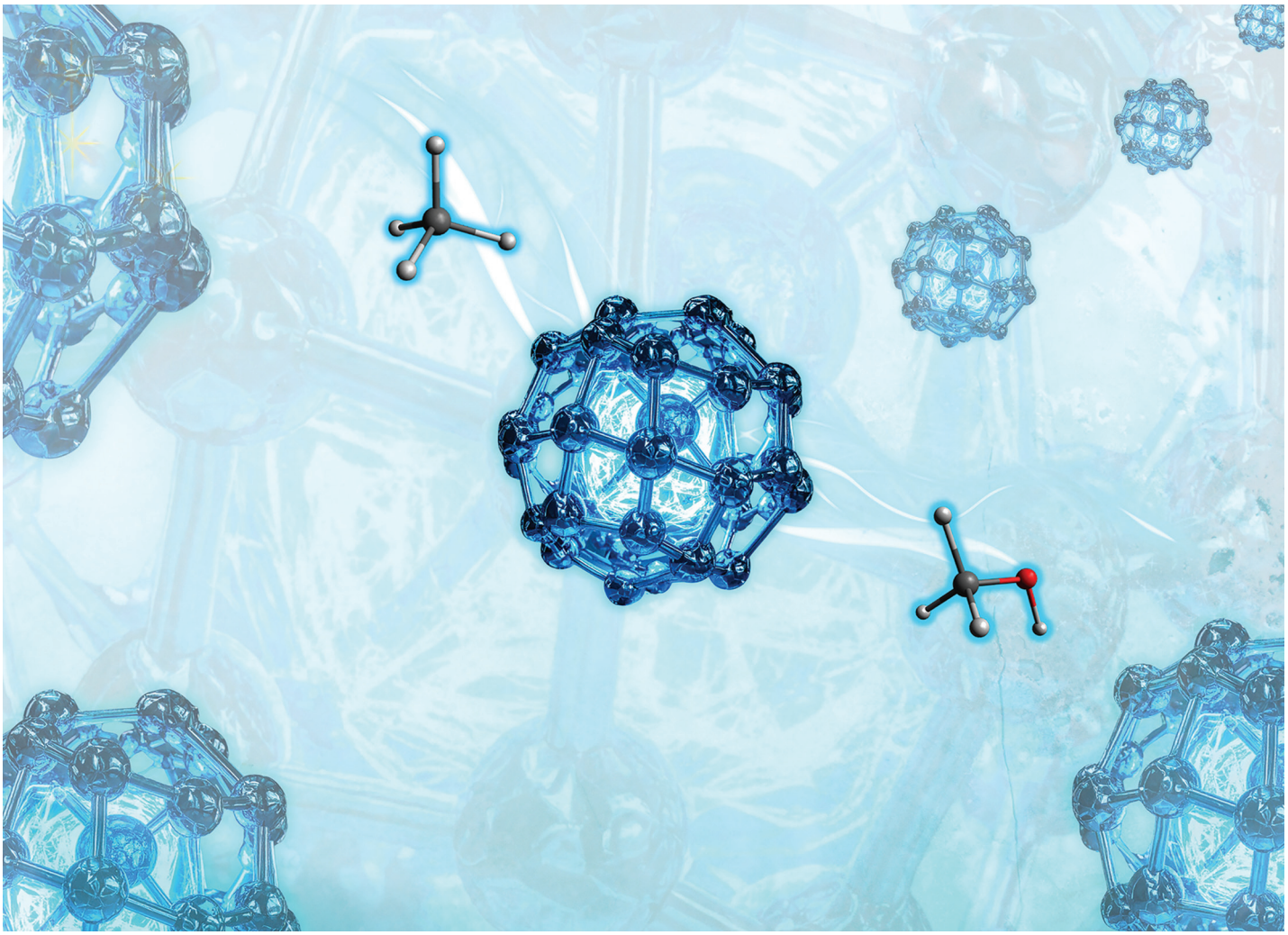

Showcasing research from Dr Samudrala's group, Chemical & Biological Engineering, Monash University, Australia.

Nanozymes for clean energy catalysis: unlocking potential, progress and perspectives

This work highlights the emerging role of nanozymes—engineered nanomaterials that mimic enzymes in enabling next-generation clean-energy reactions. The review explores biomimetic nanozymes that unite biological inspiration with nanoscale engineering to achieve selective and efficient catalytic transformations for sustainable energy applications. By emulating key features of natural enzymes while offering superior stability and tunability, nanozymes open new pathways for methane upgrading, biofuel production, hydrogen and oxygen electrocatalysis, and CO_2 conversion. The work showcases how controlled, robust and bio-inspired mechanisms can advance cleaner and more sustainable catalytic technologies.

Image reproduced by permission of Dr Shanthi Priya Samudrala, Harshita, and Murali Sastry from *Nanoscale*, 2026, **18**, 1121.

Dark blue spherical molecular illustration generated with Adobe Firefly. Additional images created with Avogrado. Cover designed with Canva.com.

As featured in:

See Shanthi Priya Samudrala *et al.*, *Nanoscale*, 2026, **18**, 1121.

ROYAL SOCIETY OF CHEMISTRY

rsc.li/nanoscale

Registered charity number: 207890

Nanoscale

REVIEW

View Article Online
View Journal | View Issue

Cite this: *Nanoscale*, 2026, **18**, 1121

Nanozymes for clean energy catalysis: unlocking potential, progress and perspectives

Harshita,[a] Murali Sastry[a,b] and Shanthi Priya Samudrala *[a]

The growing need for sustainable and efficient energy conversion has driven the development of advanced catalytic materials. In this quest, nanozymes—nanomaterials that mimic the catalytic functions of natural enzymes emerge as promising candidates due to their tunable catalytic properties, high operational stability, and cost-effectiveness. This review presents recent advancements in the applications of nanozymes for clean energy technologies, focusing on their mechanistic roles and engineering strategies within the scope of key reactions, including hydrogen evolution reaction (HER), oxygen evolution and reduction reactions (OER, ORR), CO_2 reduction, biofuel production, and methane-to-methanol conversion. The fundamental classes of nanozymes, their structure–activity relationships, and how their fine-tuned properties aid energy conversion in systems such as biofuel cells, electrolyzers, and fuel cells are also discussed. To underscore their practical advantages, nanozymes are benchmarked against conventional catalysts using key performance metrics such as turnover frequency, cost, and stability. Additionally, the review addresses challenges associated with limited selectivity, incomplete mechanistic understanding, and scalability while also highlighting emerging technologies such as nanostructuring, doping, hybridization, and 3D printing. By mapping recent advances and identifying critical research gaps, this review underscores the potential of established nanozymes and nanozyme-inspired catalytic systems as next-generation catalysts for clean energy applications and their role in advancing the transition toward a carbon-neutral and circular energy economy.

Received 30th September 2025,
Accepted 30th November 2025

DOI: 10.1039/d5nr04138d

rsc.li/nanoscale

1. Introduction

1.1 Clean energy transition and key technological challenges

As nations race to decarbonize their economies, clean energy has emerged as both a scientific frontier and a societal imperative, driving the development of power sources that emit little to no greenhouse gases while meeting the world's growing energy demands. Clean energy technologies—including solar,[1] wind,[2] hydropower,[3] geothermal,[4] and bioenergy[5]—are widely adopted to reduce dependence on fossil fuels, improve energy security, and support economic growth.[6] According to the International Renewable Energy Agency (IRENA), renewable resources accounted for approximately 33% of global electricity generation in 2024, up from around 30% in 2023, where various sources are highlighted in Fig. 1.[7] This upward trend indicates a clear global shift towards sustainable energy. The transition to renewable energy is essential for mitigating greenhouse gas emissions, reducing pollution, and curbing fossil–fuel depletion.[8,9] The Intergovernmental Panel on Climate Change (IPCC, 2021) indicates that limiting global warming to below 1.5 °C will require rapid and far-reaching changes in global energy systems, including large-scale substitution of fossil fuels with renewable sources, widespread electrification, and significant improvements in energy efficiency.[10] However, persistent scientific, technical, economic, environmental, and political challenges, as illustrated in Fig. 2, continue to impede large-scale deployment of clean energy technologies.

Clean energy systems such as batteries, fuel cells, and solar panels depend heavily on a narrow set of critical raw materials

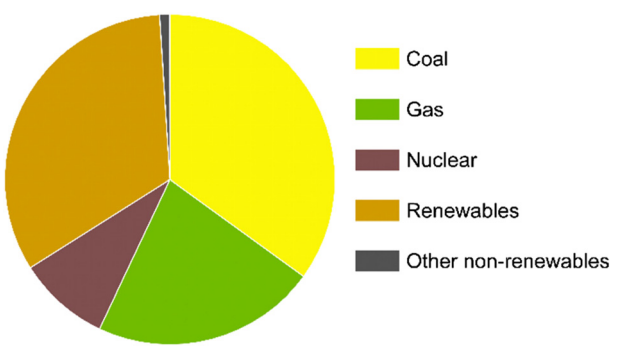

Fig. 1 Global electricity generation by source, 2024.

[a]*Department of Chemical and Biological Engineering, Monash University, Australia. E-mail: priya.shanthipriya@monash.edu*
[b]*Department of Materials Science and Engineering, Monash University, Australia*

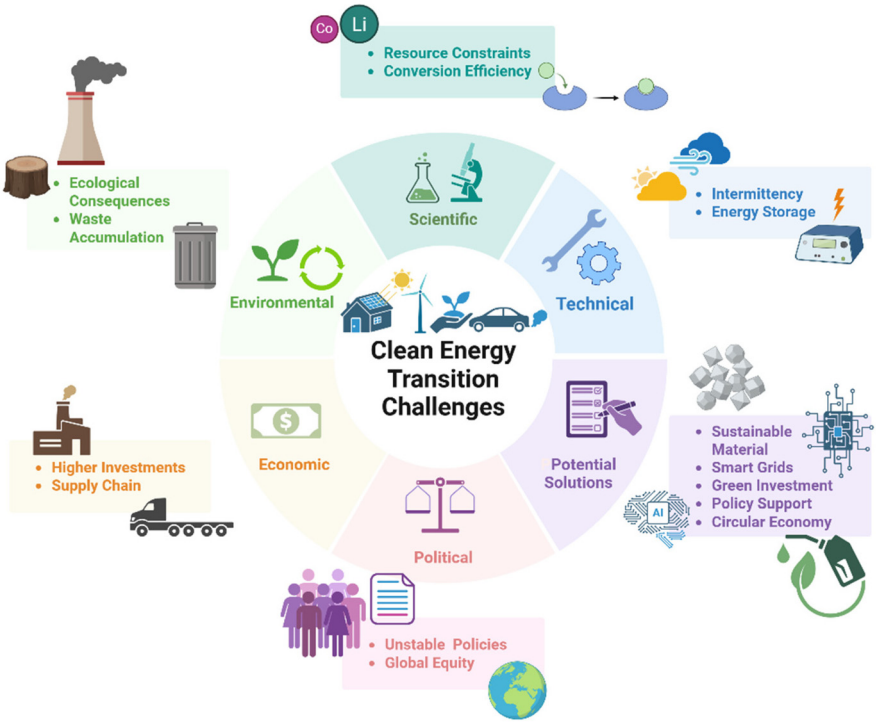

Fig. 2 Overview of multifaceted challenges and key solutions in the clean energy transition.

—lithium, cobalt, platinum, and rare-earth elements, raising concerns about supply security, price volatility, and intensified mining activities.[11] Furthermore, converting renewable energy into storable chemical or electrochemical forms involves multi-step processes with substantial energy losses, lowering overall system efficiency.[12] Overcoming these barriers requires the development of advanced materials and catalytic systems capable of enabling faster, more efficient, and low-energy-input conversion pathways.[13]

Intermittency is another major technical challenge: solar and wind availability varies with weather and time, introducing fluctuations that affect grid reliability.[14] Integrating smart or AI-enabled grid systems with advanced storage and power-balancing mechanisms has been proposed as one pathway to mitigate these fluctuations.[15]

Yet such solutions require complementary advances at the materials, catalysis, and reaction-engineering levels to ensure efficient conversion and storage of harvested energy. Finally,

Harshita

Harshita is a current PhD student in the Department of Chemical and Biological Engineering, Monash University, Australia. She completed her bachelor's degree in Biotechnology at Panjab University, India, followed by further studies at RMIT University, Australia, where she conducted a research project on the stability of DNA encapsulated within metal–organic frameworks (MOFs). Her doctoral research is highly interdisciplinary, focusing on the development of sustainable and clean-energy solutions using bio-mimicking catalysts.

Murali Sastry

Professor Murali Sastry is an internationally recognized expert in nanomaterials and surface science, currently a Professor at Monash University and CEO of the IITB-Monash Research Academy. He has made pioneering contributions in thin films, nanotechnology, and materials chemistry, with over 300 publications and numerous patents. Professor Sastry has held key positions in academia and industry, including Chief Scientist at Tata Chemicals. He is a recipient of many awards, including the prestigious Shanti Swarup Bhatnagar Prize, and is a Fellow of several leading scientific academies. His research continues to impact innovations in science and technology.

the energy transition is shaped by global coordination challenges, as unequal technological capacity, infrastructure, and financial resources create disparities in adoption and implementation.[16,17] Alongside these system-level barriers, a central scientific challenge lies in improving the efficiency of fundamental energy-conversion reactions—an area where catalysts play a decisive enabling role.

1.2 Catalysis as a central enabler of efficient energy conversion

When considering the scientific challenges in clean energy, efficient energy conversion stands out as a major issue. Several barriers in energy conversion can be addressed through catalysis, most notably reducing energy losses, improving efficiency, and enabling sustainable pathways for fuel and electricity production.[18,19] By lowering activation energies, catalysts allow reactions to proceed more efficiently and under milder conditions, enhancing both kinetics and thermodynamics while reducing system costs and enabling scalable, commercially viable technologies.[20]

These catalytic enhancements are critical for renewable energy processes including water splitting, CO_2 reduction, oxygen reduction, and fuel oxidation, all of which involve multi-electron transfers, high energy inputs, and inherently slow kinetics. Catalysts are indispensable for the Hydrogen Evolution Reaction (HER) and Oxygen Evolution Reaction (OER), where highly active and stable electrocatalysts are required to reduce overpotentials and accelerate reaction rates; without them, these reactions proceed too slowly and demand excessive electrical input.[21] Similarly, the Oxygen Reduction Reaction (ORR), a four-electron process, governs the performance of proton exchange membrane fuel cells and metal–air batteries, necessitating catalysts with high activity and selectivity to reach commercial performance. Furthermore, in CO_2 reduction and biomass-derived fuel production, redox reactions dominate, steering product selectivity and mimicking metabolic pathways, while maintaining industrial robustness. These objectives can only be achieved through the strategic design and application of advanced catalytic systems.

1.3 Emergence of nanozymes as enzyme-mimicking catalysts

In response to the limitations of conventional catalysts and natural enzymes, such as poor stability, high cost, or limited tunability, researchers have increasingly turned to emerging materials known as nanozymes: engineered nanomaterials that exhibit intrinsic enzyme-like activity while offering enhanced physicochemical robustness. Nanotechnology has enabled this shift by leveraging the unique features of materials at the 1–100 nm scale through precise control over composition, structure, and surface chemistry.[22] As a result, nanozymes have rapidly advanced to the forefront of renewable energy research due to their tunable catalytic properties, excellent stability under harsh conditions, and cost-efficiency relative to both natural enzymes and traditional metal-based catalysts.[23] Unlike conventional nanocatalysts, nanozymes specifically mimic the function of natural enzymes—such as substrate activation, redox cycling, or intermediate stabilization—with some systems even exhibiting substrate specificity or cascade-type catalytic behavior. Nanozymes are often inspired by structural or functional motifs present in natural enzymatic active sites.[24] Although the definition retains some "fuzzy boundaries", nanozymes are broadly recognized as nanomaterials that exhibit intrinsic and quantifiable enzyme-mimicking activity, rather than simply acting as supports for immobilized enzymes or catalytic ligands.[25] Importantly, while all nanozymes are nanoscale materials, not all nanoparticles qualify as nanozymes, a distinction that becomes essential when differentiating them from conventional or purely structural catalysts.

Recent literature further recognizes that nanozymes encompass a broader class of catalytic systems, including certain single-atom catalysts (SACs), dual single-atom catalysts (DSACs) and structurally well-defined porous materials such as zeolites, MOFs, and COFs, due to their resemblance to biological and homogeneous single-site catalytic centers.[26–30] SAC-based nanozymes, often referred to as single-atom nanozymes (SANs), have demonstrated oxidase-, peroxidase-, and dehydrogenase-like behavior in biocatalysis and electrochemical energy applications.[31,32] Likewise, zeolite and MOF catalysts featuring isolated metal nodes, confined reaction pockets, and substrate pre-organization have been described as "nanoenzyme-like" materials, reflecting mechanistic parallels with natural enzymatic catalysis.[33–35] Taken together, these developments highlight that nanozymes represent an evolving continuum of biomimetic catalytic systems rather than a single mechanistic category.

As detailed in the later sections, nanozyme activity spans diverse mechanisms, including peroxidase-, oxidase-, catalase-, and superoxide dismutase-like functions, enabled by material platforms such as transition metal oxides, MOFs, carbon nanomaterials, and M–N–C frameworks. Beyond mimicking enzyme behavior, nanozymes offer practical advantages in clean-

Shanthi Priya Samudrala

Shanthi Priya Samudrala is a Senior Lecturer in the Department of Chemical and Biological Engineering at Monash University, Australia. She earned her M.Sc. degree in Organic Chemistry from Osmania University (Gold Medal, 2008) and Ph.D. in Applied Chemistry from RMIT University (Research Excellence Award, 2016). She subsequently carried out postdoctoral research and teaching roles at RMIT University and Monash University. Her research focuses on advanced heterogeneous catalysts, nanozymes, and bio-inspired catalytic systems, with emphasis on transforming renewable and waste feedstocks into value-added chemicals and clean fuels, integrating molecular-level catalysis with sustainable reaction engineering.

energy systems: enhancing biomass conversion in biofuel cells,[36] improving hydrogen and oxygen evolution in electrolyzers, facilitating oxygen reduction in fuel cells, and maintaining durability under operational stress. Collectively, these features position nanozymes as a promising class of catalytic materials for next-generation sustainable-energy technologies.

1.4 Advantages of nanozymes over conventional catalytic systems

Compared with conventional homogeneous or heterogeneous catalysts, nanozymes possess unique catalytic behaviours arising from their nanoscale structural tunability and controllable surface chemistry.[37,38] Their activity can be modulated through parameters such as composition, morphology, coordination environment, and defect engineering, enabling precise adjustment of reaction pathways and catalytic performance. Nanozymes demonstrate superior stability, tolerance to extreme reaction environments, and resistance to deactivation compared with both natural enzymes and traditional metal-based catalysts.[39] Their nanoscale architecture allows straightforward surface functionalisation, integration with co-catalysts, and recyclability, while typically maintaining lower production costs and better storage stability.[39,40] These attributes make nanozymes particularly attractive for clean-energy transformations where high selectivity, durability, and controllable reaction pathways are required. A detailed benchmarking of nanozymes against natural enzymes and conventional catalysts is provided in section 5.1.

1.5 Scope, framework and objectives of this review

In the global quest for transitioning towards sustainable and clean energy, the development of cost-effective, durable, and efficient catalysts to facilitate energy conversion and storage has gained significant attention. Nanozymes, a promising class of synthetic catalysts that are not only highly specific and efficient like natural enzymes, but also tunable and robust due to their nanomaterial-based design, offer an effective solution to many of these challenges. With the recent surge in research on nanozymes for clean energy, a systematic synthesis of current knowledge and future directions is both timely and necessary.

This review aims to comprehensively explore the fundamentals, design strategies, and catalytic applications of nanozymes within the context of clean energy reactions. By delving into structure–activity relationships and mechanistic insights, we highlight the role of nanozymes in key reactions, namely hydrogen evolution, oxygen reduction and evolution, carbon dioxide reduction, biofuel production, and methane oxidation. The objective is not only to highlight the contribution of nanozymes in renewable energy systems but also to identify their potential in overcoming the limitations posed by traditional catalysts and biological enzymes.

In addition to established nanozymes, this review also examines a set of nanozyme-inspired catalytic systems—including selected MOFs, COFs, SACs, DSACs, and composite materials—that were not explicitly labelled as nanozymes in their original publications but nonetheless exhibit key features consistent with emerging nanozyme design principles. These systems display attributes such as isolated metal centers, enzyme-like coordination environments, substrate pre-organization, confined catalytic pockets, or cascade-type reaction pathways, positioning them conceptually along a continuum between conventional catalysts and established nanozymes. Throughout this review, the term "established nanozymes" is used to denote catalytic systems explicitly identified in their original sources as exhibiting intrinsic enzyme-mimetic activity, whereas catalytic systems not originally labelled as nanozymes but demonstrate defining biomimetic catalytic features are referred to as "nanozyme-inspired" catalytic systems. Their inclusion is not intended to retroactively reclassify these materials, but rather to highlight the expanding scope and evolving boundaries of nanozyme research and to provide a comparative baseline for identifying future candidates suitable for rational nanozyme design.

Additionally, this review systematically surveys recent advances in nanozyme engineering, including nanostructuring, doping, defect manipulation, and hybridization with co-catalyst or natural enzymes, to enhance catalytic ability, selectivity, and stability altogether. The integration of nanozymes into reactor systems and scalable synthetic approaches is also discussed, with an emphasis on pathways toward real-world applications. A holistic view of nanozyme performance is provided by comparing them with other catalytic materials in terms of turnover frequencies and economic feasibility. Moreover, the knowledge gaps and challenges contributing to mechanistic ambiguities and product selectivity control are highlighted, helping to lay the foundation for targeted future research efforts.

While most existing research on clean energy catalysts and nanozymes remains confined to specific applications, this review adopts a broader lens – charting future opportunities for clean energy conversion, cross-disciplinary directions, and pathways toward transformative impact. It discusses emerging trends in nanozyme research, including innovative fabrication techniques like 3D printed catalyst architectures, and explores the potential impact of nanozymes on the commercialization of clean energy technologies. This provides a roadmap for advancing nanozymes from mere laboratory curiosity to industrial reality. In essence, this review serves as a bridge between fundamental principles and applied science, providing a multidimensional view of how nanozymes can shape the future of sustainable energy technologies. It aspires to inform and inspire researchers and engineers who seek to leverage nanozymes in advancing global sustainable energy outcomes.

2. Fundamentals of nanozymes

2.1 Definition, discovery, and mechanisms

Nanozymes are a class of nanomaterials that inherently exhibit enzyme-like catalytic behavior, distinguishing them from systems in which natural enzymes or catalytic ligands are

merely immobilized on nanomaterials. Mechanistically, a major distinction between nanozymes and protein-based enzymes is that nanozyme activity is strongly influenced by surface valency, coordination environment, and electronic structure. Recent efforts to formalize the definition of nanozymes, including the perspective by Robert *et al.* (2022), propose that a nanoparticle should be considered a nanozyme only when it demonstrates intrinsic catalytic activity analogous to natural enzymes—for example, the peroxidase-like behavior first observed in Fe_3O_4 nanoparticles.[41] This definition has played an important role in establishing rigorous activity-based criteria. However, it is now widely recognized that this framework is intentionally narrow and does not encompass the broader range of biomimetic catalytic behaviors reported across emerging nanozyme systems. Many modern nanozymes derive their functionality not only from peroxidase-like activity, but also from enzyme-inspired coordination environments, substrate pre-organization, confined reaction spaces, redox cycling, or cascade-like reactivity—features that extend beyond a strict activity checklist. Consequently, the term "nanozyme" continues to evolve in parallel with advances in nanoscale catalyst design.

The term "nanozymes" was initially introduced by Manea *et al.* in 2004, referring to the transphosphorylation activity displayed by triazacyclononane-functionalized gold nanoparticles.[42]

However, the concept gained broader recognition following the 2007 discovery of Fe_3O_4 nanoparticles possessing intrinsic peroxidase-like activity as seen in Fig. 3.[43]

It was demonstrated that Fe_3O_4 nanoparticles could facilitate the oxidation of conventional peroxidase substrates, such as diazo-aminobenzene (DAB), 3,3′,5,5′-tetramethylbenzidine (TMB), and *o*-phenylenediamine (OPD) in the presence of hydrogen peroxide, resulting in observable colorimetric changes. These findings highlighted their peroxidase-mimicking properties. Subsequent kinetic studies identified a ping–pong catalytic mechanism, also called a double-displacement mechanism, in which the catalyst temporarily forms an intermediate state before regenerating to its original form during the reaction process. Compared to horseradish peroxidase (HRP), Fe_3O_4 nanozymes displayed a higher catalytic turnover (K_{cat} = 8.58 × 10^4 s^{-1}) but a lower substrate affinity (K_M = 154 mM). This led to the formulation of catalytic activity units and standardized evaluation methods, enabling quantitative comparison of various nanozyme systems.[44]

Since the initial discovery of Fe_3O_4's peroxidase-like properties in 2007,[43] the field has expanded rapidly, with over 200 research groups worldwide contributing to the development of nanozymes based on diverse nanomaterial platforms.[45,46] The surge in related publications reflects growing scientific interest and the wide-ranging potential applications of these materials.

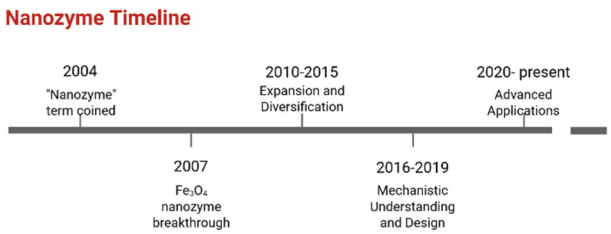

Fig. 3 Timeline showing key milestones in the development of nanozymes.

2.2 Types and catalytic functions

Nanozymes have garnered significant attention because of their promising catalytic capabilities. This section provides an overview of the underlying mechanisms and kinetic behaviors of representative nanozymes exhibiting distinct enzyme-like activities (Table 1).

2.2.1 Peroxidase-like activity. Peroxidase-mimicking nanozymes operate mainly through two catalytic pathways: the

Table 1 Overview of enzyme-mimicry in nanozymes: functions and energy relevance

Enzyme type	Reaction catalyzed	Example nanozyme	Mechanism	Application (energy/other)
Peroxidase-like	$H_2O_2 + AH_2 \rightarrow 2H_2O + A$	Co_3O_4 [47]	Fenton-like mechanism	Fuel cell cathodes, biosensing, oxidative pollution degradation, lignin valorization, oxidative desulfurization
Oxidase-like	$O_2 + AH_2 \rightarrow H_2O_2 + A$	CeO_2 [48]	Surface Ce^{3+}/Ce^{4+} redox cycling to generate superoxide anion from O_2	Oxygen activation (methane-to-methanol), oxygen reduction in metal–air batteries, photocatalytic fuel production, aerobic biomass conversion
Superoxide dismutase-like	$2O_2^{-\bullet} + 2H^+ \rightarrow H_2O_2 + O_2$	*Tris*-malonic acid derivative of fullerene C_{60} (C_3) [49]	Electron-deficient zones attract $O_2^{-\bullet}$ anions, enabling surface-based dismutation	Protection of active sites in oxidative catalysis, redox balancing in the O_2 evolution reaction
Catalase-like	$2H_2O_2 \rightarrow 2H_2O + O_2$	CeO_2 [50]	Surface-mediated decomposition of H_2O_2	H_2O_2 stabilization in biofuel cells, O_2 generation in photo/electrochemical water splitting.
Reductase-like	$A + e^- + H^+ \rightarrow AH$	Fe_3O_4/poly *m*-phenylenediamine (PmPD) [51]	Electron relay through the metal centre	Electrocatalytic CO_2 or nitrate reduction, hydrogenation of renewable feedstocks, and detoxification of aqueous Cr (VI)

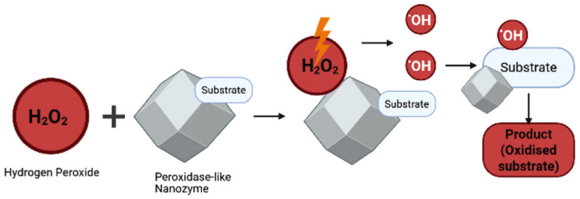

Fig. 4 Schematic representation of peroxidase-like activity of nanozymes.

generation of reactive oxygen species (ROS) and electron transfer mechanisms.[52,53] A widely accepted mechanism involves Fenton or Fenton-like reactions.[43] Initially, hydrogen peroxide (H_2O_2) is adsorbed onto the nanozyme's surface (Fig. 4), facilitating cleavage of the O–O bond and yielding hydroxyl radicals (•OH). These radicals are stabilized by partial electron exchange interactions with the nanozyme surface[54,55] and subsequently oxidize the substrate to generate colored intermediates or products, which may further dimerize or decompose into carbon dioxide, water, and salts.[56]

Distinct from the Fenton mechanism, certain nanozymes catalyze peroxidase-like reactions *via* direct electron transfer without the production of hydroxyl (•OH) radicals.[47,53] In this process, the nanoparticle acts as a mediator, enabling electron flow between H_2O_2 and the substrate. Moreover, upon excitation by localized surface plasmon resonance, hot electrons are produced and injected into H_2O_2 orbitals, promoting its decomposition into hydroxyl radicals and hydroxide ions.[57] Simultaneously, holes generated during this process are neutralized by OH^-, water, or other electron donors, preventing recombination and accelerating the catalytic breakdown of H_2O_2.[57,58]

2.2.2 Oxidase-like nanozymes. Oxidase enzymes catalyze substrate oxidation using molecular oxygen (O_2) as the electron acceptor. These enzymes are often named based on their target substrate, such as glucose oxidase, lactate oxidase, alcohol oxidase, and uric acid oxidase, which facilitate the oxidation of glucose, lactate, ethanol, and uric acid, respectively. Recently, nanomaterials such as gold (Au) nanoparticles,[59,60] manganese dioxide (MnO_2),[61] and cerium oxide (CeO_2)[48] have been identified as oxidase mimics. Moreover, oxidase-mimicking nanoparticles are being increasingly applied in colorimetric detection assays, where they catalyze the oxidation of substrates using O_2, often producing H_2O_2 as a byproduct[62–64] (Fig. 5). These catalytic processes depend on both the structural and electronic characteristics of the nanoparticle and the substrate. However, in contrast to natural oxidases, most nanozymes exhibit broader substrate ranges and often lack the high substrate specificity of their biological counterparts, making the enhancement of selectivity an ongoing research challenge.

2.2.3 Superoxide dismutase-like activity. Numerous nanoparticles have shown the ability to mimic superoxide dismutase (SOD) activity by converting superoxide radicals ($O_2^{-\bullet}$) into H_2O_2 and O_2 (Fig. 6). The underlying mechanisms, however, vary depending on the nanozyme's structure. For example, $C_{60}[C(COOH)_2]_3$-based nanozymes feature electron-deficient zones that electrostatically attract $O_2^{-\bullet}$ anions, enabling surface-mediated dismutation. The carboxyl groups on the nanozyme contribute protons, aiding the catalytic cycle.[49] For cerium oxide (CeO_2), SOD-like activity arises from Ce^{3+}/Ce^{4+} redox cycling, supported by oxygen vacancies on the nanoparticle surface.[50] Here, superoxide anions interact with surface vacancies and, in the presence of protons, are *trans* formed into H_2O_2, a mechanism analogous to that observed in Fe and Mn-based SOD mimics.[65]

2.2.4 Catalase-like activity. Catalase-mimicking nanozymes catalyze the conversion of H_2O_2 into water and oxygen (Fig. 7). Similar to their SOD-like function, cerium oxide-based nanozymes perform this reaction through Ce^{3+}/Ce^{4+} redox cycling. In this mechanism, the O–O bond of adsorbed H_2O_2 is cleaved with proton assistance, leading to water release from the nanozyme's surface.[50]

2.2.5 Reductase-like activity. Nanozymes with reductase-like (R-like) catalytic activity have been widely reported for the reduction of various substrates (Fig. 8).[66,67] For example, hexavalent chromium (Cr(VI)) can be reduced to the less toxic trivalent chromium (Cr(III)) using magnetite-based or cobalt oxide-based nanocomposites.[51,68] Similarly, peroxynitrite can be

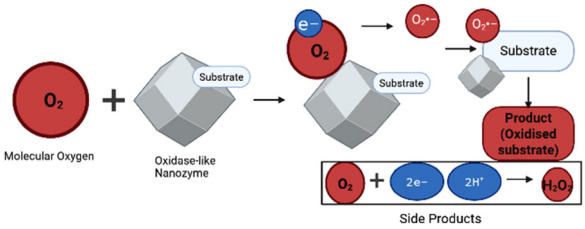

Fig. 5 Schematic representation of oxidase-like activity of nanozymes.

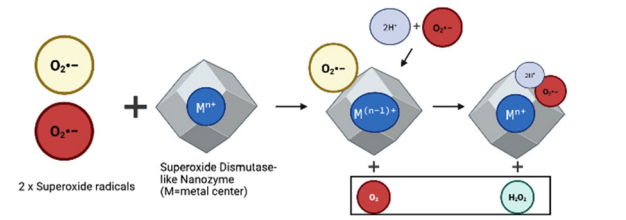

Fig. 6 Schematic representation of superoxide-dismutase-like activity of nanozymes.

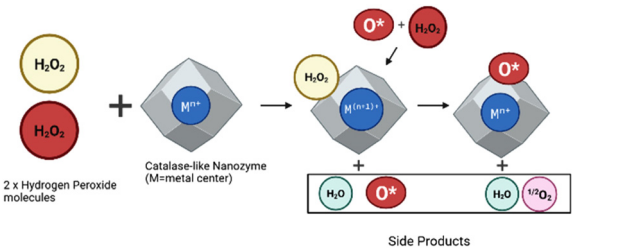

Fig. 7 Schematic representation of catalase-like activity of nanozymes.

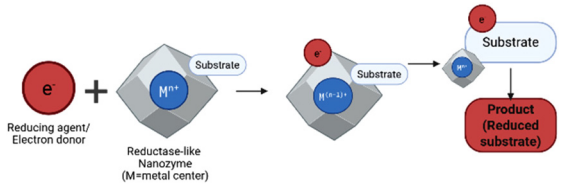

Fig. 8 Schematic representation of reductase-like activity of nanozymes.

reduced by graphene–hemin hybrids,[69] while zeolitic imidazolate frameworks (ZIFs) encapsulated in polyethylenimine catalyze the reduction of cytochrome c (Cyt c).[66] Several nanozymes also facilitate the reduction of 4-nitrophenol to 4-aminophenol in the presence of sodium borohydride, a widely used model reaction for benchmarking reductase-like activity. This has been demonstrated using gold (Au) and silver (Ag) nanoparticles, cobalt oxide-reduced graphene oxide composites, platinum nanoparticles, and iron oxide incorporated in alginate–bentonite hydrogels.[70]

2.3 Structure–activity relationships

2.3.1 Composition. The composition of nanozymes is a primary detriment to their catalytic activity, largely governed by the density and accessibility of metal active centers.[71,72] For instance, Wu *et al.*,[73] employed a salt-template technique to synthesize a Cu–N–C nanozyme featuring atomically dispersed copper with high loading, which exhibited outstanding peroxidase-like activity. Moreover, the size of nanozymes also significantly affects their catalytic efficiency.[74,75]

Another strategy to boost catalytic functionality is the incorporation of additional metals.[76] The group led by Ma *et al.*[77] developed a dual single-atom Mo/Zn nanozyme, where synergistic interactions between Mo and Zn atoms resulted in K_m = 40.32 mM, a remarkable peroxidase-like performance. Designing nanozymes with high metal loading or multiple active centers is an exciting and promising direction. Surface engineering further boosts catalytic and biological performance.[78–80] For example, Xin *et al.*[81] created polyethylene glycol-coated Fe single-atom nanocatalysts (PSAF NCs), with improved stability and biocompatibility, enabling efficient H_2O_2-to-hydroxyl radical conversion under acidic conditions for targeted tumor cell destruction.

2.3.2 Coordination number. The catalytic efficiency of nanozymes is strongly influenced by the coordination environment surrounding their active metal centers. Cui *et al.* developed a suite of single-atom Fe-based nanozymes utilizing Fe–NX coordination structures. Their studies demonstrated that altering the coordination number can fine-tune the nanozyme's oxidase-like performance. Notably, nanozymes with Fe–N_3 coordination showed superior oxidase-mimicking activity, suggesting promising applications in tissue repair.[82] Building on this, Zheng's group synthesized Mo-based nanozymes with Mo–NX–C structures and evaluated how variations in coordination number impacted peroxidase-like behavior.[83,84] Both simulations and lab results confirmed that the Mo–N_3–C single-atom configuration provided exceptional catalytic capability. Additionally, when compared with other M–N_3 type nanozymes (including Fe–N_3, Co–N_3, and Ni–N_3), Mo–N_3–C demonstrated superior activity and specificity. However, a common limitation of single-atom catalysts is the absence of neighboring active sites. To address this, an atomically dispersed copper cluster nanozyme (Cu_3) was recently developed.[85] Advanced characterization using Aberration-Corrected High-Angle Annular Dark-Field Scanning Transmission Electron Microscopy (AC-HAADF-STEM) and Extended X-ray Absorption Fine Structure (EXAFS) confirmed the successful synthesis of this Cu_3 cluster nanozyme. Unlike traditional single-atom or bulk nanoparticle systems, these cluster-type nanozymes contain adjacent copper atoms, which contribute to a denser electron environment at the active sites. This enhances both oxygen adsorption and O–O bond cleavage, yielding significantly stronger oxidase-like activity.[86] Therefore, modifying the coordination number, either through metal–metal interactions or metal–support interfaces, emerges as a powerful strategy for tailoring the catalytic performance of atomically dispersed nanozymes.

2.3.3 Heteroatom doping. Heteroatom doping has emerged as a crucial method for enhancing the catalytic efficiency of nanozymes.[87–89] Fan *et al.*[90] introduced nitrogen-doped carbon nanospheres exhibiting multiple enzyme-mimicking behaviors. X-ray Photoelectron Spectroscopy (XPS) revealed pyridinic N (N-6), pyrrolic N (N-5), quaternary N (N–Q), and pyridinic N-oxide (N–OX) species, which serve as anchoring sites for metal active centers. Wu *et al.*[91] developed Fe–N–C (FeNGR) nanozymes that mimic the function of nicotinamide adenine dinucleotide phosphate (NADPH) oxidase. In another study, Xu's group[92] synthesized a single-atom Zn nanozyme, *i.e.*, carbon nanospheres consisting of a zinc-centered porphyrin-like structure (PMCS) by pyrolyzing mono-dispersed ZIF-8 at high temperatures. The graphitized nitrogen altered the electronic structure around the Zn sites, thereby enhancing the peroxidase-mimetic behavior of PMCS. Their comparative study, based on the coordination configuration of Zn sites, revealed that PMCS containing Zn–N_4 unsaturated coordination displayed the most pronounced catalytic efficiency. Beyond nitrogen, other heteroatoms doped into carbon frameworks also refine nanozyme activity. Jiao *et al.*[26] designed boron (B)-doped single-atom Fe nanozymes where charge modulation by B reduced reaction barriers near the Fe active site and improved peroxidase-like activity. A near-linear correlation was also found between the energy required to form hydroxyl radicals and the local positive charge at Fe centers, offering insights for rational nanozyme design. Furthermore, Ji's group[93] reported a FeN_3P-based single-atom nanozyme (FeN_3P-SAzyme), wherein phosphorus (P) and nitrogen (N) atoms coordinated precisely with Fe to tune its electronic environment. The presence of phosphorus (P) as an electron-donating dopant increased electron density at the Fe site, improving catalytic performance. Computational data indicated that FeN_3P-SAzyme exhibited stronger peroxidase-like activity than both FeN_4-SAzyme and Fe_3O_4 nanozymes.

3. Applications of nanozymes in clean energy conversion

Nanozymes, owing to their structural versatility, tunable active sites, and robustness under harsh conditions, have emerged as promising catalysts for advancing clean energy technologies. They play key roles in processes such as carbon dioxide reduction and valorization into fuels, as well as in water splitting reactions, including the Hydrogen Evolution Reaction (HER), Oxygen Evolution Reaction (OER), and Oxygen Reduction Reaction (ORR). In particular, nanozymes have been explored as electrocatalysts for fuel cell applications, enabling efficient conversion of chemical energy into electrical power. Additionally, nanozymes facilitate the transformation of organic matter and biogas into renewable energy carriers such as biofuels. The following subsections highlight how nanozymes contribute to these clean energy pathways across several key reactions. Fig. 9 provides an overview of these applications and serves as a roadmap for the discussion that follows.

3.1. Hydrogen evolution reaction (HER)

The rapid depletion of fossil fuel reserves and the growing global energy demand present significant challenges, prompting the pursuit of alternative, earth-abundant energy sources and efficient energy storage systems. Among these, electrochemical water splitting has emerged as a highly promising approach, enabling the production of clean hydrogen fuel.[94] Hydrogen is a vital clean energy option and a sustainable substitute for fossil fuels. The Hydrogen Evolution Reaction (HER) is a crucial process in water splitting and ranks among the most significant processes for the generation of sustainable energy, leading to the design and discovery of numerous active catalysts. It occurs in three elementary steps: Volmer, Tafel, and Heyrovsky. In acidic media, the Volmer step includes the reduction of a proton to form adsorbed hydrogen on the active site. In the Tafel and Heyrovsky steps, two adsorbed hydrogen atoms recombine chemically, and a single adsorbed hydrogen atom reacts electrochemically with a proton and an electron to release hydrogen gas, respectively. Whereas, in alkaline media, water molecules are first dissociated to produce hydrogen, as depicted in Fig. 10.[95–101] An efficient catalyst is characterized by high intrinsic performance, a large surface area, and rapid electron transfer. Fabrication method, whether intrinsic (composition-related) or extrinsic (structural tuning), generally does not affect the structural or electrical properties of the catalytic materials; instead, they often enhance both aspects simultaneously. For example, nanomaterials with a narrow size distribution expose a greater number of catalytic sites (an electronic impact) and increase the interfacial area (a structural impact), both of which are important for electrocatalytic effectiveness.[102,103] Notably, nanozymes have emerged as promising HER catalysts, offering both structural tunability and catalytic versatility. The synthesis of nanozymes is often complex, making it difficult to achieve consistent reproducibility and uniformity.[40] Moreover, their industrial application under different pH and temperature conditions remains insufficiently explored and requires further research.[45]

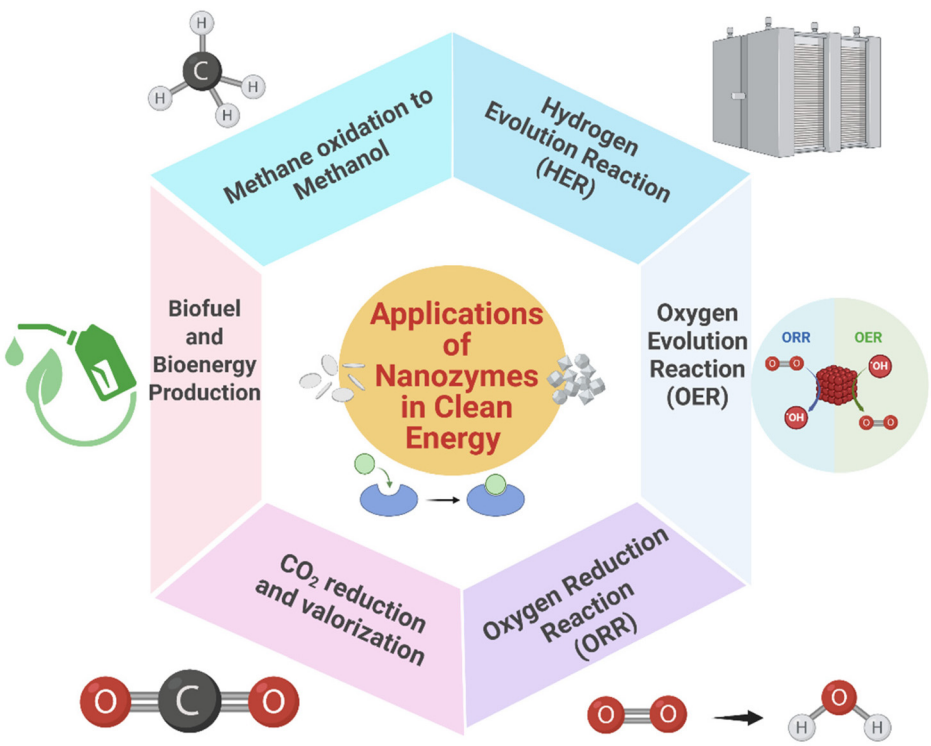

Fig. 9 Schematic overview of nanozyme applications in clean energy conversion covered in this review.

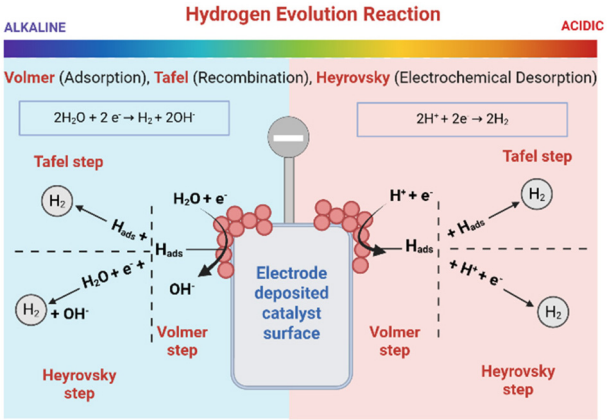

Fig. 10 Schematic representation of the Volmer–Tafel and Volmer–Heyrovsky reactions taking place on nanozyme surface in both acidic and alkaline environments.

3.1.1 Mechanistic pathways of nanozymes in HER. The catalytic mechanism of most nanozymes consists of two main steps: an electron transfer pathway and a reactive oxygen species (ROS)-induced pathway (Fig. 11). In the electron transfer pathway, the electrons are transferred by nanozymes from biomolecules to the oxygen molecule (O_2) or hydrogen peroxide (H_2O_2). The biomolecules work as electron donors, where O_2 or H_2O_2 act as electron acceptors.[104,105] The ROS-driven pathway can be further categorized into two distinct types: free ROS and bound ROS. The kinetic mechanism of the free ROS pathway involves the interaction of H_2O_2 with peroxidase (POD)-like nanozymes, resulting in the formation of hydroxyl radicals. These radicals oxidize the substrate by abstracting a proton (H^+) from the biomolecule, which serves as the hydrogen donor.[43,106]

In the bound ROS pathway, a single H_2O_2 molecule reacts with a POD-like nanozyme to form a metal–oxide intermediate, which abstracts a proton (H^+) from the substrate and drives

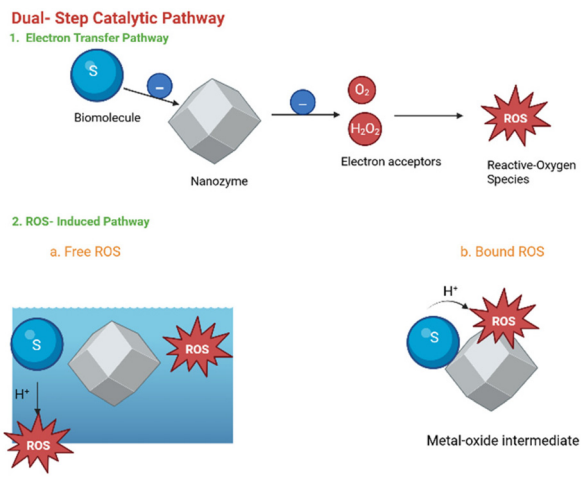

Fig. 11 Schematic representation of a dual-step catalytic mechanism followed by nanozymes.

the catalytic peroxidase reaction.[107,108] The main difference between these two pathways lies in how the substrate interacts with the nanozyme: in the bound ROS pathway, the substrate engages directly with the ROS intermediate; whereas in the free ROS pathway, the reaction proceeds through freely diffusing ROS in solution.[108,109] Due to the structural inhomogeneity of nanozymes, it is difficult to determine the geometry of active sites, which substantially hinders mechanistic elucidation.

3.1.2 Design strategies for efficient and stable HER nanozymes. Over the years, a broad array of nanomaterials has been investigated and designed for their enzyme-mimicking capabilities, following general design principles. This progress has stimulated interest in catalytic nanomaterials, including noble metals like silver, platinum, and gold,[110,111] metal oxides such as Co_3O_4,[112] and metal–organic frameworks (MOFs).[113,114] Nevertheless, challenges remain, especially relating to water stability and the potential release of toxic metal ions.[115] These limitations underscore the ongoing need for new nanomaterials that can effectively mimic natural enzyme functions.

Single-atom catalysts (SACs), featuring atomically dispersed metal active sites and optimal atom utilization, serve as ideal models to study catalytic mechanisms. In some studies, where single metal atoms are dispersed on a support, they have shown superior HER activity.[116] Another promising direction is the design of hybrid nanozymes, especially those built around multi-metal centers. For example, Bar-Hen *et al.*[117] developed a hybrid catalyst made from Ag, Ag_2S, and MoS_2, measuring 610 mV and 455 mV overpotential in 0.5 M KOH and 0.5 M H_2SO_4, respectively. Many catalytic systems tend to suffer from poor stability. To address this, Zhang *et al.*[118] adopted a different approach, introducing a bioinspired sulfur–Fe-heme nanozyme designed to enhance both activity and stability. These examples illustrate how composite metal-based nanozymes represent promising steps toward practical and scalable HER catalyst development. Table 2 highlights representative examples of established nanozymes and nanozyme-inspired catalytic systems developed for efficient HER catalysis.

3.2 Oxygen evolution and reduction reactions (OER & ORR)

The oxygen evolution reaction (OER) and oxygen reduction reaction (ORR) play pivotal roles in artificial energy conversion technologies. Central to these processes are the formation and cleavage of H–H and O–O bonds, which are critical reaction steps (Fig. 12). In natural systems, the intermediates involved in these bond transformations are typically highly reactive and transient, making their detection and study particularly challenging. In artificial catalytic systems, achieving these reactions at practical rates and near their thermodynamic equilibrium remains a significant hurdle. As such, uncovering the underlying reaction mechanisms and establishing clear structure–function relationships is crucial for advancing catalyst design and improving efficiency.[126]

3.2.1 ORR and oxidase-like (OXD-like) catalysis. Motivated by the catalytic parallels between natural enzymes and syn-

Table 2 Representative examples of established nanozymes and nanozyme-inspired catalytic systems for HER

Catalyst	Pathway/reaction conditions	Highlights	Ref.
$NiCo_2O_4$@Al–Sn [a]	Sea water (4 wt% NaCl solution), Room Temperature	Hydrogen production rate–915 L h^{-1} per gram of nanozymes Mimics hydrogenase-like activity.	119
$NiCo_2S_4$ [a]	0.5 M Na_2SO_4	Decorated on $CaTiO_3$, hydrogen production rate-307.76 μmol g^{-1} h^{-1}	120
$FeSe_2$, FeS_2 [a]	0.5 M H_2SO_4 (pH-0.8)	$FeSe_2$ depicts lower onset potential than FeS_2	121
$NiCo_2O_4$ [a]	Room temperature	Hydrogen production rate −0.61 L min^{-1} g^{-1}	122
OVs-TiO_2/Pd HNSs [a]	Photocatalytic	Hydrogen production rate −22.15 mmol h^{-1} g^{-1}	123
Au–Rh [a]	Hydrolysis of $B_2(OH)_4$	Au–Rh nanoparticles encapsulated in a "click" dendrimer TOFs = 6000 mol_{H_2} mol_{cat}^{-1} min^{-1}	124
$Ti_{n+1}C_n$ T_x–Pt_{SA} [b]	Volmer–Heyrovsky mechanism	Thickness effects catalytic performance Best performing catalyst-Ti_2CF_2–Pt_{SA} and $Ti_2CH_2O_2$–Pt_{SA}	116
Ag@MoS_2 [b]	Ar-saturated 0.5 M H_2SO_4 and 0.5 M KOH	Higher activity in alkaline media. Ag drives water dissociation, MoS_2 drives hydrogen recombination.	117
Ni_xCo_y-BTC [b]	1 M KOH	Requires only −0.203 V *vs.* RHE @ 10 mA cm^{-2} Best performing catalyst-$Ni_{0.8}Co_{0.2}$-BTC	125

[a] Established nanozymes: explicitly identified as nanozymes with experimentally verified intrinsic enzyme-mimetic activity in the original publication. [b] Nanozyme-inspired catalytic systems: not originally labelled as nanozymes but consistent with emerging nanozyme design principles.

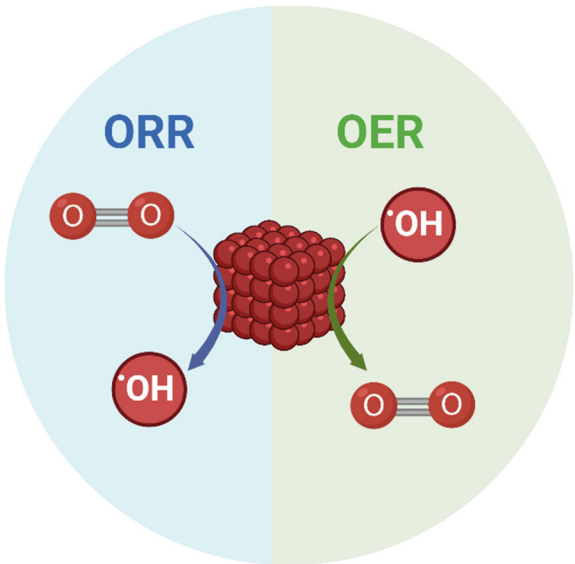

Fig. 12 Typical representation of oxygen evolution and oxygen reduction reactions.

thetic catalysts, researchers have examined various natural oxidases as promising electrocatalysts for ORR.[127] From a mechanistic standpoint, ORR electrocatalysts typically demand high electrical conductivity to ensure efficient electron transfer from the electrode to the catalyst surface and ultimately to oxygen molecules. Whereas, in nanozyme-catalyzed oxidase reactions, electron transfer occurs directly between the oxygen species and substrates confined on the catalyst surface, without requiring long-range conductivity. Combining the distinct kinetic characteristics of ORR and oxidase-like (OXD-like) catalysis offers a promising strategy to enhance reaction selectivity. In ORR electrocatalysis, electrons are continuously delivered from the working electrode, making H_2O_2 selectivity largely dependent on the intrinsic electronic and structural properties of the catalyst. In contrast, in enzyme-like systems, electron donation is limited by the dehydrogenation of substrate molecules. Each catalytic site typically abstracts only two electrons per substrate molecule, thereby limiting oxygen reduction to the $2e^-$ pathway and enabling H_2O_2 production.[128]

3.2.2 Role of OER and ORR nanozymes in electrolyzers and fuel cells. The oxygen reduction reaction (ORR) is a critical electrochemical process underpinning the performance of fuel cells and related energy technologies.[129,130] Similar to the oxygen evolution reaction (OER), the ORR entails a series of multi-electron transfer steps, resulting in inherently slow kinetics (Fig. 13). Platinum-based electrocatalysts currently exhibit the highest ORR activity, but their limited availability and high cost restrict widespread practical applications. One partial solution lies in enhancing the atomic utilization efficiency of platinum. For instance, Pt single-atom catalysts (SACs) supported on carbon black have been developed with power densities reaching up to 680 mW cm^{-2} at 80 °C in acidic fuel cells.[131]

Beyond noble metals, significant attention has turned to non-noble metal SACs for the ORR. Zhang *et al.*[132] developed a modular synthesis strategy to embed isolated cobalt centers into a multichannel carbon matrix (Co@MCM). Han, *et al.*[133] introduced chlorine ligands to FeN_4 centers ($FeCl_1N_4$/CNS), which significantly enhanced the catalytic performance. The modified catalyst achieved a half-wave potential ($E_{1/2}$) of 0.921 V in alkaline media, surpassing both unmodified FeN_4/CN and commercial Pt/C catalysts.

Owing to their outstanding catalytic activity in the oxygen reduction reaction (ORR), single-atom catalysts (SACs) have been extensively investigated as cathode materials for zinc–air batteries. In one study, Chen *et al.*[134] synthesized Fe-based SACs by anchoring isolated iron atoms onto a hollow carbon matrix co-doped with nitrogen, phosphorus, and sulfur

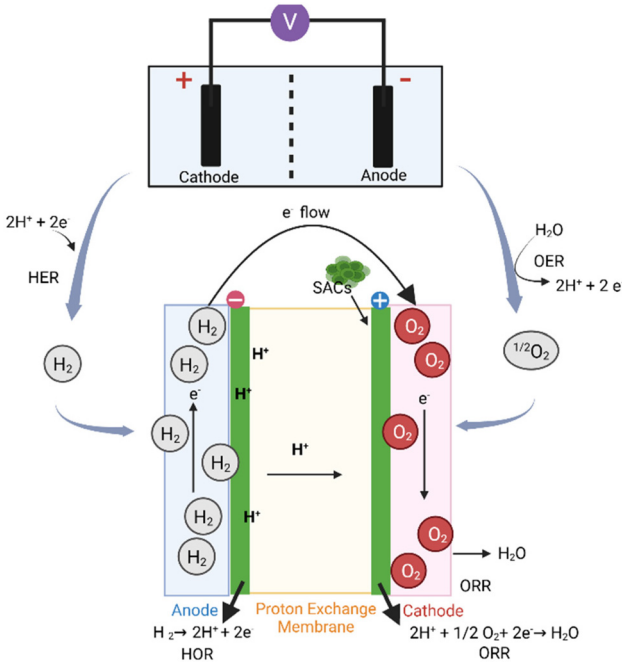

Fig. 13 Schematic representation of the role of nanozymes in OER and ORR.

(Fe–SAs/NPS–HC). This catalyst exhibited a peak power density of 195 mW cm^{-2} at a current density of 375 mA cm^{-2}. Density functional theory (DFT) calculations suggested that this high efficiency and favorable reaction kinetics stem from electron donation by coordinated S and P atoms to the Fe centers. This electron transfer reduced the positive charge on iron ($Fe^{\delta+}$), thereby weakening the adsorption of intermediate $^{*}OH$ species and facilitating the overall ORR process.

The oxygen evolution reaction (OER) involves a complex four-electron transfer process, which imposes high energy barriers.[135] Ru- and Ir-based oxides are recognized as benchmark OER electrocatalysts, but their practical applications in acidic media are hindered by their limited stability due to surface degradation. To address this, researchers have explored anchoring isolated Ru or Ir atoms onto acid-resistant supports to simultaneously enhance their catalytic efficiency and durability.[136] Other transition metal SACs have also shown strong OER activity.[137] Drawing inspiration from the natural oxygen-evolving complex $CaMn_4O_5$ in chlorophyll, researchers have also developed mononuclear manganese embedded in nitrogen-doped graphene (Mn–NG), which achieved a turnover frequency (TOF) exceeding 200 s^{-1}.[138] Table 3 summarizes representative examples of established nanozymes and nanozyme-inspired catalytic systems developed for ORR and OER across electrolyzers, fuel cells, zinc-air batteries, *etc.*

3.3 CO_2 reduction reaction

Following the critical role of nanozymes in the HER, OER, and ORR, another frontier lies in CO_2 utilization, which not only addresses greenhouse gas emissions but also provides sustainable routes to fuels and value-added chemicals. CO_2 is a thermodynamically stable compound with a standard enthalpy of formation of 393.5 kJ mol^{-1}.[150] Its linear and symmetric molecular geometry contributes to its kinetic inertness, making activation more challenging. Consequently, converting CO_2 into value-added products (Fig. 14) necessitates effective activation strategies and substantial energy input, either from high-energy substrates or through external sources such as light or electricity.

3.3.1 Mechanistic pathways in electrochemical CO_2 reduction. The CO_2 reduction reaction (CO_2RR) is inherently complex, involving multiple electron and proton transfer steps

Table 3 Representative examples of established nanozymes and nanozyme-inspired catalytic systems for ORR and OER

Catalyst	Reaction conditions	Active site	Performance metrics and selectivity	Ref.
Rh_1/NC [a]	125 mM H_3PO_3 + 125 mM KH_2PO_3	Rh–N_4	0.48 mol $g_{catalyst}^{-1}$ h^{-1}, 100%	139
NiFe–P_{Zn}@PNTA [a]	1 M KOH	NiFe–Zn^{2+}	300 mV@100 mA cm^{-2}	140
Co_3O_4 [a]	1 M KOH	Co_3O_4	TOF was 0.0117 at η of 400 mV	141
NFCL(70)-LDH@NF [a]	1 M KOH	NiFe–LDH	224 mV@100 mA cm^{-2}	142
FeCu-DA/NC [a]	0.1 M KOH, 0.5 M H_2SO_4	FeN_4CuN_4	$E_{1/2}$ gap of 20 mV to Pt/C in an acid	143
Fe–N–C [a]	O_2- and N_2-saturated HAc–NaAc buffer solution (0.1 M, pH 5)	FeNC	Fe-N–C > N–C	144
FeN_5 SAs [a]	Three-electrode electrochemical system	FeN_5	K_m = 4.2 × 10^{-5} M	145
Pt@PMOF [a]	0.1 M PBS with N2	Pt NPs	Not stated	146
O-CNTs [b]	0.1 M KOH or 0.1 M phosphate-buffered saline	Quinone type C=O	~3950 mg L^{-1} h^{-1} @ 0.4–0.65 V, 90%	147
h-Pt_1–CuS_x [b]	1.1 V, 0.1 M $HClO_4$, 1600 rpm	Pt–CuS	35±4 A g_{cat}^{-1} @ 0.4 V, 96%	148
Pt-supported sulfur-doped zeolite-templated carbon [b]	0.1 M $HClO_4$, V_{RHE} = $V_{Ag/AgCl}$ + 0.287 V, 900 rpm	Pt nanoparticles	97.5 μmol h^{-1}@0 V, 96%	149
Ru–N–C [b]	0.5 M H_2SO_4	Ru–N_4	3571 A g_{metal}^{-1}, TOF-3348 O_2 h^{-1},	136
HCM@Ni–N [b]	1 M KOH electrolyte at 25 °C	Ni–N	Overpotential-403 mV, current density-10 mA cm^{-2}	137

[a] Established nanozymes: explicitly identified as nanozymes with experimentally verified intrinsic enzyme-mimetic activity in the original publication. [b] Nanozyme-inspired catalytic systems: not originally labelled as nanozymes but consistent with emerging nanozyme design principles.

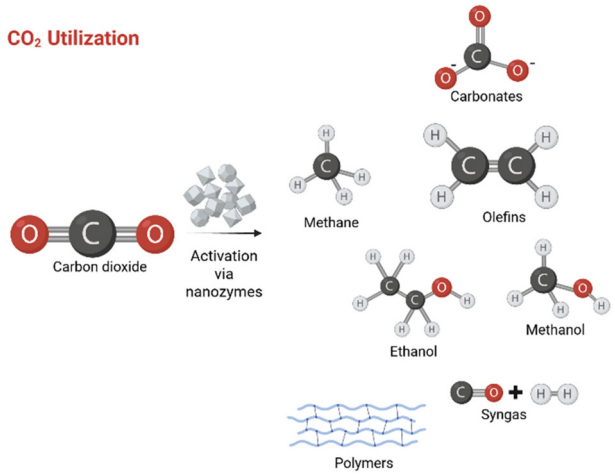

Fig. 14 Schematic representation of CO_2 valorization products.

that give rise to a diverse range of products. Establishing a definitive reaction mechanism, therefore, remains a significant challenge. As reported by Kuhl *et al.*,[151] up to 16 distinct products, including alkanes, alkenes, aldehydes, ketones, alcohols, and carboxylic acids, have been observed from CO_2RR on copper-based catalysts. This intricate reaction network arises because many products share common intermediates. However, despite substantial progress, many elementary steps and mechanistic details remain incompletely validated experimentally.

Adding to the complexity is the wide array of possible intermediates in CO_2RR. In contrast, the hydrogen evolution reaction (HER), which often competes with CO_2RR, it is kinetically more favorable and can be predicted using the Sabatier principle. This principle qualitatively states that optimal catalytic performance occurs when the interaction between a catalyst and its substrate is balanced – neither too weak nor too strong.[152]

Achieving selective CO_2RR toward specific value-added products is particularly difficult due to the linear scaling relationships among the binding energies of similar surface intermediates.[153] For example, the transformation of *CO to *CHO, an essential step in CH_4 formation, has the largest free energy barrier (0.75 eV), making it the rate-determining step. Improving this transformation would require a catalyst surface that binds *CHO more strongly than *CO, which is inherently challenging due to the scaling constraints.[154]

3.3.2 Nanozyme strategies for selectivity and product control in CO2RR. Activation through thermal, photo-, or electrocatalytic routes is essential for CO_2 utilization. To date, homogeneous catalytic systems have been extensively studied for CO_2 transformations through the formation of activated intermediates. Insights gained from these homogeneous systems have guided the development of heterogeneous catalysts, which address key issues like poor thermal stability and lack of recyclability. Among various fabrication approaches, immobilizing molecular catalysts onto nanomaterials has proven particularly effective due to its straightforwardness. Alternatively, designing nanostructures with inherent catalytic activity presents a robust and promising strategy.[155] Selectivity and stability are therefore vital parameters when evaluating catalysts for CO_2RR.

A coordination-number-dependent trend was noted for copper-based catalysts,[156] where catalytic activity and product distribution varied significantly with particle size. Nanoparticles of 1.9 and 2.3 nm exhibited abrupt increases in activity, showing 2-fold and 1.5-fold higher current densities compared to Cu foils at −1.1 V *vs.* RHE. This trend also extends to other metals. Gao *et al.*[157] revealed a size-affected divergence in the adsorption energies of *COOH and *H, for Pd NPs, which favored CO production over HER. Unlike Au and Cu NPs, where HER often dominates, Pd NPs selectively promoted CO generation due to these altered adsorption characteristics. Table 4 provides an overview of representative classes of established nanozymes and nanozyme-inspired catalytic systems designed for the effective valorization of CO_2 into high-value products.

3.4 Biofuel and bioenergy production

3.4.1 Enzyme mimicry in biological energy systems. Enzymes, which are nature's catalysts, are generally classified into six distinct categories according to the type of catalytic reaction they facilitate: oxidoreductases, transferases, hydrolases, lyases, ligases, and isomerases. In the context of bioenergy, nanozymes that mimic natural enzymes such as glucose

Table 4 Representative examples of established nanozymes and nanozyme-inspired catalytic systems for CO_2 valorization

Catalyst	Type of catalysis	Performance metrics	Product targeted	Ref.
PPF-100 [a]	Electrocatalysis	Faradaic Efficiency-72.4%	Carbon monoxide	158
Cu_6-Cotpy [a]	Photocatalysis	Yield-740.7 μmol g^{-1} h^{-1}	Carbon monoxide	159
Co@ZIF-8/Ag [a]	Hydration/dehydration catalysis	44.4% yield compared to the control group	CO_3^{2-} and HCO_3^- ions	160
Au NPs@SiO_2 [b]	Electrocatalysis	Faradaic Efficiency-90%	Carbon monoxide	161
$CdIn_2S_4$ [b]	Photocatalysis	Yield-41.1 μmol g^{-1} h^{-1}	Carbon monoxide	162
$[Cu_6M(\mu\text{-adeninato})_6(\mu_3\text{-OH})_6(\mu\text{-}H_2O)_6]^{2+}$ [b]	Thermocatalysis	Yield-114 $mmol_{CO}$ g^{-1} h^{-1}	Carbon monoxide	163

[a] Established nanozymes: explicitly identified as nanozymes with experimentally verified intrinsic enzyme-mimetic activity in the original publication. [b] Nanozyme-inspired catalytic systems: not originally labelled as nanozymes but consistent with emerging nanozyme design principles.

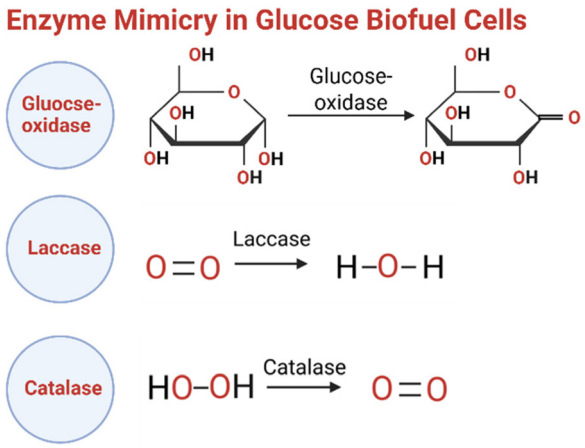

Fig. 15 Schematic representation of enzyme mimicry types in glucose biofuel cells.

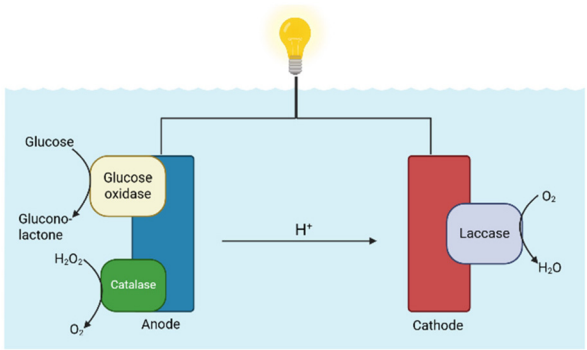

Fig. 16 Schematic representation of enzymes involved in the operation of a biofuel cell.

oxidase, catalase, and laccase, play a pivotal role in powering glucose biofuel cells (Fig. 15). This section highlights their catalytic behavior and design principles.

3.4.1.1 Glucose oxidase-like activity. Glucose oxidase is essential in biofuel cells, as it facilitates electron production by catalyzing glucose oxidation (Fig. 16). In theory, complete oxidation of a single glucose molecule can release up to 24 electrons; however, achieving this requires a series of catalytic processes. Specifically, in glucose oxidase-mediated reactions, the oxidation of one glucose molecule generates two electrons through the formation of one gluconolactone molecule and one molecule of H_2O_2. Due to its research and practical significance, a variety of nanomaterials, *e.g.*, Au NPs, have been explored as nanozymes that emulate glucose oxidase activity.[59,164,165] Beyond gold, other nanomaterials, comprising noble metals and metal oxides (CeO_2), also exhibit glucose oxidase-like activity, making them promising candidates for biofuel cell applications.[166] These nanozymes can be employed to catalyze glucose oxidation at the anode, generating electrons for glucose biofuel cells. However, challenges such as low catalytic performance and substrate specificity remain unresolved.

3.4.1.2 Catalase-like activity. Natural glucose oxidase and its nanozyme counterparts produce H_2O_2 as a by-product. Accumulated H_2O_2 can damage electrode surfaces, resulting in diminished catalytic performance, reduced power output, and shorter operational lifespan. To address these drawbacks, catalase, which decomposes H_2O_2 into oxygen and water, is crucial in designing glucose biofuel cell anodes (Fig. 16). Its activity not only protects glucose oxidase but also enhances the anode's current density by enabling the electrochemical reduction of H_2O_2.[167] Cerium oxide (CeO_2) nanoparticles represent a prominent example of catalase-like nanozymes.[50,168] While catalase-like nanozymes alone cannot form complete glucose biofuel cells, dual-function nanozymes that possess both glucose oxidase and catalase-like activities have been developed for use as anodes in these systems.[169]

3.4.1.3 Laccase-like activity. Laccase enzymes catalyze the reduction of molecular oxygen to water by accepting electrons. A natural laccase enzyme features an active site with four copper ions categorized into three types: T1, T2, and T3.[170] Inspired by this structural motif, recent efforts have focused on designing laccase-mimicking nanozymes that replicate these molecular architectures.[170] Within biofuel cell systems, laccase-like nanozymes are employed at the cathode, and metals such as Pt, Fe, Mn, Co, and Ni are typically effective in cathode fabrication.[171,172] When selecting laccase-like nanozymes for cathodes, a crucial consideration is maximizing the open circuit voltage (OCV), which depends on the specific nanozymes employed at the anode to achieve optimal power output. Therefore, advancing the design of laccase-like nanozymes with both excellent catalytic ability and high electrical conductivity is pivotal for the next generation of glucose biofuel cell technologies.

3.4.2 Advances in nanozyme integration for bioelectrochemical sensing. The integration of nanozymes into bioelectrochemical devices has emerged as a transformative advancement in biosensing technologies. In comparison to natural enzymes, nanozymes offer numerous advantages, including superior stability and durability, lower production costs, tunable catalytic characteristics, and remarkable electrical conductivity.[173] Nanozymes can also function as electrode materials for specific analyte recognition while simultaneously serving as labels for signal enhancement. Their large surface areas offer numerous adsorption sites, thereby increasing the loading of electroactive species and facilitating electrochemical reactions. Recent classes of nanozymes, including metal–organic frameworks (MOFs)[174] and two-dimensional MXenes,[175] have shown remarkable success in electrochemical sensing applications. Their performance is attributed to excellent electrical conductivity, expansive surface areas, and unique physicochemical properties.[176] Table 5 summarizes some examples of established nanozymes and nanozyme-inspired catalytic systems integrated into various fuel cell systems.

3.5 Methane oxidation to methanol

Methane serves as a crucial feedstock for producing various valuable chemicals, including methanol, acetic acid, aromatic

Table 5 Representative examples of established nanozymes and nanozyme-inspired catalytic systems used in bioelectrochemical devices (anode/cathode)

Anode	Cathode	Application	Ref.
Fe–N–S–C [a]	3D carbon brush	Bioelectricity generation in microbial fuel cells	177
Au nanozyme[a]	BOD-N_{pyo}-CDs	Glucose/oxygen fuel cell	178
Alumina-polished carbon electrode	Cu_2O Nanocubes[a]	Laccase-mimic in a biofuel cell	179
$Cu_3(PO_4)_2$ (HNF)/ ACF [a]	$Cu_3(PO_4)_2$ (HNF)/ACF	Mediatorless glucose biofuel cell	169
Ni/PDI-Au NP [b]	PDI/FePc	Hydrogen peroxide fuel cell	180

[a] Established nanozymes: explicitly identified as nanozymes with experimentally verified intrinsic enzyme-mimetic activity in the original publication. [b] Nanozyme-inspired catalytic systems: not originally labelled as nanozymes but consistent with emerging nanozyme design principles.

hydrocarbons, olefins, and dimethyl ether, among others.[181] Efficient utilization of methane holds substantial promise for mitigating both energy shortages and environmental pollution. However, methane (CH_4) is the most inert hydrocarbon, with a high C–H bond dissociation energy (ΔH C–H = 104 kcal mol^{-1} or 4.55 eV at 298 K), and its initial bond cleavage demands significant energy (approximately 435 kJ mol^{-1}) due to its low polarizability (2.84×10^{-40} C^2 m^2 J^{-1}).[182] Designing catalysts that can selectively activate the C–H bond to produce desirable products, therefore, remains a vital area of research,

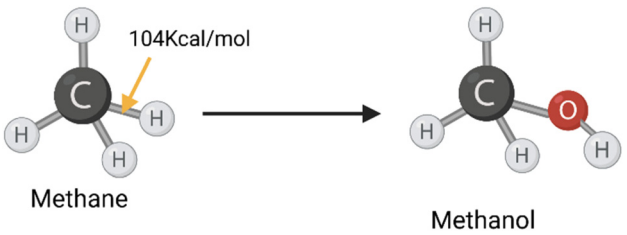

Fig. 17 Schematic representation of methane to methanol oxidation.

with direct implications for both energy sustainability and climate change.

While biological enzymes such as soluble and particulate methane monooxygenases (sMMO and pMMO) are capable of selectively activating methane to methanol under ambient conditions, their scalability and stability outside biological environments remain limited. A range of catalytic systems, including metal complexes based on Pd, Hg, Au, Pt, Ru, Rh, and V, molecular sieves (*e.g.*, ZSM-5), and metal–organic frameworks (MOFs)[183–185] have been studied for methane oxidation to methanol (Fig. 17). However, these systems suffer from drawbacks such as low activity, poor selectivity, reliance on corrosive reaction conditions, and difficulties in product separation.[186,187] Reducing the size of transition metal catalysts to the nanometer scale has shown improved catalytic performance by increasing the surface energy and exposing more active sites. However, maintaining such nanoparticles is problematic due to their tendency to agglomerate, which leads to deactivation.[188]

In conventional catalytic systems, activating methane's C–H bonds typically demands high temperatures. The methanol produced under these conditions is highly susceptible to further oxidation, yielding thermodynamically more stable by-products. Moreover, the inherent polarity of methanol, in comparison to non-polar methane, leads to its stronger adsorption on catalyst surfaces, making it more prone to overoxidation. Thus, an ideal catalyst must promote methane activation while simultaneously suppressing methanol overoxidation.[189,190] In order to address this challenge, various approaches have been explored across biological, homogeneous, and heterogeneous catalysis (Table 6).

3.5.1 Reaction pathways and selectivity control. A major hurdle in the catalytic transformation of methane to methanol lies in the reaction's stoichiometry, which operates on a 1 : 1 ratio.[194] This challenge has led to the development of the "stepped conversion" technique. In this method, initial catalyst activation is performed using an oxidant at elevated temperatures. Subsequently, methane is introduced at a lower temperature to facilitate methanol formation, after which steam is employed to extract the methanol product. This sequential exposure ensures that the catalyst interacts separately with the

Table 6 Comparative overview of various catalytic systems reported in the literature

Catalyst system	Catalyst name	Catalytic mechanism of action	Challenges in oxidation reaction	Reaction conditions (pressure, temperature, oxidants)	Limitations	Ref.
Heterogenous catalysis	Fe–Cu–ZSM-5	Activation of methane *via* Fe-oxo and Cu species in the zeolite framework	Overoxidation of methanol to CO_2, H_2O_2 instability	50 °C, atmospheric pressure, H_2O_2 oxidant	Expensive H_2O_2 oxidant, catalyst deactivation over time	191
Homogeneous catalysis	Bipyrimidyl-Pt complex	Electrophilic activation of methane to form methyl bisulfate in sulfuric acid medium	High acidity of the medium; potential overoxidation of methanol	220 °C, 35 bar, SO_3 oxidant in concentrated sulfuric acid	Requires oleum (sulfuric acid with SO_3); methyl bisulfate needs hydrolysis to yield methanol	192
Enzyme-based catalysis (sMMO)	sMMO	Diiron active site activates O_2 to form a reactive species that oxidizes methane	Difficulty in isolation, instability outside the natural environment	Ambient temperature, requires NADH as a cofactor	Enzyme degradation, low scalability	193

oxidant and methane, thereby enhancing methanol selectivity. However, significant obstacles persist, as industrial-scale processes still demand substantial energy input due to the high activation barriers inherent in methane conversion, making these methods energy-intensive and less feasible for large-scale applications.[195]

Temperature and pressure are critical variables influencing methane's partial oxidation to methanol, both for catalyst activation and the C–H bond cleavage process. Apart from the economic burden associated with maintaining high temperatures, the risk of methanol overoxidation under these conditions poses another significant challenge. A promising alternative for achieving methane conversion at moderate temperatures is photocatalysis. Photocatalysis offers a viable solution by utilizing high-energy photons to generate reactive intermediates capable of cleaving the C–H bond under milder conditions. Such an approach mitigates the agglomeration and sintering of active sites that typically occur at high temperatures. Fig. 18 illustrates how biological inspiration from methane monooxygenase enzymes informs the design of nanozyme platforms, enabling photocatalytic methane conversion through selective C–H activation.

For instance, Sastre *et al.*[196] observed that photoirradiation leads to the dissociation of surface O–H bonds in silica-zeolite structures, producing siloxyl radicals capable of forming methyl radicals from methane. The choice of oxidant is equally vital in photocatalytic methane conversion. Therefore, gaining precise control over reaction pathways and selectivity is not only fundamental to catalytic efficiency but also central to designing nanozyme materials rationally. This has driven a growing interest in highly tunable platforms such as metal–organic frameworks (MOFs) and single-atom nanozymes (SAzymes), discussed in the next section.

3.5.2 Robust nanozyme platforms for methane conversion. Metal–organic frameworks (MOFs) are crystalline porous materials composed of metal ions or clusters coordinated with organic ligands, forming multidimensional lattices.[197] Single-atom catalysts (SACs), featuring isolated metal atoms dispersed on active supports, have emerged as highly promising alternatives to conventional catalytic systems, primarily due to their distinctive geometric structures, enhanced reactivity, and high product selectivity.[31,198] The specific coordination of metal atoms with the support matrix also contributes to the thermal and chemical robustness of these catalysts *via* ensemble effects.[108] Metal nanoparticles have increasingly attracted attention in catalytic applications in recent years. Nevertheless, their high surface energies render them thermodynamically unstable and prone to aggregation during catalytic processes. An effective strategy to stabilize these nanoparticles involves embedding them within porous materials,[199,200] for which MOFs have emerged as highly suitable host materials. Several studies employing established nanozymes and nanozyme-inspired catalytic systems for methane oxidation are highlighted in Table 7 below.

The main objective in recent studies has been to mimic the activity of soluble methane monooxygenase (sMMO) by stabilizing isolated redox-active centers within MOF nodes. For example, Chauhan *et al.*[212] studied monomeric $Fe(OH)_2$ catalyst within DUT-5 (Al-MOF) frameworks. Their study reported high turnover frequencies of 38 592 $\mu mol_{meth}\ g_{Fe}^{-1}\ h^{-1}$ using oxygen as an oxidant at 125 °C and 30 bar methane pressure. Methane's low solubility in water, highlighted in studies involving Pt/polyoxometalate-loaded UiO-67,[204] hampers conversion efficiency unless addressed by alternative solvents or gas-phase conditions.

In the context of methane oxidation reactions (CH_4OR), SAzymes share mechanistic similarities with cytochrome P450 enzymes and have demonstrated the capability to promote room-temperature oxidation of methane to oxygenates. Photoactive SACs offer an appealing alternative, as they can generate H_2O_2 directly from water oxidation, enabling *in situ* CH_4OR using sunlight as the energy source.[213] Likewise, Cu single atoms stabilized within the nitrogen cavities of heptazine frameworks have achieved selective oxidation of methane to methanol with a high TOF of 6.7 h^{-1} at 25 °C.[210] A new class of catalysts, homonuclear and heteronuclear Dual Single-Atom Catalyst (DSACs), is also emerging, featuring two or more isolated metal centers working cooperatively. For instance, Fe_2N_6 dimers anchored on graphene have shown the capacity to activate molecular oxygen through a peroxo-like adsorption configuration.[214] Despite significant progress, heteronuclear DSACs remain largely unexplored in methane oxidation, offering considerable opportunities for future research.

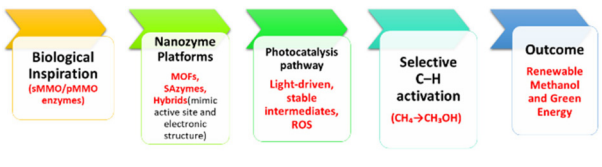

Fig. 18 Schematic representation of the enzyme-inspired nanozyme pathway for methane conversion.

4. Engineering and optimization of nanozyme catalysts

Optimizing the catalytic activity, specificity, and practical utility of nanozymes relies on precise engineering of their structural and compositional characteristics. Various engineering strategies such as nanostructuring, doping, alloying, defect engineering, and hybridization have been widely applied (Fig. 19). Recent advances show that nanozymes can be rationally designed to mimic natural enzymes (peroxidase, catalase, *etc.*), supporting applications in biosensing and environmental remediation.[215] Furthermore, data-driven approaches, including machine learning (ML) techniques, have opened new avenues for optimizing nanozyme synthesis and performance.

4.1 Nanostructuring and surface modification

Despite significant advances in nanozyme research,[216–218] several obstacles still hinder their advancement. One major limitation lies in the narrow spectrum of reactions they catalyze, which are primarily redox processes. Since catalytic

Table 7 Representative examples of established nanozymes and nanozyme-inspired catalytic systems for methane oxidation

Catalyst/system	Temp. (°C)	Pressure (bar)	Oxidant	Reactor/medium	CH_4 conversion or yield	CH_3OH selectivity	Ref.
Fe/Al-MIL-53 [a]	40–60 °C	30.5 bar (700 rpm)	H_2O_2	Batch, aqueous	50 mmol g_{cat}^{-1}	90%	35
Cu-Bzz-MOF-808 [a]	150 °C	Not stated	N_2O	Pretreated 2 h at 150 °C, continuous flow	71.8 μmol g_{cat}^{-1} h^{-1}	100% at 150 °C (only MeOH)	201
Cu-ZIF-7 [a]	50 °C	30 bar	H_2O_2	Batch, aqueous	177.4 μmol g_{cat}^{-1}	Not stated	202
Cu oxide in UiO-bpy [b]	200 °C	1 atm	O_2	Continuous, gas phase 3-step: activation, loading, extraction	24.33 μmol g_{cat}^{-1}	88.1%	203
Pt-POM in UiO-67 [b]	60 °C	50 bar	H_2O_2	Batch, aqueous	12.4% MeOH (2 h); drops to 3.5% (4 h)	71.3% EtOH, 15.9% AcOH	204
AuPd@ZIF-8 [b]	50 °C	30 bar	H_2O_2 (700 μmol), 5 bar O_2 for 30 min	Batch, aqueous	84 μmol g_{cat}^{-1} h^{-1}	89.5%	205
Cu-Oxo NU-1000 [b]	150 °C	1 bar	O_2	3 h, continuous flow	17.7 μmol g_{cat}^{-1}	45% (MeOH + DME)	206
Fe^{2+}@MIL-100 [b]	200 °C	Not stated	N_2O	Furnace bed reactor, pretreated 12 h at 250 °C	0.34 mol (mol Fe)$^{-1}$	94%, 6% CO_2 only	207
Fe-ZSM-5@ZIF-8 [b]	50 °C (adsorption), 150 °C (reaction) for 2 h	1 atm	No oxidant, pre-oxidation done	Fixed bed reactor	0.12 μmol g_{cat}^{-1} (steaming)	Not stated	208
CNT@PNC/Ni (~0.68 wt%) [b]	50 °C	2 MPa CH4 for 10 hours	H_2O_2	Batch, aqueous	1.063 μmol R_{cat} (h^{-1} mg^{-1}), TOF-1.4 h^{-1}	94.2%	209
Cu-SAs/C_3N_4 [b]	25 °C	3 MPa (95% CH4 in Ar)	H_2O_2	Batch, aqueous	397 μmol g^{-1}, TOF-6.7 h^{-1}	95%	210
Cu_2@C_3N_4 [b]	50 °C	3 MPa	O_2	Continuous	1399.3 mmol g Cu^{-1} h^{-1}	>98%	211

[a] Established nanozymes: explicitly identified as nanozymes with experimentally verified intrinsic enzyme-mimetic activity in the original publication. [b] Nanozyme-inspired catalytic systems: not originally labelled as nanozymes but consistent with emerging nanozyme design principles.

activity mostly occurs at the surface, precise control of surface chemistry is crucial for understanding functional mechanisms and enhancing performance. This need has made surface engineering a central design strategy. In recent years, research has increasingly focused on modifying substrate interactions, altering surface electronic characteristics, and enhancing the overall catalytic performance. To reflect these advancements, this section reviews selected studies where the emphasis is placed on how surface engineering and structural design contribute to optimizing nanozyme functionality.

Yu *et al.*[219] investigated the significance of surface modification in influencing catalytic behavior by coating iron oxide nanoparticles (NPs) with ligands bearing different charges and functional groups. Their findings demonstrated that surface charge strongly influences peroxidase-like activity. Positively charged iron oxide NPs modified with glycine (Gly), polylysine (PLL), and poly(ethyleneimine) (PEI) exhibited enhanced catalytic efficiency toward ABTS oxidation. In contrast, negatively charged coatings such as citrate (Cit), carboxymethyl dextran (CMD), and heparin (Hep) favored 3,3′,5,5′-tetramethylbenzidine (TMB) oxidation. Notably, PEI-modified NPs, with a ζ-potential of +47.1 mV, displayed ~12 times higher activity than Hep-coated NPs (ζ-potential −51.2 mV). Additionally, Fe_3O_4 NPs have been integrated into polymeric hydrogels to enhance colloidal stability,[220,221] representing a surface engineering approach. These NPs can be synthesized *in situ* within pre-formed hydrogels[222] or co-generated during hydrogel formation *via* a co-precipitation. The resulting Fe_3O_4 NP-hydrogel composites demonstrate high catalytic activity and can detect hydrogen peroxide concentrations as low as 1.5 μM.[220]

Hydrophilic surface modifiers such as polyethylene glycol (PEG) are also widely employed to improve biocompatibility and dispersion. For instance, Huo *et al.*[223] synthesized Fe-based SAzymes by first immobilizing Fe(III) acetylacetonate in ZIF-8 *via* a hydrothermal process, followed by pyrolysis under an argon atmosphere to produce nitrogen-doped carbon-supported Fe SAzymes (designated as SAF NCs). To improve their hydrophilicity and compatibility, DSPE–PEG–NH_2 was anchored onto the SAF NCs through hydrophobic interactions, yielding PEG-functionalized Fe SAzymes (PSAF NCs). This surface modification not only reduced particle size distribution and increased negative surface potential but also significantly improved dispersion in physiological saline. In addition to PEG, polyvinylpyrrolidone (PVP) is another commonly used polymer to enhance the colloidal stability and biocompatibility of SAzymes.[224] Moreover, Covalent Organic Frameworks (COFs) are an emerging class of crystalline materials composed of lightweight elements such as carbon, nitrogen, oxygen, and hydrogen. Their enzyme-like catalytic performance is largely attributed to their rich C–N framework, which supports a high density of active sites for mimicking enzymatic functions.[225] COFs can be endowed with specific catalytic activities by incorporating functional elements such as iron porphyrins, chiral groups, or metal ions (Cu^{2+} and Fe^{3+}) either during synthesis or *via* post-synthetic modification. A notable example is the work by Zhou *et al.*,[226] who

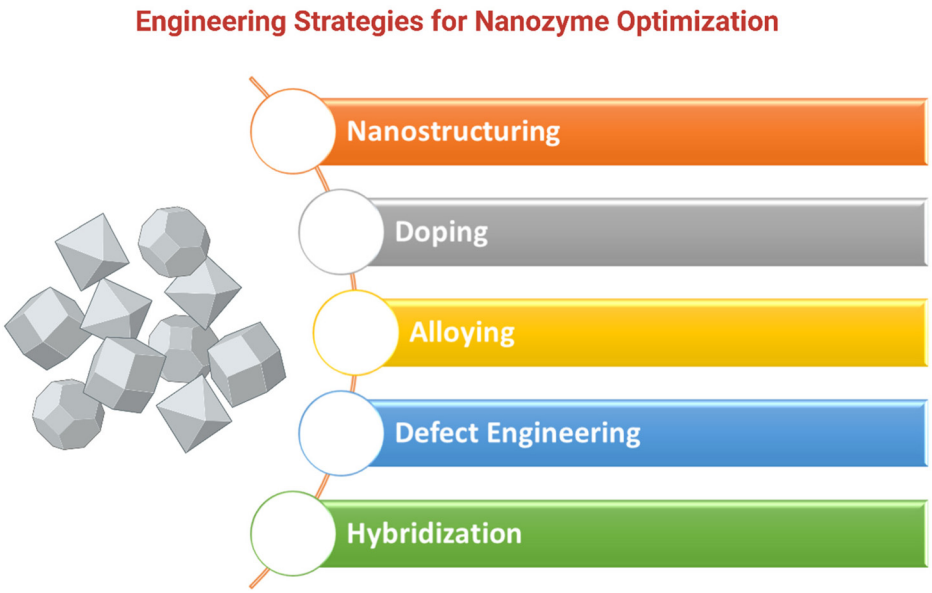

Fig. 19 Engineering strategies employed for nanozyme optimization.

first integrated the chiral molecule L-histidine (L-His) into a COF structure, significantly enhancing the catalytic performance of the resulting nanozyme beyond that of natural horseradish peroxidase. Furthermore, the inherent porosity of COFs can provide a favorable environment for other materials by improving substrate diffusion and preventing enzyme aggregation, thereby supporting more efficient catalytic processes.[227]

4.2 Doping, alloying, and defect engineering

4.2.1 Doping. Elemental doping is a powerful strategy to modulate the coordination environment of active metal centers in single-atom enzyme mimics (SAzymes), thereby significantly affecting catalytic performance. For instance, Jiao *et al.*[26] synthesized a boron-doped Fe SAzyme (FeBNC) by pyrolyzing a precursor mixture of $FeCl_2$ (iron source), dicyandiamide (nitrogen source), and boric acid (boron source). Boron introduction induced charge redistribution around Fe centers, altered their coordination environment, and significantly enhanced peroxidase (POD)-like activity, demonstrating a novel approach to tuning SAzyme functionality. Similarly, Feng *et al.*[228] produced a boron-doped Zn SAzyme (ZnBNC), where boron incorporation improved nitrogen and oxygen content, water dispersibility, and POD-like activity. Boron doping also introduced structural defects, which further contributed to catalytic enhancement. Wang *et al.*[229] developed a copper-based single-atom catalyst, with Cu single-atom sites embedded in nitrogen-doped porous carbon (Cu SASs/NPC) using a pyrolysis–etching–adsorption–pyrolysis sequence. Cu incorporation boosted POD-like activity, enhanced glutathione (GSH) depletion, and improved photothermal properties. Overall, doping strategies during synthesis modulate the coordination environment of active sites in SAzymes, allowing rational tuning of enzymatic activity. This principle forms the basis for developing more advanced strategies for regulating SAzyme activity and broadening their potential applications.[230]

4.2.2 Alloying. Alloying is an effective strategy to fine-tune the catalytic behavior of noble metals by modifying their electronic and geometric configurations through the incorporation of additional elements.[231] To achieve this, a variety of synthesis methods have been employed, including chemical co-reduction,[232] galvanic replacement,[233] seed-mediated growth,[234] and thermal decomposition.[235] Alloy nanozymes are typically classified into three main categories: random alloys, intermetallic alloys, and high-entropy alloys (HEAs) (Fig. 20), each offering distinct structural characteristics and catalytic properties.

4.2.2.1 Random alloys. Random alloys, also known as solid-solution alloys, are characterized by the random atomic distribution within their crystal lattice.[236] Compared to monometallic counterparts, multi-metallic alloy nanozymes often exhibit superior chemical stability and enhanced enzyme-mimicking activity. For example, Meng *et al.*[237] synthesized AuPd alloy

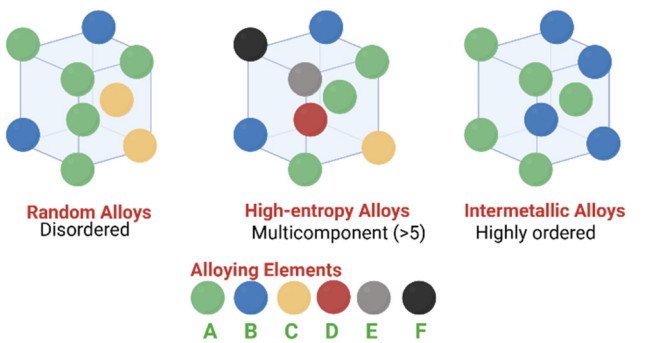

Fig. 20 Schematic representation of alloying categories.

nanozymes that showed markedly improved superoxide dismutase (SOD)- and myeloperoxidase (MPO)-like activities compared to pure Au or Pd. These nanozymes also maintained their activity over a broad temperature range (25–80 °C), demonstrating robust thermal stability.[237]

The performance enhancement arises mainly from electronic structure modulation through alloying.[238,239] Yan *et al.*[240] investigated PdSn nanozymes and confirmed a uniform distribution of Pd and Sn atoms *via* EDS mapping. Projected density of states (PDOS) analysis revealed strong p–d orbital hybridization, which raised the d-band energy level, improved substrate adsorption, and reduced antibonding electron filling. As a result, PdSn nanozymes showed remarkable peroxidase (POD)-like activity, exhibiting high maximum reaction velocities (V_{max}) for both hydrogen peroxide (H_2O_2) and 3,3′,5,5′-tetramethylbenzidine (TMB) substrates. Notably, they also displayed substrate specificity, with low activation energies (1.03 kJ mol^{-1} for POD-like activity and −4.64 kJ mol^{-1} for oxidase-like behavior), underscoring their catalytic efficiency and selectivity.

An effective approach to engineering multifunctional alloy nanozymes involves incorporating functional elements into noble metal frameworks to tailor their physicochemical properties.[241] For instance, oxophilic metals such as bismuth (Bi), tin (Sn), and nickel (Ni) are commonly alloyed with noble metals to enhance activity by promoting the formation of surface-bound oxygen species.[242] Xia *et al.*[243] demonstrated that the peroxidase-mimicking activity of PdBi nanozymes was closely linked to the surface Bi content, which enhanced H_2O_2 adsorption and significantly reduced the decomposition barrier. In another study, PtSn nanozymes benefited from oxygen vacancy sites derived from SnO_{2-x} phases. These vacancies promoted H_2O_2 adsorption and decomposition into reactive oxygen species such as O_2 and hydroxyl radicals, further enhancing catalytic performance.[242]

4.2.2.2 Intermetallic alloy. Intermetallic alloys are metallic compounds with well-ordered atomic structures that significantly impact their catalytic behavior through unique electronic and geometric configurations.[244–246] A recent study by Zhu *et al.*[247] introduced a high-indexed intermetallic Pt_3Sn nanozyme, synthesized through a one-step solvothermal approach. High-resolution structural analysis confirmed the formation of the intermetallic phase, showing lattice spacings of 0.283 nm and 0.179 nm, indicative of a high-index crystalline structure. The resulting nanozyme (H-Pt_3Sn) exhibited the strongest absorbance of oxidized TMB (ox-TMB) at 371 nm and 652 nm when compared with cubic Pt_3Sn, monometallic Pt, and other control samples, highlighting its superior peroxidase (POD)-like activity. Notably, its specific activity (345.32 U mg^{-1}) was nearly double that of the monometallic Pt counterpart (190.12 U mg^{-1}).

In another example, intermetallic Pd_2Sn nanorods (NRs) were engineered as multifunctional nanozymes for cancer immunotherapy applications.[248] Modified with soybean phospholipid and glucose oxidase (GOx), these NRs exhibited excellent colloidal stability, maintaining a consistent hydrated size for seven days in phosphate-buffered solution. The incorporation of plasmonic Pd imparted strong light absorption and efficient photothermal conversion. This localized surface plasmon resonance (LSPR) effect enabled Pd_2Sn NRs to function not only as catalytic agents but also as effective contrast agents for photoacoustic imaging (PAI), demonstrating the dual utility of intermetallic nanozymes in therapy and diagnostics.

4.2.2.3 High-entropy alloys (HEAs). High-entropy alloys (HEAs) have recently emerged as promising candidates in various domains, including energy, engineering, and catalysis, due to their unique compositional and structural characteristics.[249,250] Unlike conventional alloys, HEAs typically comprise five or more principal elements in near-equimolar ratios (5–35%).[251,252] This multicomponent configuration offers greater tunability of the local coordination environment, enabling precise modulation of catalytic activity. Additionally, their high configurational entropy imparts exceptional structural and thermal stability.[253]

In nanozyme research, HEAs have shown great potential as high-performance artificial enzymes.[254,255] For instance, Ai *et al.* synthesized ultra-small PtPdRuRhIr HEA nanoparticles (HEANPs) using a metal–ligand cross-linking strategy.[254] These nanoparticles, averaging (~1.5 nm in size), consisted of uniformly distributed Pt, Pd, Ru, Rh, and Ir. The resulting HEA nanozymes (HEAzymes) exhibited exceptional peroxidase (POD)-like activity, evidenced by a low Michaelis constant (K_M) and high maximum reaction velocity (V_{max}) with H_2O_2 and TMB. Their superior enzymatic activity was attributed to the synergistic effects arising from atomic-level random mismatches and variable site occupancies, which facilitated efficient electron transfer. The sluggish diffusion kinetics and enhanced conformational entropy of the HEAs further contributed to their remarkable structural stability. Importantly, HEAzymes are not limited to noble metal-based systems. More cost-effective and diverse elemental combinations, such as Fe, Cu, Ag, Ce, and Gd[255] and Mn, Fe, Co, Ni, and Cu,[256] have also been developed. These examples highlight both the versatility and the expanding application space of HEAs in nanozyme catalysis.[257]

4.2.3 Defect engineering. Defect Engineering is a powerful strategy to enhance the catalytic performance by selectively generating and manipulating structural imperfections. For instance, Wan *et al.*[258] developed a single-atom gold (Au) catalyst anchored on TiO_2 nanosheets, containing abundant oxygen vacancies, as confirmed by electron paramagnetic resonance (EPR) spectroscopy. The atomic dispersion of Au was stabilized *via* Ti–Au–Ti coordination, and the catalyst exhibited significantly lower CO oxidation temperatures than Au on defect-free TiO_2, highlighting the role of surface defects in enhancing catalytic activity.

Metal–organic frameworks (MOFs), with their complex porous architectures, naturally possess structural defects due to their complex architectures,[259] making them ideal candidates for defect-engineered single-atom enzyme mimics (SAzymes). Zirconium (Zr)-based MOFs, such as UiO-66,

UiO-67, and UiO-68,[260] are especially attractive due to the robust carboxylate–Zr bonds and high connectivity of Zr_6 clusters[261] conferring excellent thermal,[262] solvent,[263] and pressure stability.[264] Defects in MOFs typically fall into two categories: missing-linker defects and missing-cluster defects (Fig. 21),[265,266] which can be introduced either during synthesis (*de novo*) or through post-synthetic modification.[267,268]

De novo synthesis involves altering reaction parameters, often *via* addition of *modulators*, such as water,[269] hydrochloric acid (HCl),[270] acetic acid (HAc),[271] or trifluoroacetic acid (TFA).[272] These modulators possess stronger coordination affinities toward metal clusters than organic linkers, leading to competitive binding and defect formation. The defect concentration can be precisely tuned by varying the type and amount of modulator used.[270,273] Post-synthetic treatments offer additional control. Post-synthetic exchange (PSE), also called solvent-assisted exchange, allows for the substitution of metal ions[274] or linkers,[275] introducing desired defects without altering the overall framework. Alternatively, etching methods, which employ acids, bases, or salts, can generate defects and even create meso- or macroporous architectures within MOFs, thereby enhancing mass transport and catalytic properties.[276,277]

A study conducted by Li *et al.*[270] employed HCl and HAc as modulators to synthesize defective NH_2–UiO66 nanoparticles, referred to as HCl–NH_2–UiO66 and Ac–NH_2–UiO66, respectively. Incorporation of Fe^{3+} ions into defect sites produced SAzymes with superior peroxidase-like activity effective for detecting trace H_2O_2.

The amount of modulator added during synthesis significantly influences defect concentration and, consequently, catalytic performance.[278] Despite these advances, robust strategies for reliably fine-tuning the catalytic performance of defect-engineered SAzymes remain limited. Currently, most reported applications are focused on industrial catalysis, with limited progress in other domains. Nevertheless, defect engineering presents a promising, energy-efficient, and cost-effective route for the rational design of SAzymes.

4.3 Hybrid systems with natural enzymes or co-catalysts

Electrocatalysis is an effective method for interconverting electrical and chemical energy, making it a cornerstone of sustainable energy systems.[279] Covalent organic frameworks (COFs) have emerged as suitable candidates in this context due to their structural tunability. By extending conjugated systems and modifying band structures, COFs enhance light absorption and increase the efficiency of visible-light-driven photocatalysis. Additionally, the integration of functional moieties into COF frameworks or pores facilitates efficient separation and migration of photo-induced charge carriers.[280] While these features have driven the growing use of COFs in energy conversion technologies, to improve catalytic efficiency and enhance enzyme specificity, researchers frequently combine covalent organic frameworks (COFs) with metal nanoparticles and natural enzymes, creating hybrid systems. COFs serve as excellent immobilization carriers due to their structural versatility and compatibility.[281,282] Similarly, integrating COFs with metal–organic frameworks (MOFs) not only improves enzymatic performance but also provides a novel pathway for designing advanced nanozymes.

A notable example is the pioneering work by Zhang *et al.*, who developed a nature-inspired MOF@COF hybrid nanozyme (NMC_{TP-TTA}).[283] Building on this innovation, COF-based nanozymes have rapidly advanced since their application as heterogeneous biomimetic oxidation catalysts in 2014.[284] For instance, the covalent triazine framework CTF-1 was reported to mimic peroxidase activity.[225] In 2020, a chiral COF-based nanozyme was introduced, outperforming natural enzymes in catalytic performance.[226] In 2021, a light-responsive COF nanozyme with a donor–acceptor structure was developed.[285] Most recently, in 2022, researchers synthesized an ultrathin two-dimensional COF nanosheet with oxidase-like activity.[286]

4.4 Immobilization strategies and reactor-level integration

Enzyme immobilization refers to the confinement of enzymes within a defined spatial domain using either physical or chemical approaches. This approach not only protects enzymes from external environmental influences but also improves their operational stability.[287] Widely used immobilization techniques include adsorption,[288–290] encapsulation,[291] and cross-linking.[292,293] In recent years, nanomaterial-based immobilization strategies have garnered considerable attention.[294,295] These strategies utilize nanocarriers, characterized by simple synthesis protocols, gentle reaction conditions, shorter processing durations, and reduced enzyme

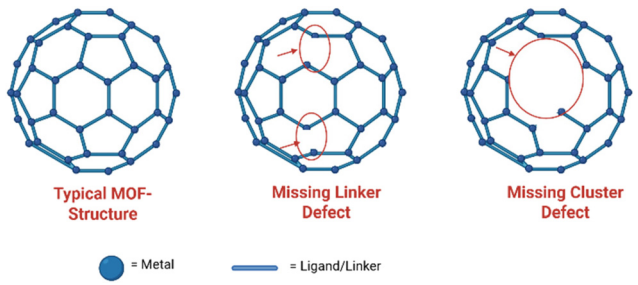

Fig. 21 Schematic representation of defect-engineering strategies in MOFs.

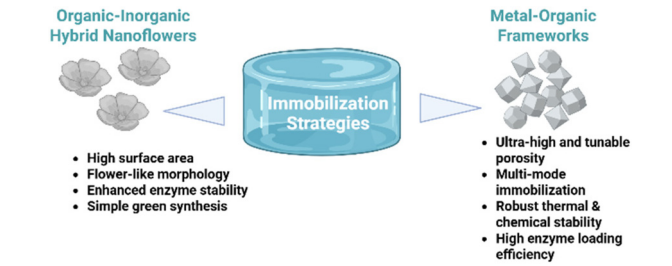

Fig. 22 Schematic representation of various enzyme immobilization strategies.

inactivation. Among the most innovative strategies are organic–inorganic hybrid nanoflowers and metal–organic frameworks (MOFs) (Fig. 22), which are discussed in the following subsections.

4.4.1 Organic–inorganic hybrid nanoflowers. Nanoflowers are nanostructured materials recognized for their distinctive flower-like shapes at the nanoscale. Their unique morphology and high surface-to-volume ratio have positioned them as promising candidates for diverse applications, including catalysis, energy conversion and storage, sensing technologies, and biomedical imaging. The specific architecture of nanoflowers enhances their catalytic performance, optical features, and detection sensitivity. Notably, their petal-like structures provide an extended surface area that facilitates effective biomolecular interactions. Depending on their chemical composition, nanoflowers can be categorized as inorganic,[296,297] organic,[298,299] and hybrid organic–inorganic.[297] A significant breakthrough came in 2012 when Ge *et al.*[300] reported the formation of hybrid nanoflowers by co-incubating proteins with copper ions and phosphate. This process led to protein-directed precipitation and assembly of inorganic materials, yielding flower-like structures approximately 100–500 nm in diameter, known as organic–inorganic hybrid nanoflowers (HNFs).[301]

Typically, the formation of enzyme-based HNFs involves three sequential steps: coordination, precipitation, and self-assembly.[301,302] Initially, metal ions interact with phosphate ions, forming metal phosphate seeds. Functional groups on the enzyme (such as amide, hydroxyl, or carboxyl groups) coordinate with metal ions, providing nucleation sites that anchor initial crystal growth. These nucleation sites promote the growth of metal phosphate petals through repeated enzyme-ion interactions. Finally, anisotropic growth culminates in the formation of the complete flower-like nanostructure.

4.4.2 Metal–organic frameworks. MOFs have gained considerable attention as carriers for enzyme immobilization recently. A widely studied approach is *in situ* immobilization *via* bottom-up synthesis.[303,304] In this method, enzyme molecules function as nucleation centers that direct the growth of MOF frameworks, resulting in a stable and ordered MOF shell that encapsulates the enzyme.[305] This strategy effectively immobilizes enzymes during MOF growth, preserving their catalytic function while providing structural protection.[306] The structural characteristics of MOFs, such as surface area, pore size, shape, and volume, can be precisely tailored.[307] Furthermore, the MOF shell functions as a protective barrier, increasing enzyme resistance to extreme conditions and enhancing long-term stability during storage, temperature shifts, pH variations, and solvent exposure.

The enhanced stability of enzymes within MOFs can be attributed to several factors: (1) the confinement of enzymes within the MOF's porous structure stabilizes their active conformation and minimizes leaching during reuse; (2) the selective pore architecture can regulate substrate access, protecting the enzyme and improving catalytic efficiency; and (3) the physical encapsulation prevents enzyme aggregation.[308] The bottom-up method (*in situ* encapsulation) is further classified into co-precipitation and biomimetic mineralization techniques, depending on whether auxiliary co-precipitants are used during enzyme immobilization.[309]

4.5 Synthesis optimization for enhanced performance

In recent years, metallic and single-atom nanozymes have gained significant attention as a new class of catalysts due to their superior catalytic activity and selectivity.[310,311] Their synthesis typically involves the strategic selection and combination of metal elements, enabling synergistic interactions that enhance overall catalytic performance. Despite their potential, the development of metal-based nanozymes is often hindered by their intrinsic thermodynamic instability, which creates challenges for establishing robust and scalable synthesis techniques. This section highlights the principal fabrication methods for nanozymes, including conventional wet chemistry approaches, ultrafast synthetic techniques, and machine learning-assisted strategies (Fig. 23).[310,312]

4.5.1 Wet chemistry approach. In a study by Xu *et al.*,[313] AuPtCu alloy nanoparticles were synthesized in aqueous media using ascorbic acid as both a reducing and stabilizing agent, leading to the formation of $AuPt_3Cux$ alloys upon Cu incorporation. These Cu-doped alloy nanoparticles exhibited multifunctional enzyme-like behaviors, mimicking oxidase (OXD), peroxidase (POD), and catalase (CAT). In another study, Qu *et al.*[314] developed MnO_2@PtCo nanoparticles using a self-assembly technique, where pre-synthesized PtCo nanoparticles served as templates for the controlled growth of MnO_2. By tuning the reactant ratio, the resulting MnO_2@PtCo nanostructures demonstrated outstanding catalytic properties, with PtCo acting as an oxidase mimic and MnO_2 as a catalase mimic. Zhang *et al.*[315] used a hot injection method to produce a flower-like Co–$FeSe_2$ nanomaterial (~113 nm in diameter), which exhibited strong glutathione-degrading ability and promoted reactive oxygen species (ROS) generation.

Traditional thermal decomposition remains a commonly used strategy for fabricating multi-metallic nanozymes.[316,317] In this approach, metal precursors are decomposed under heat to yield nanoparticles with desired compositions and morphologies. The selection of solvents and ligands plays a critical role in controlling particle shape, size, and alloy distribution.[318,319] For instance,

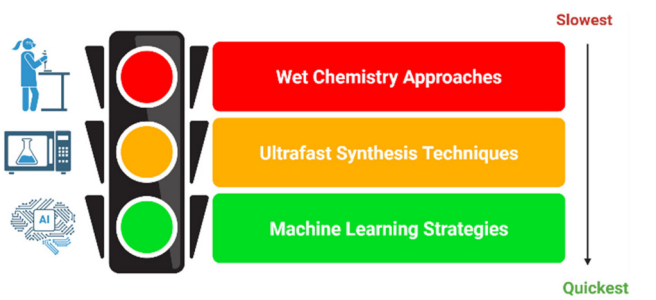

Fig. 23 Infographic of techniques for nanozyme synthesis optimization.

Yang *et al.*[320] synthesized Mn-doped VSe_2 nanosheets (180–250 nm) *via* a high-temperature organic solution method. These nanosheets were further modified with chitosan to enhance water solubility and biocompatibility, producing VSe_2/Mn-chitosan nanosheets. Similarly, Deblin[321] utilized a wet chemical route to create ultrasmall trimetallic PdCuFe nanozymes, further improving their biocompatibility through Dopapimapeg surface modification using a ligand exchange technique. The dopamine groups provided a strong affinity to Fe and Pd surfaces. The resulting PdCuFe nanozymes served as pH-responsive Fenton-like catalysts, mimicking glucose oxidase (GOx) and peroxidase (POD) activities to generate hydroxyl radicals. A recent study by Ai *et al*[254] explored the synthesis of ultrasmall high-entropy nanozymes composed of Pt, Pd, Ru, Rh, and Ir fabricated *via* a straightforward and scalable metal–ligand crosslinking reaction through aldol condensation. The resulting particles displayed exceptional peroxidase-like activity, efficiently converting endogenous hydrogen peroxide (H_2O_2) into hydroxyl radicals.

Among available synthesis techniques, the wet chemical method is widely regarded for its versatility, scalability, and control over particle properties. It enables precise control over particle size, morphology, and uniform dispersion, all of which are essential traits for enhanced catalytic activity. A major advantage lies in its ability to form alloys from elements with similar or slightly mismatched miscibility. However, it faces limitations with strongly immiscible elements, often leading to phase separation and heterogeneity.[322–324] Addressing these challenges may require advanced high-energy synthesis techniques or stabilizing agents to maintain homogeneity and catalytic efficiency.

4.5.2 Ultrafast synthesis approach. Ultrafast synthesis strategies, which utilize rapid energy input such as thermal shockwaves and immediate quenching, enable the fabrication of multi-metallic nanomaterials. Yao *et al.*[325] and Cui *et al.*[326] pioneered an efficient approach known as the facile and ultrafast high-temperature carbon shock method. Their technique enables the synthesis of multi-metallic nanoparticles within just 55 milliseconds, reaching temperatures of nearly 2000 K with heating ramp rates around 10^5 K s^{-1}. The extremely high temperatures facilitate salt decomposition and promote uniform elemental mixing, allowing the formation of nanoparticles with a narrow size distribution and uniform dispersion within the carbon matrix.

Beyond the carbon shock strategy, other approaches such as microwave-assisted synthesis, ultrasonication, laser ablation, arc discharge, and flame-assisted strategies have gained prominence for their speed and effectiveness in nanoparticle fabrication.[327–330] While these high-speed methods offer promising advantages, they also pose challenges, most notably the need for precise control and monitoring of reaction temperatures, which are essential for ensuring reproducibility and scalability. Despite these limitations, ultrafast synthesis techniques remain highly attractive due to their ability to generate nanomaterials with superior catalytic performance across a wide range of applications.

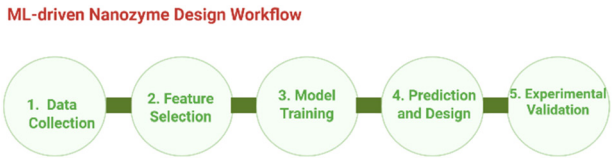

Fig. 24 Flowchart depicting various steps in ML-driven nanozyme design workflow.

4.5.3. Machine learning approach. Machine learning (ML) has emerged as a transformative tool in the development of nanozymes. It enhances their efficiency by predicting critical parameters such as particle size, morphology, and surface properties, thereby reducing the time and resources required for experimental optimization (Fig. 24). ML is particularly valuable for forecasting key nanozyme attributes, including catalytic activity, substrate specificity, and environmental stability.[331] These data-driven insights play a crucial role in guiding the rational design and optimization of nanozymes.

For instance, regression-based ML models are often employed to predict optimal catalytic conditions, such as pH, temperature, and reactant concentrations, to maximize enzymatic performance.[332] By identifying the most favorable parameters from a vast range of possibilities, these models streamline the experimental workflows and reduce reliance on time-consuming trial-and-error methods.[333] They have also enabled researchers to accurately determine the ideal nanoparticle dimensions and surface features needed to tailor nanozymes for specific catalytic applications. In another example, a combination of clustering and regression analysis was employed to improve the environmental stability of gold nanozymes under varying pH and temperature conditions, leading to the development of more durable and reliable biosensors.[334]

In addition, reinforcement learning has emerged as a promising method for optimizing the synthesis conditions of carbon-based nanozymes. This approach iteratively adjusts parameters such as reaction time, precursor concentration, and temperature based on feedback from previous synthesis cycles.[335,336] Together, these advances underscore the pivotal role of ML in shaping the future of nanozyme development.[337,338] Incorporating ML into this domain represents a paradigm shift, enabling the tailored design of nanozymes for catalysis, biotechnology, environmental monitoring, and medical diagnostics. As algorithms grow more sophisticated and computational capabilities expand, the scope of ML applications in nanozyme research will continue to broaden.

5. Comparative assessment of nanozymes with other catalytic systems

5.1 Benchmarking

Nanozymes have emerged as one of the most widely studied and practically relevant classes of artificial enzymes (AEs).

While AEs in general have gained growing interest as alternatives to conventional catalysts, nanozymes stand out due to their structural tunability, robustness, and versatility across applications. AEs comprise a diverse array of organic and inorganic substances designed to function within nanoscale architectures, such as nanoparticles or nanocoatings, and are capable of replicating the catalytic behaviour of natural enzymes under defined conditions.[339] Comparable in size and catalytic mechanism to natural enzymes, AEs also exhibit multivalency, a critical feature that facilitates strong substrate interactions, enhancing both selectivity and specificity.[340] Based on composition, AEs are generally categorized into two types: nanozymes and semi-artificial enzymes (SAEs).[341] Among these, nanozymes are particularly important as they effectively bridge the functional gap between traditional chemical catalysts and biological enzymes (Fig. 25).

5.1.1 How nanozymes outperform traditional catalysts. Traditional catalytic systems often rely on noble metals or transition metal oxides, which, although effective, frequently suffer from poor durability and limited adaptability under variable environmental conditions. Nanozymes, by contrast, not only deliver comparable or superior catalytic activity but also provide exceptional structural tunability and operational robustness. For example, gold nanoparticles (AuNPs) supported on graphitic carbon nitride (g-C_3N_4) have shown higher catalytic efficiency than unsupported particles due to increased active site exposure and enhanced charge transfer at the interface.[342] Similarly, Fe_3O_4 nanoparticles and porous 3D graphene frameworks have been tailored for oxidase- or peroxidase-like behavior, maintaining activity across a broad pH range and under extreme temperatures.[80,343] These properties are especially beneficial in energy conversion technologies such as fuel cells, electrocatalytic reactors, and pollutant degradation modules, where conventional catalysts often suffer from low activity or deactivation.

Nanozymes also play an important role in advanced oxidation processes (AOPs), where the catalytic decomposition of hydrogen peroxide (H_2O_2) generates hydroxyl radicals ($^{\bullet}OH$), capable of breaking down organic pollutants into harmless byproducts. Iron-based nanozymes, particularly when integrated into porous carbon or metal–organic frameworks, are highly effective in degrading compounds like phenols, synthetic dyes, lignins, and melamine, contaminants often found in industrial wastewater or agrochemical residues.[343–345] Beyond chemical activation, nanozymes can also be activated by light, ultrasound, or electric fields, enabling multimodal strategies for clean energy and environmental remediation.

5.1.2 How nanozymes overcome the limitations of natural enzymes. Natural enzymes such as catalase, horseradish peroxidase (HRP), and superoxide dismutase (SOD) show significant catalytic efficiency; however, under extreme physiological conditions, they present significant limitations. Many lose activity in the presence of organic solvents, high temperatures, or oxidative stress, all of which are common in industrial, biomedical, and energy-related processes. On the other hand, nanozymes retain activity under such harsh conditions and can be readily synthesized from cost-effective, abundant materials. Hybrid constructs that combine enzymatic and inorganic functions are particularly promising. For instance, AuNPs@MIL-101, when com-

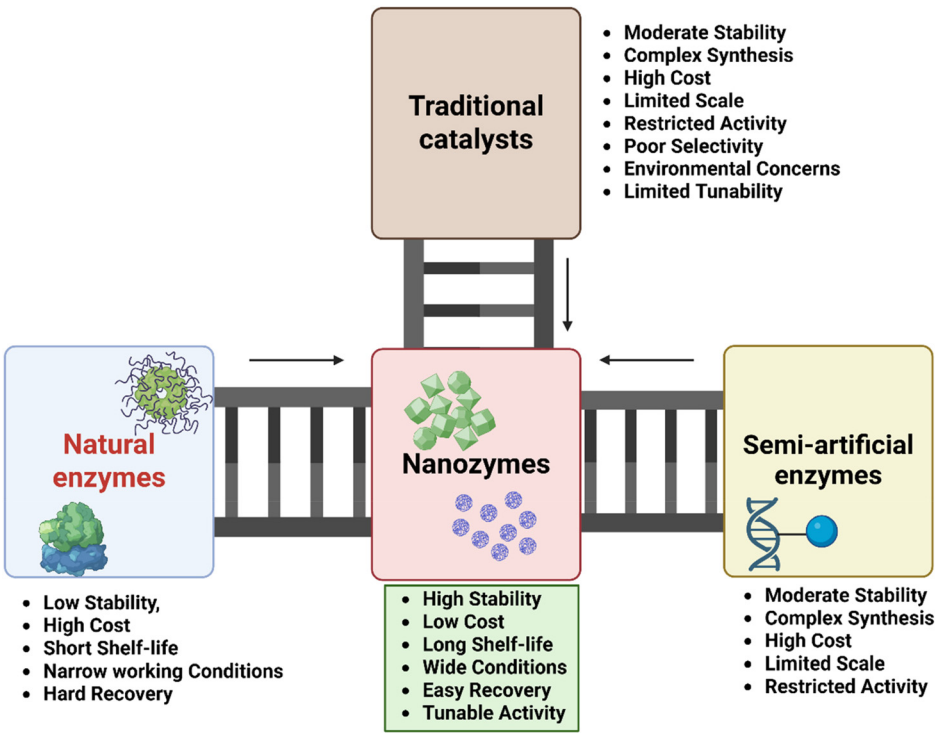

Fig. 25 Schematic representation of nanozymes bridging the gap between natural enzymes, semi-artificial enzymes, and traditional catalysts.

bined with enzymes such as glucose oxidase or lactate oxidase, display a substantial increase in catalytic output. This is attributed to efficient electron mediation between the enzyme and the nanozyme component.[346] Another strategy involves encapsulating natural enzymes within nanoparticles to stabilize their tertiary structure, shield them from denaturation, and extend operational lifetime while broadening their functional range.[347]

Many nanozyme reactions occur at the particle surface, and dense ligand coatings used for bioconjugation can obstruct access to active sites. This has been observed in oxidase-type nanozymes, where excessive surface functionalization leads to notable activity loss.[348] Some progress has been made using polysaccharide coatings, such as dextran-functionalized nanoceria, which balance colloidal stability with active site accessibility.[349] Similarly, encapsulating homogeneous catalysts within polymer or hybrid matrices is emerging as a method for preserving reactivity in biologically or chemically complex environments.[350,351] Overall, the adaptability of nanozymes to different types of substrates, reaction mechanisms, and harsh environmental conditions makes them well-suited for future deployment in clean energy, environmental remediation, and smart biomedical devices. Intriguingly, some nanozymes are also capable of catalyzing non-natural biological reactions, such as bioorthogonal catalysis.[352–354] A comparative overview of various catalytic systems can be seen in Table 8.

5.2 Economic and environmental viability

In the context of growing environmental concerns, nanozymes serve as green catalysts that support the creation of more sustainable products and eco-friendly processes. The circular economy concept challenges the traditional linear production model by emphasizing waste reduction and efficient resource management. Nanozymes function as 'circular catalysts', maintaining catalytic activity over multiple cycles and enabling closed-loop systems in manufacturing. Their robustness and reusability make them particularly valuable in areas such as pharmaceutical synthesis and environmental remediation, such as pollutant degradation and wastewater treatment, where they facilitate greener reaction routes.[360] Nanozymes also offer benefits such as reduced energy consumption, minimal chemical usage, safer processing conditions, and the use of renewable resources.[360]

The nanoscale physicochemical properties of Fe-doped and carbon-based nanostructures are especially important in replicating peroxidase-like activities, enhancing the performance of microbial electrochemical technologies (METs). However, environmental concerns such as metal toxicity, dissolution, excessive reactive oxygen species generation, and oxidative stress-induced toxicity have raised questions about the sustainability and safety of conventional doping and synthesis strategies.[361] As a result, there is growing interest in developing simpler, cost-effective, and friendly methods suitable for industrial-scale implementation. One such approach involves the use of the electroactive bacterium *Geobacter sulfurreducens* combined with an oxygen evolution reaction (OER) – active element such as iron, and further integration with reduced graphene oxide (rGO). This hybrid nanoelectrocatalyst demonstrated enhanced bioelectric performance, reduced overpotential, and improved operational stability. Specifically, the system achieved a geometric current density of 10 mA cm^{-2} at 270 mV during a 10 hour stability test, because of the peroxidase-like behavior of the Fe sites.[362]

In another study, a bioanode modified with a magnetite–carbon nanotube (Fe_3O_4/CNT) yielded a power density of 1050 mW m^{-2} in a microbial fuel cell (MFC) catalyzed by *Escherichia coli*. The magnetic field generated by Fe_3O_4 enhanced microbial adhesion to the electrode surface, promoting faster electron transfer and delivering a 30% increase in power output compared to traditional mediated MFCs. Fe_3O_4 preserved the integrity of the biocatalytic layer, while CNTs formed microchannels that improved electron transport at the biofilm-electrode interface.[363] Additionally, coating electrodes with a reduced graphene oxide/tin oxide (rGO/SnO_2) nanohybrid boosted power density to 1624 mW m^{-2} due to the promotion of electroactive biofilm formation, which facilitated extracellular electron transfer.[364,365]

6. Challenges and knowledge gaps

6.1 Selectivity and reaction control

Achieving selectivity in reactions that yield multiple products remains one of the major challenges in catalysis, as it depends on numerous factors, including the applied potential or

Table 8 Key performance metrics: natural enzymes *vs.* traditional catalysts *vs.* nanozymes

Metrics	Natural enzymes[355]	Traditional catalysts[356]	Nanozymes[355]
Operational stability	Low; denatures under extreme pH/temperature	High; thermally stable but may deactivate in harsh media[357]	Very high; withstand broad conditions
pH tolerance	Narrow (optimum pH only)	Broader (metal oxides tolerant)	Wide (material-dependent)
Temperature stability	Limited (optimum ~37 °C; denature >40 °C)	Stable >1300 °C	Stable 4–90 °C
Substrate specificity	Very high (lock-and-key model)	Low	Moderate; tunable *via* ligand/dopant engineering
Scalability	Low; requires bioproduction and purification	Limited to high; mature industrial processes	Good; scalable synthesis
Cost	High; low yield	Low to high (metal/rare earth cost)	Low
TOF, K_m	K_m = 3.7 mM; V_{max} = 3.34 × 10^{-8} M s^{-1} for native HRP[358]	K_m = 2.3 mM; K_{cat} = 33 s^{-1} for 8-formyl-heme (8F)-HRP[359]	K_m = 154 mM; V_{max} = 9.78 × 10^{-8} M s^{-1} for Fe_3O_4 MNPs[358]

current, the catalyst's properties, and the pH. A comprehensive understanding of the reaction mechanisms and the influence of specific parameters is essential for effective selectivity control, as these processes often involve multiple pathways and intermediates. A well-known example is the electrochemical reduction of CO_2, which can yield up to 16 distinct products.[151] The initial mode of CO_2 adsorption and activation plays a crucial role in determining the overall product outcome. Among these, carbon-rich products (C_{2+}) are considered particularly valuable. However, their formation typically occurs at potentials that also favor the hydrogen evolution reaction (HER), which competes with CO_2 reduction. Thus, suppressing HER is key to steering the process toward multicarbon product formation. The synthesis of C_{2+} products is associated with reaction pathways that enable C–C coupling, which is strongly catalyst dependent.

Copper (Cu) has remained the most extensively researched catalyst for CO_2 reduction, owing to its unique capability to support C–C coupling mechanisms, producing high-value chemicals like ethylene and ethanol.[366] Strategies to enhance Cu's performance have focused on altering its structural and chemical properties through alloying and controlled nanostructuring. However, a limitation of these strategies, and similar approaches that prioritize identifying catalysts with high faradaic efficiency before tailoring their selectivity, is that they may overlook catalysts with inherently high selectivity but low faradaic efficiency.

Recent advancements have introduced novel catalyst systems capable of selectively producing C_2, C_3, and C_4 products. For instance, boron-doped copper achieved ~79% efficiency in reducing CO_2 to C_2 products, attributed to boron's role in stabilizing the $Cu^{\delta+}/Cu^0$ surface ratio.[367] Similarly, a tandem Au/Cu catalytic system efficiently converted CO_2 into C_2 alcohols such as ethanol and *n*-propanol. This system operates *via* a two-step cascade where CO_2 is first reduced to CO at gold sites, which is then further converted into alcohols at adjacent Cu sites.[368]

In comparison to natural enzymes, which exhibit high substrate selectivity (for example, glucose oxidase specifically targets glucose), gold nanoparticles (AuNPs) tend to oxidize multiple reducing sugars indiscriminately.[348] This broad reactivity is largely due to the absence of defined substrate-binding pockets on nanozyme surfaces, allowing multiple substrates to interact freely and undergo reactions, as can be seen in Fig. 26. One strategy to address this issue involves incorporating substrate-binding ligands like antibodies or aptamers. Although feasible in principle, these ligands are limited by high cost and poor stability, undermining the practical advantages of nanozymes.

To overcome these challenges, one approach utilizes molecularly imprinted polymers (MIPs).[369,370] For example, when the substrate TMB was first adsorbed onto iron oxide nanozymes, a hydrogel layer was synthesized around it. Upon removing TMB (serving as the template), the resulting cavities exhibited nearly 100-fold selectivity for TMB. MIPs present a compelling solution due to their robustness, cost-effectiveness, and compatibility with the synthetic nature of nanozymes.

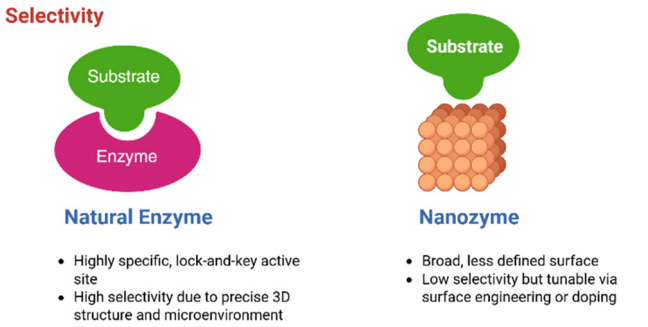

Fig. 26 Schematic representation depicting active sites of natural enzymes and nanozymes.

To advance specificity, one promising direction involves mimicking the three-dimensional substrate-binding pockets found in natural enzymes. However, rationally engineering such structures on nanozyme surfaces remains a difficult challenge. Another viable strategy to improve specificity is the use of biorthogonal nanozymes, which define both the catalyst and the substrate, often relying on synthetic compounds for highly specific reactions.[371] For instance, palladium-based bioorthogonal nanozymes have been employed in prodrug activation within tumor microenvironments, enabling localized chemotherapy with minimal off-target toxicity.[372]

These examples highlight the importance of deepening our understanding of catalyst materials and the mechanisms through which they promote product formation. A shift in focus toward achieving high product selectivity rather than merely enhancing faradaic activity could offer practical benefits such as reducing the cost of product separation. However, predicting product selectivity remains complex even with computational methods, due to the significant influence of multiple catalyst features, including particle size, morphology, crystal structure, and exposed facets.[373,374] A fundamental change in catalyst design philosophy appears necessary to drive significant advances.

6.2 Mechanistic understanding and active site identification

While current research on nanozymes has largely focused on their observed enzymatic activities and practical applications, the continued advancement of this field requires a deeper investigation into the underlying reaction mechanisms that govern their behavior. A much-detailed mechanistic understanding would not only strengthen and refine the definition and classification criteria for nanozymes but also reveal opportunities to exploit enzyme-like catalytic principles in emerging or as-yet unrecognized materials. Such insights could expand the library of nanozyme candidates and accelerate their translation across diverse clean-energy and environmental applications. At their core, nanozyme-catalyzed reactions are surface-mediated and typically proceed through a series of steps, including substrate adsorption, diffusion, chemical transformation, and subsequent product desorption. These steps have been well-characterized in gas-phase catalytic

systems involving crystalline surfaces. However, in aqueous media, often containing buffers and electrolytes, the reaction environment becomes significantly more complex (Fig. 27). So far, elucidating the precise mechanisms of electron transfer in redox reactions has proven to be a major challenge. Among the various nanozymes studied, nanoceria remains one of the most thoroughly investigated. Peng *et al.*[375] proposed that its catalytic behavior occurs through a dissolution-based mechanism. Other mechanistic models include the interconversion between Ce^{3+} and Ce^{4+} oxidation states,[50] and its functioning as an "electron sponge".[350,376] These differing views highlight the lack of consensus and underscore the complexity of defining a clear, unified mechanism.

Going forward, bridging the gap between experimental conditions in wet chemistry and conventional surface characterization techniques (often conducted under ultrahigh vacuum) will be critical to ensure their relevance to reactions occurring in solution-phase environments. Operando techniques, such as *operando* spectroscopy and *in situ* Transmission Electron Microscopy (TEM) or Atomic Force Microscopy (AFM), are emerging as powerful tools to monitor active site behavior and track reaction mechanisms in real time under realistic conditions. In addition, using nanomaterials as scaffolds for homogeneous catalysts has enabled more detailed mechanistic insights. A notable example is the work by Cao-Milán *et al.*[377] who employed ~2 nm gold nanoparticles coated with protective ligand shells to immobilize a bioorthogonal ruthenium catalyst. By altering the ligand structures, they observed variations in kinetic behavior, indicating that the ligand shell significantly influenced the catalytic process. This study shed light on the effect of the local environment on reactivity and provided a framework for the systematic study of nanozyme mechanisms and their rational design.

6.3 Scalability and integration into practical systems

Recent progress in nanozyme-based systems has revealed considerable potential for energy and environmental applications. Nevertheless, multiple obstacles must be addressed before their full potential can be realized. One major challenge is scaling up nanozyme technologies while maintaining consistent quality and performance.[310,378] Shifting from laboratory-scale procedures to industrial-scale production is complex, particularly when aiming to meet the stringent quality benchmarks for each formulation.[379,380] Another critical limitation is the lack of unified protocols for nanozyme synthesis, evaluation, and validation.[381–383] Developing standardized procedures would ensure experimental reproducibility, improve cross-study comparisons, and simplify regulatory approval processes, all of which are crucial for commercial applications.

A major issue lies in achieving consistent synthesis and characterization of nanozymes. Factors such as the synthesis method, reaction conditions, and post-synthesis surface modifications can significantly influence the final catalytic performance. Even minor deviations may lead to substantial variations in activity. In addition, scalability is a significant hurdle. Many nanozyme synthesis techniques involve intricate procedures that are labor-intensive and time-consuming.[384,385] Moreover, certain synthesis routes rely on costly or hazardous reagents, which not only raise production costs but also present environmental and safety concerns (Fig. 28).[386,387] Addressing these issues will be critical for translating nanozyme technologies from laboratory research to commercial and clinical use.

As highlighted by Mohamed's research group,[388,389] existing regulatory systems are not yet fully equipped to accommodate the complexity of nanoparticle-based applications, creating a major obstacle to product development and regulatory approval. Techno-economic analysis (TEA) and life-cycle assessment (LCA) are essential tools to provide a holistic view of both economic competitiveness by assessing cost, scalability, economic feasibility, and environmental responsibility across the entire product life-cycle. Screening synthesized materials using these tools together can guide the optimization of nanozyme design and manufacturing. Thus, future research efforts must focus on resolving challenges related to production scalability and method

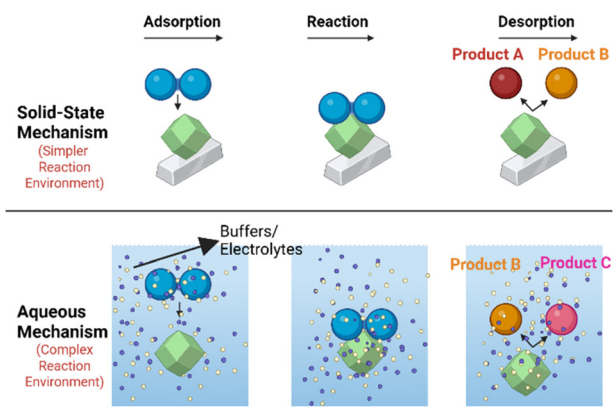

Fig. 27 Schematic representation of solid-state and aqueous catalytic mechanisms.

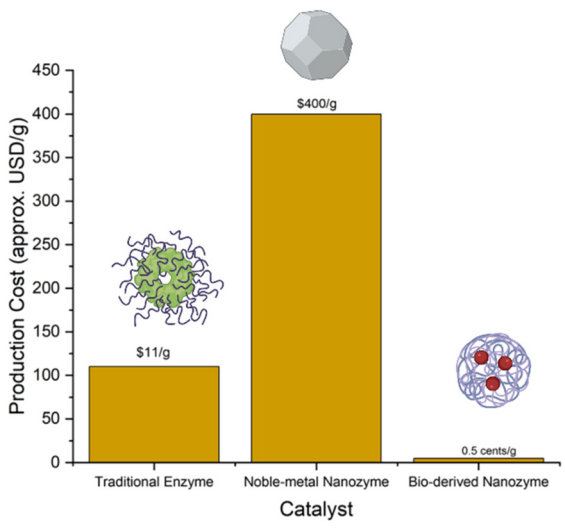

Fig. 28 Graphical representation of approximated costs of traditional enzymes, noble-metal nanozymes, and bio-derived nanozymes.

standardization. These developments will pave the way for nanozyme-based applications that are accurate, dependable, and commercially viable.

7. Future perspectives

7.1 Emerging trends in nanozyme research

The landscape of enzyme immobilization is undergoing a significant transformation, shifting from traditional immobilization methods toward dynamic, responsive systems that integrate artificial intelligence, innovative nanocarriers, and bioprinted scaffolds. These next-generation systems offer refined control over enzymatic behavior, spatial organization, and catalytic reactivity. Designed for high selectivity, sensitivity, and cost-effectiveness, nanomaterials serve multiple critical roles, including acting as support matrices for enzymes, enhancing signal transduction, or functioning directly as enzyme mimics (nanozymes).[390] Notably, artificial intelligence (AI) and machine learning (ML) tools are increasingly being employed to predict interactions and forecast catalytic performance based on structural and physicochemical features. These models accelerate nanozyme design and optimization by enabling rapid screening of enzyme-support combinations and reaction conditions.[391]

In a study by Pandey *et al.*,[392] α-amylase was immobilized onto Halloysite nanotubes (HNTs), which markedly improved the enzyme's thermal stability and reusability, attributes that make it suitable for industrial applications. Shin *et al.*[393] developed a hydrogen peroxide biosensor by encapsulating horseradish peroxidase in protein nanoparticles and integrating it with a reduced graphene oxide-coated gold electrode to improve both the catalytic stability of the enzyme and the electrical conductivity of the electrode. This resulted in a sensor with excellent accuracy, low detection limits, and a wide detection range. While these studies demonstrate significant improvements in stability and functionality, a major limitation remains the lack of standardized metrics, such as turnover frequency, half-life under operational conditions, and number of reuse cycles, for quantitatively benchmarking immobilized enzyme performance. Establishing consistent evaluation criteria would not only enhance comparability across different immobilization platforms but also accelerate the translation of these biocatalysts into industrial and clinical applications.[394]

Beyond sensing, immobilized enzymes play a vital role in environmental applications such as wastewater treatment, where they efficiently break down organic pollutants. Their contribution to bioremediation is equally impactful, aiding in the degradation of oil spills and hazardous chemicals, thus supporting environmental sustainability. In industrial catalysis, immobilized enzymes such as cellulases are essential for the efficient production of bioethanol, while lipases are instrumental in biodiesel synthesis. Their use in the manufacture of active pharmaceutical ingredients further highlights their importance in green chemistry and environmentally friendly manufacturing practices.[388,395–397]

7.2 3D-printed catalyst architectures

Recent advancements in 3D printing technology have introduced innovative approaches for fabricating microarchitectures that facilitate enzyme immobilization, improving reaction specificity and catalytic efficiency (Fig. 29). These benefits stem from the enhanced surface-to-volume ratios and customizable geometries achievable through 3D printing. A widely adopted method involves designing 3D-printed scaffolds with functionalized polymer surfaces, which enable enzyme immobilization through covalent bonding or physical entrapment. Notably, enzymes such as Esterase 2 from *Alicyclobacillus acidocaldarius* and *Candida antarctica* lipase B have been successfully immobilized on polymer-grafted 3D architectures, showing marked improvements in stability and reusability, particularly in solvent-rich environments.[398] The enzyme systems demonstrated up to 0.61 U g^{-1} support, no observable leaching, and stable performance across at least five consecutive reuse cycles.[398]

Hydrogels and polymer-based substances yield structures with extensive surface areas that stabilize enzymes, promote reusability, and enhance catalytic efficiency.[399] A prominent strategy involves entrapping enzymes in 3D-printed hydrogel matrices. For example, researchers designed a 3D-printed hydrogel using poly (ethylene glycol) diacrylate (PEGDA) that preserved around 95% of initial enzymatic activity after 35 days at 4 °C.[400] Shen and colleagues,[399] further showed that 3D gel printing for immobilizing enzymes like lipase, glucose oxidase, and horseradish peroxidase produced engineered porous structures with a threefold increase in catalytic efficiency compared to non-printed controls, owing to improved substrate access and enzyme activity. The synergy between 3D printing technologies and innovations in material design continues to drive the development of cutting-edge biocatalytic platforms.

7.3 Roadmap to commercial deployment

Scaling up nanoparticle production while maintaining control over their structural and functional attributes remains a core technological barrier.[401] Moreover, the high cost of materials, particularly for noble-metal-based nanoparticles like gold, continues to limit widespread industrial adoption. To address this, researchers are actively exploring biodegradable and cost-effective alternatives to traditional materials. However, striking the right balance between cost-efficiency and functional performance is essential to ensure that the technology meets both industrial practicality and regulatory standards.[401] Addressing additional concerns, such as biodegradability, bioavailability, and economic viability of enzyme-conjugated carriers, is necessary to pave the way for real-world implementation.[402] The industrial-scale production of enzymes is also central to advancing nanozyme applications and supporting commercialization. This growth is driven by major international firms such as DuPont (USA), Sunhy Biology and Shandong Longda Biology Engineering (China), Novozymes (Denmark), and AB Enzymes (Germany), all of which are investing heavily in

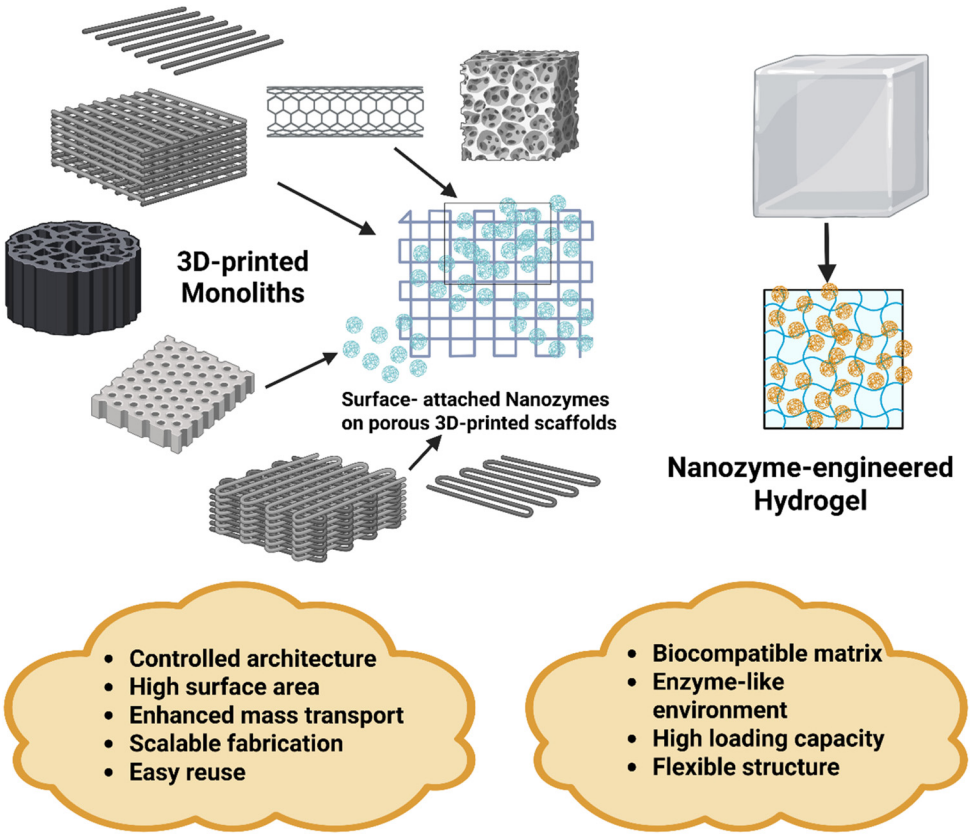

Fig. 29 Schematic representation of 3D-printed monoliths and nanozyme-engineered hydrogels, highlighting potential advantages.

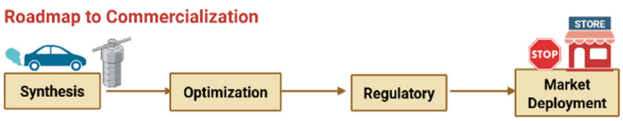

Fig. 30 Flowchart depicting the roadmap towards the commercialization of nanozymes.

enzyme technologies and anticipate rapid market expansion. These companies are developing enzyme-based solutions for diverse biotechnological and industrial applications. Fig. 30 shows a brief overview of the commercialization pathway for nanozymes. Overall, the unique catalytic properties of nanozymes position them as highly valuable across multiple domains. With sustained research, innovation, and the establishment of standardized production methods, nanozyme-based systems hold tremendous potential for industrial deployment.[403]

8. Conclusion

In conclusion, nanozymes have established themselves as a potent class of catalytic materials by bridging the gap between nanotechnology and enzymology. Their future in clean energy applications is highly promising owing to their extraordinary enzyme-mimicking properties, versatile structural designs, tunable activity, and robustness under harsh conditions. These features make nanozymes suitable for diverse sustainable energy production pathways, including hydrogen production, water splitting, oxygen electrocatalysis, biofuel generation, CO_2 reduction, and methane-to-methanol conversion. With ongoing research addressing limitations in long-term operational stability, cost-effectiveness, and compatibility with existing infrastructure, their commercial potential can be significantly enhanced.

Through strategic design and engineering approaches, such as doping, nanostructuring, and hybridization, nanozymes can achieve higher selectivity, efficiency, and operational stability compared to both traditional catalysts and natural enzymes. Despite considerable progress in nanozyme research, significant challenges remain, particularly in achieving precise control of active sites, advancing mechanistic understanding, enhancing scalability, and integrating nanozymes into real-world industrial systems. Furthermore, the field suffers from a lack of standardized benchmarking protocols, deeper structure–activity insights, and more sustainable synthetic approaches. Moreover, there remains an urgent need for clearer and more universally accepted definitions and categorizations of nanozymes, particularly as the field continues to evolve rapidly. Many nanomaterials that exhibit enzyme-like activities—here referred to as nanozyme-inspired catalytic

systems—are still not formally recognized as nanozymes. With further mechanistic study, these materials may reveal valuable catalytic principles and significantly broaden the scope of nanozyme applications.

Looking ahead, novel immobilization strategies based on 3D printing, bio-hybrid materials, and reactor-level engineering are paving the way for large-scale applications and unlocking their potential in transformative green energy projects. Interdisciplinary research combining materials science, catalysis, and systems engineering will be critical to bridging current knowledge gaps and deployment hurdles in the clean energy field. With their adaptability and multifunctionality, nanozymes are poised not only to enhance existing catalytic systems but also to open new avenues of innovation in the global transition toward decarbonization.

Author contributions

Harshita: writing – original draft, conceptualization, formal analysis, investigation. Murali Sastry: writing – review & editing, supervision. Shanthi Priya Samudrala: writing – review & editing, conceptualization, validation, resources, supervision.

Conflicts of interest

The authors declare that they have no known competing financial interests or personal relationships that could have appeared to influence the work reported in this paper.

Data availability

No primary research results, software or code have been included, and no new data were generated or analysed as part of this review.

Acknowledgements

Harshita gratefully acknowledges Monash University for the award of Monash Graduate Scholarship and Monash International Tuition Scholarship. The authors acknowledge BioRender for assistance in developing figures.

References

1 M. E. Mackay, *Solar energy: An introduction*, Oxford University Press (UK), 2015.
2 J. F. Manwell, J. G. McGowan and A. L. Rogers, *Wind energy explained: theory, design and application*, John Wiley & Sons, 2010.
3 Å. Killingtveit, in *Managing global warming*, Elsevier, 2019, pp. 265–315.
4 I. Stober and K. Bucher, *Geothermal energy*, Germany, Springer-Verlag Berlin Heidelberg, 2013, vol. 10, pp. 978–973.
5 S. M. Asaad, M. Tawalbeh, A. Ali, S. R. Al Kindi and A. Al-Othman, in *Renewable Energy-Volume 2: Wave, Geothermal, and Bioenergy*, Elsevier, 2024, pp. 215–243.
6 B. Lin and Z. Li, *Appl. Energy*, 2022, **307**, 118160.
7 I. E. A. (IEA), Global electricity generation by source, 2014–2027, (accessed July, 2025), https://www.iea.org/data-and-statistics/charts/global-electricity-generation-by-source-2014-2027.
8 J.-H. Chang, M. Kumar, S. Selvaraj, M. S. Samuel, S. Ethiraj, A. Senthilkumar, C.-D. Dong and M. Shkir, *Ind. Crops Prod.*, 2024, **215**, 118527.
9 K. K. Jaiswal, C. R. Chowdhury, D. Yadav, R. Verma, S. Dutta, K. S. Jaiswal, B Sangmesh and K. S. K. Karuppasamy, *Energy Nexus*, 2022, **7**, 100118.
10 I. P. o. C. C. (IPCC), *Climate Change 2021: The Physical Science Basis*, 2021.
11 M. N. Ojiambo and T. Adachi, *Miner. Econ.*, 2023, **36**, 519–534.
12 E. Rozzi, F. D. Minuto, A. Lanzini and P. Leone, *Energies*, 2020, **13**, 420.
13 D. Liu and Y. Zhang, *Matter*, 2021, **4**, 2678–2680.
14 N. Mlilo, J. Brown and T. Ahfock, *Technol. Econ. Smart Grids Sustain. Energy*, 2021, **6**, 25.
15 M. B. Blarke and B. M. Jenkins, *Energy Policy*, 2013, **58**, 381–390.
16 A. Bhattacharya, J. Oppenheim and N. Stern, *Brookings Global Working Paper Series*, 2015.
17 C. Okereke and P. Coventry, *Wiley Interdiscip. Rev. Clim. Change*, 2016, **7**, 834–851.
18 L. Peng and Z. Wei, *Engineering*, 2020, **6**, 653–679.
19 Y. Wang, Y. Tian, S.-Y. Pan and S. W. Snyder, *ChemSusChem*, 2022, **15**, e202201290.
20 M. V. Twigg, *Catalyst handbook*, Routledge, 2018.
21 J. Masa, C. Andronescu and W. Schuhmann, *Angew. Chem., Int. Ed.*, 2020, **59**, 15298–15312.
22 R. Saini, S. Saini and S. Sharma, *J. Cutan. Aesthet. Surg.*, 2010, **3**, 32–33.
23 L. Zheng, F. Wang, C. Jiang, S. Ye, J. Tong, P. Dramou and H. He, *Coord. Chem. Rev.*, 2022, **471**, 214760.
24 S. Liu, J. Xu, Y. Xing, T. Yan, S. Yu, H. Sun and J. Liu, *View*, 2022, **3**, 20200147.
25 H. Wei, L. Gao, K. Fan, J. Liu, J. He, X. Qu, S. Dong, E. Wang and X. Yan, *Nano Today*, 2021, **40**, 101269.
26 L. Jiao, W. Xu, Y. Zhang, Y. Wu, W. Gu, X. Ge, B. Chen, C. Zhu and S. Guo, *Nano Today*, 2020, **35**, 100971.
27 R. Gounder and E. Iglesia, *Chem. Commun.*, 2013, **49**, 3491–3509.
28 J. M. Thomas, R. Raja and D. W. Lewis, *Angew. Chem., Int. Ed.*, 2005, **44**, 6456–6482.
29 A. Wang, J. Li and T. Zhang, *Nat. Rev. Chem.*, 2018, **2**, 65–81.
30 Z. Liu, J.-L. Ling, Y.-Y. Liu, B.-H. Zheng and C.-D. Wu, *Chem. Commun.*, 2024, **60**, 12964–12976.

31 L. Jiao, H. Yan, Y. Wu, W. Gu, C. Zhu, D. Du and Y. Lin, *Angew. Chem., Int. Ed.*, 2020, **59**, 2565–2576.
32 W. Zhang, W. Yuan, X. Zhang, Q. Liu, B. Zhao, B. Pan, Y. Xie and Y. Tang, *Matter*, 2025, **8**, 102034.
33 P. Vanelderen, R. G. Hadt, P. J. Smeets, E. I. Solomon, R. A. Schoonheydt and B. F. Sels, *J. Catal.*, 2011, **284**, 157–164.
34 B. E. R. Snyder, M. L. Bols, R. A. Schoonheydt, B. F. Sels and E. I. Solomon, *Chem. Rev.*, 2018, **118**, 2718–2768.
35 D. Y. Osadchii, A. I. Olivos-Suarez, Á. Szécsényi, G. Li, M. A. Nasalevich, I. A. Dugulan, P. S. Crespo, E. J. M. Hensen, S. L. Veber, M. V. Fedin, G. Sankar, E. A. Pidko and J. Gascon, *ACS Catal.*, 2018, **8**, 5542–5548.
36 Y. Meng, W. Li, X. Pan and G. M. Gadd, *Environ. Sci.:Nano*, 2020, **7**, 1305–1318.
37 R. Zhang, X. Yan and K. Fan, *Acc. Mater. Res.*, 2021, **2**, 534–547.
38 Z. Feng, Y. Guo, Y. Zhang, A. Zhang, M. Jia, J. Yin and G. Shen, *J Nanobiotechnol.*, 2024, **22**, 704.
39 S. H. Elagamy, R. H. Obaydo, A. Ashkar and H. M. Lotfy, *Sens. Actuator Rep.*, 2025, **10**, 100394.
40 M. Liang and X. Yan, *Acc. Chem. Res.*, 2019, **52**, 2190–2200.
41 A. Robert and B. Meunier, *ACS Nano*, 2022, **16**, 6956–6959.
42 F. Manea, F. Houillon, L. Pasquato and P. Scrimin, *Angew. Chem., Int. Ed.*, 2004, **43**, 6165–6169.
43 L. Gao, J. Zhuang, L. Nie, J. Zhang, Y. Zhang, N. Gu, T. Wang, J. Feng, D. Yang and S. Perrett, *Nat. Nanotechnol.*, 2007, **2**, 577–583.
44 B. Jiang, D. Duan, L. Gao, M. Zhou, K. Fan, Y. Tang, J. Xi, Y. Bi, Z. Tong and G. F. Gao, *Nat. Protoc.*, 2018, **13**, 1506–1520.
45 J. Wu, X. Wang, Q. Wang, Z. Lou, S. Li, Y. Zhu, L. Qin and H. Wei, *Chem. Soc. Rev.*, 2019, **48**, 1004–1076.
46 K. Korschelt, M. N. Tahir and W. Tremel, *Chem. – Eur. J.*, 2018, **24**, 9703–9713.
47 H. Jia, D. Yang, X. Han, J. Cai, H. Liu and W. He, *Nanoscale*, 2016, **8**, 5938–5945.
48 R. Pautler, E. Y. Kelly, P.-J. J. Huang, J. Cao, B. Liu and J. Liu, *ACS Appl. Mater. Interfaces*, 2013, **5**, 6820–6825.
49 S. S. Ali, J. I. Hardt, K. L. Quick, J. S. Kim-Han, B. F. Erlanger, T.-t. Huang, C. J. Epstein and L. L. Dugan, *Free Radicals Biol. Med.*, 2004, **37**, 1191–1202.
50 I. Celardo, J. Z. Pedersen, E. Traversa and L. Ghibelli, *Nanoscale*, 2011, **3**, 1411–1420.
51 R. Acharya, A. Lenka and K. Parida, *J. Mol. Liq.*, 2021, **337**, 116487.
52 H. Su, D.-D. Liu, M. Zhao, W.-L. Hu, S.-S. Xue, Q. Cao, X.-Y. Le, L.-N. Ji and Z.-W. Mao, *ACS Appl. Mater. Interfaces*, 2015, **7**, 8233–8242.
53 T. Chen, X. Wu, J. Wang and G. Yang, *Nanoscale*, 2017, **9**, 11806–11813.
54 Y. Jv, B. Li and R. Cao, *Chem. Commun.*, 2010, **46**, 8017–8019.
55 K. Herget, P. Hubach, S. Pusch, P. Deglmann, H. Götz, T. E. Gorelik, I. y. A. Gural'skiy, F. Pfitzner, T. Link and S. Schenk, *Adv. Mater.*, 2017, **29**, 1603823.
56 X. Zuo, C. Peng, Q. Huang, S. Song, L. Wang, D. Li and C. Fan, *Nano Res.*, 2009, **2**, 617–623.
57 C. Wang, Y. Shi, Y. Y. Dan, X. G. Nie, J. Li and X. H. Xia, *Chem. – Eur. J.*, 2017, **23**, 6717–6723.
58 I. K. Konstantinou and T. A. Albanis, *Appl. Catal., B*, 2004, **49**, 1–14.
59 W. Luo, C. Zhu, S. Su, D. Li, Y. He, Q. Huang and C. Fan, *ACS Nano*, 2010, **4**, 7451–7458.
60 Y. Lin, J. Ren and X. Qu, *Adv. Mater.*, 2014, **26**, 4200–4217.
61 D. Fan, C. Shang, W. Gu, E. Wang and S. Dong, *ACS Appl. Mater. Interfaces*, 2017, **9**, 25870–25877.
62 W. Zhang, D. Ma and J. Du, *Talanta*, 2014, **120**, 362–367.
63 Y. Xiong, S. Chen, F. Ye, L. Su, C. Zhang, S. Shen and S. Zhao, *Chem. Commun.*, 2015, **51**, 4635–4638.
64 Q. Chang and H. Tang, *Microchim. Acta*, 2014, **181**, 527–534.
65 C. Korsvik, S. Patil, S. Seal and W. Self, *Chem. Commun.*, 2007, **35**, 1056–1058.
66 J. Chen, Q. Ma, M. Li, W. Wu, L. Huang, L. Liu, Y. Fang and S. Dong, *Nanoscale*, 2020, **12**, 23578–23585.
67 D. Besold, S. Risse, Y. Lu, J. Dzubiella and M. Ballauff, *Ind. Eng. Chem. Res.*, 2021, **60**, 3922–3935.
68 A. Al Nafiey, A. Addad, B. Sieber, G. Chastanet, A. Barras, S. Szunerits and R. Boukherroub, *Chem. Eng. J.*, 2017, **322**, 375–384.
69 A. A. Vernekar and G. Mugesh, *Chem. – Eur. J.*, 2012, **18**, 15122–15132.
70 N. Stasyuk, G. Gayda, T. Kavetskyy and M. Gonchar, *RSC Adv.*, 2022, **12**, 2026–2035.
71 D. Sun, X. Pang, Y. Cheng, J. Ming, S. Xiang, C. Zhang, P. Lv, C. Chu, X. Chen and G. Liu, *ACS Nano*, 2020, **14**, 2063–2076.
72 F. Wu, C. Pan, C.-T. He, Y. Han, W. Ma, H. Wei, W. Ji, W. Chen, J. Mao and P. Yu, *J. Am. Chem. Soc.*, 2020, **142**, 16861–16867.
73 Y. Wu, J. Wu, L. Jiao, W. Xu, H. Wang, X. Wei, W. Gu, G. Ren, N. Zhang and Q. Zhang, *Anal. Chem.*, 2020, **92**, 3373–3379.
74 R. Zhao, Z. Liang, S. Gao, C. Yang, B. Zhu, J. Zhao, C. Qu, R. Zou and Q. Xu, *Angew. Chem., Int. Ed.*, 2019, **58**, 1975–1979.
75 X. Wei, S. Song, W. Song, W. Xu, L. Jiao, X. Luo, N. Wu, H. Yan, X. Wang and W. Gu, *Anal. Chem.*, 2021, **93**, 5334–5342.
76 X. Lai, G. Zhang, L. Zeng, X. Xiao, J. Peng, P. Guo, W. Zhang and W. Lai, *ACS Appl. Mater. Interfaces*, 2020, **13**, 1413–1423.
77 C. B. Ma, Y. Xu, L. Wu, Q. Wang, J. J. Zheng, G. Ren, X. Wang, X. Gao, M. Zhou and M. Wang, *Angew. Chem., Int. Ed.*, 2022, **61**, e202116170.
78 J. Chen, X. Wei, H. Tang, J. C. Munyemana, M. Guan, S. Zhang and H. Qiu, *Talanta*, 2021, **222**, 121680.
79 M. Sharifi, S. H. Hosseinali, P. Yousefvand, A. Salihi, M. S. Shekha, F. M. Aziz, A. JouyaTalaei, A. Hasan and M. Falahati, *Mater. Sci. Eng., C*, 2020, **108**, 110422.
80 K. Fan, H. Wang, J. Xi, Q. Liu, X. Meng, D. Duan, L. Gao and X. Yan, *Chem. Commun.*, 2017, **53**, 424–427.

81 Q. Xin, X. Jia, A. Nawaz, W. Xie, L. Li and J. R. Gong, *Nano Res.*, 2020, **13**, 1427–1433.
82 Z. Fu, K. Fan, X. He, Q. Wang, J. Yuan, K. S. Lim, J.-N. Tang, F. Xie and X. Cui, *ACS Nano*, 2024, **18**, 12639–12671.
83 F. Meng, P. Zhu, L. Yang, L. Xia and H. Liu, *Chem. Eng. J.*, 2023, **452**, 139411.
84 Y. Wang, G. Jia, X. Cui, X. Zhao, Q. Zhang, L. Gu, L. Zheng, L. H. Li, Q. Wu and D. J. Singh, *Chem*, 2021, **7**, 436–449.
85 F. Meng, M. Peng, Y. Chen, X. Cai, F. Huang, L. Yang, X. Liu, T. Li, X. Wen and N. Wang, *Appl. Catal., B*, 2022, **301**, 120826.
86 J. Zhang, T. S. Wu, H. V. Thang, K. Y. Tseng, X. Hao, B. Xu, H. Y. T. Chen and Y. K. Peng, *Small*, 2022, **18**, 2104844.
87 Y. Qu, L. Wang, Z. Li, P. Li, Q. Zhang, Y. Lin, F. Zhou, H. Wang, Z. Yang and Y. Hu, *Adv. Mater.*, 2019, **31**, 1904496.
88 F.-Y. Kong, L. Yao, X.-Y. Lu, H.-Y. Li, Z.-X. Wang, H.-L. Fang and W. Wang, *Analyst*, 2020, **145**, 2191–2196.
89 Y. Wang, H. Li, L. Guo, Q. Jiang and F. Liu, *RSC Adv.*, 2019, **9**, 18815–18822.
90 K. Fan, J. Xi, L. Fan, P. Wang, C. Zhu, Y. Tang, X. Xu, M. Liang, B. Jiang and X. Yan, *Nat. Commun.*, 2018, **9**, 1440.
91 D. Wu, J. Li, S. Xu, Q. Xie, Y. Pan, X. Liu, R. Ma, H. Zheng, M. Gao and W. Wang, *J. Am. Chem. Soc.*, 2020, **142**, 19602–19610.
92 B. Xu, H. Wang, W. Wang, L. Gao, S. Li, X. Pan, H. Wang, H. Yang, X. Meng and Q. Wu, *Angew. Chem.*, 2019, **131**, 4965–4970.
93 S. Ji, B. Jiang, H. Hao, Y. Chen, J. Dong, Y. Mao, Z. Zhang, R. Gao, W. Chen and R. Zhang, *Nat. Catal.*, 2021, **4**, 407–417.
94 J. Mohammed-Ibrahim and X. Sun, *J. Energy Chem.*, 2019, **34**, 111–160.
95 R. Ge, J. Huo, T. Liao, Y. Liu, M. Zhu, Y. Li, J. Zhang and W. Li, *Appl. Catal., B*, 2020, **260**, 118196.
96 H. Yoon, H. J. Song, B. Ju and D.-W. Kim, *Nano Res.*, 2020, **13**, 2469–2477.
97 C. Jian, W. Hong, Q. Cai, J. Li and W. Liu, *Appl. Catal., B*, 2020, **266**, 118649.
98 K. Eiler, S. Suriñach, J. Sort and E. Pellicer, *Appl. Catal., B*, 2020, **265**, 118597.
99 M. Mohiuddin, A. Zavabeti, F. Haque, A. Mahmood, R. S. Datta, N. Syed, M. W. Khan, A. Jannat, K. Messalea and B. Y. Zhang, *J. Mater. Chem. A*, 2020, **8**, 2789–2797.
100 J. Xu, G. Shao, X. Tang, F. Lv, H. Xiang, C. Jing, S. Liu, S. Dai, Y. Li and J. Luo, *Nat. Commun.*, 2022, **13**, 2193.
101 G. Li, H. Jang, S. Liu, Z. Li, M. G. Kim, Q. Qin, X. Liu and J. Cho, *Nat. Commun.*, 2022, **13**, 1270.
102 M. Liu, J.-A. Wang, W. Klysubun, G.-G. Wang, S. Sattayaporn, F. Li, Y.-W. Cai, F. Zhang, J. Yu and Y. Yang, *Nat. Commun.*, 2021, **12**, 5260.
103 B. A. Yusuf, W. Yaseen, M. Xie, R. S. Zayyan, A. I. Muhammad, R. Nankya, J. Xie and Y. Xu, *Adv. Colloid Interface Sci.*, 2023, **311**, 102811.
104 W. Zhang, S. Hu, J.-J. Yin, W. He, W. Lu, M. Ma, N. Gu and Y. Zhang, *J. Am. Chem. Soc.*, 2016, **138**, 5860–5865.
105 Y. Liu, Y. Qing, L. Jing, W. Zou and R. Guo, *Langmuir*, 2021, **37**, 7364–7372.
106 H. Xia, N. Li, W. Huang, Y. Song and Y. Jiang, *ACS Appl. Mater. Interfaces*, 2021, **13**, 22240–22253.
107 F. Natalio, R. André, A. F. Hartog, B. Stoll, K. P. Jochum, R. Wever and W. Tremel, *Nat. Nanotechnol.*, 2012, **7**, 530–535.
108 C. Zhao, C. Xiong, X. Liu, M. Qiao, Z. Li, T. Yuan, J. Wang, Y. Qu, X. Wang and F. Zhou, *Chem. Commun.*, 2019, **55**, 2285–2288.
109 X. Shen, W. Liu, X. Gao, Z. Lu, X. Wu and X. Gao, *J. Am. Chem. Soc.*, 2015, **137**, 15882–15891.
110 Z. Gao, H. Wu, Z. Liu, L. Liu, Z. Zeng, X. Yang, H. Wang, J. Du, B. Zheng and Y. Guo, *ACS Appl. Nano Mater.*, 2023, **6**, 11531–11540.
111 J. Zhang, Y. Yang, F. Qin, T. Hu, X. Zhao, S. Zhao, Y. Cao, Z. Gao, Z. Zhou and R. Liang, *Adv. Healthcare Mater.*, 2023, **12**, 2302056.
112 J. Mu, L. Zhang, M. Zhao and Y. Wang, *J. Mol. Catal. A: Chem.*, 2013, **378**, 30–37.
113 N. Zhu, C. Liu, R. Liu, X. Niu, D. Xiong, K. Wang, D. Yin and Z. Zhang, *Anal. Chem.*, 2022, **94**, 4821–4830.
114 I. Chandio, Y. Ai, L. Wu and Q. Liang, *Nano Res.*, 2024, **17**, 39–64.
115 Z. Yu, X. Cao, S. Wang, H. Cui, C. Li and G. Zhu, *Water, Air, Soil Pollut.*, 2021, **232**, 1–19.
116 Z. Shu and Y. Cai, *J. Phys.: Condens. Matter*, 2023, **35**, 204001.
117 A. Bar-Hen, S. Hettler, A. Ramasubramaniam, R. Arenal, R. Bar-Ziv and M. B. Sadan, *J. Energy Chem.*, 2022, **74**, 481–488.
118 S. Zhang, X. J. Gao, Y. Ma, K. Song, M. Ge, S. Ma, L. Zhang, Y. Yuan, W. Jiang and Z. Wu, *Nat. Commun.*, 2024, **15**, 1–21.
119 N. Song, Z. Guo, S. Wang, Y. Li, Y. Liu, M. Zou and M. Liang, *Nano Res.*, 2024, **17**, 3942–3949.
120 K. Li, J. Hong, N. Song, Z. Guo and M. Liang, *Nano Res.*, 2024, **17**, 6888–6894.
121 R. Shwetharani, D. H. Nagaraju, R. G. Balakrishna and V. Suvina, *Mater. Lett.*, 2019, **248**, 39–42.
122 N. Song, Z. Guo, S. Wang, Y. Liu, M. Zou and M. Liang, *Available at SSRN* 4310470.
123 C. Li, Y. Wang, Y. Chen, H. Jia and W. He, *Mater. Today Sustain.*, 2023, **24**, 100537.
124 Q. Zhao, N. Kang, M. M. Moro, E. G. Cal, S. Moya, E. Coy, L. Salmon, X. Liu and D. Astruc, *ACS Appl. Energy Mater.*, 2022, **5**, 3834–3844.
125 Z. Li, X. Zhang, Y. Teng, H. Zhang, T. Xu and F. Teng, *ACS Appl. Mater. Interfaces*, 2024, **16**, 61921–61933.
126 X. Li, H. Lei, L. Xie, N. Wang, W. Zhang and R. Cao, *Acc. Chem. Res.*, 2022, **55**, 878–892.
127 X. Chen, C. Zhu, Y. Xu, K. Wang, X. Cao, Y. Shen, S. Liu and Y. Zhang, *Catal. Sci. Technol.*, 2021, **11**, 7255–7259.
128 Y. Xu, Z. Zhou, N. Deng, K. Fu, C. Zhu, Q. Hong, Y. Shen, S. Liu and Y. Zhang, *Sci. China: Chem.*, 2023, **66**, 1318–1335.

129 N.-I. Kim, Y. J. Sa, T. S. Yoo, S. R. Choi, R. A. Afzal, T. Choi, Y.-S. Seo, K.-S. Lee, J. Y. Hwang and W. S. Choi, *Sci. Adv.*, 2018, **4**, eaap9360.
130 X. F. Lu, B. Y. Xia, S. Q. Zang and X. W. Lou, *Angew. Chem.*, 2020, **132**, 4662–4678.
131 J. Liu, M. Jiao, L. Lu, H. M. Barkholtz, Y. Li, Y. Wang, L. Jiang, Z. Wu, D.-j. Liu and L. Zhuang, *Nat. Commun.*, 2017, **8**, 15938.
132 H. Zhang, W. Zhou, T. Chen, B. Y. Guan, Z. Li and X. W. D. Lou, *Energy Environ. Sci.*, 2018, **11**, 1980–1984.
133 Y. Han, Y. Wang, R. Xu, W. Chen, L. Zheng, A. Han, Y. Zhu, J. Zhang, H. Zhang and J. Luo, *Energy Environ. Sci.*, 2018, **11**, 2348–2352.
134 Y. Chen, S. Ji, S. Zhao, W. Chen, J. Dong, W.-C. Cheong, R. Shen, X. Wen, L. Zheng and A. I. Rykov, *Nat. Commun.*, 2018, **9**, 5422.
135 Z. P. Wu, X. F. Lu, S. Q. Zang and X. W. Lou, *Adv. Funct. Mater.*, 2020, **30**, 1910274.
136 L. Cao, Q. Luo, J. Chen, L. Wang, Y. Lin, H. Wang, X. Liu, X. Shen, W. Zhang and W. Liu, *Nat. Commun.*, 2019, **10**, 4849.
137 H. Zhang, Y. Liu, T. Chen, J. Zhang, J. Zhang and X. W. Lou, *Adv. Mater.*, 2019, **31**, 1904548.
138 J. Guan, Z. Duan, F. Zhang, S. D. Kelly, R. Si, M. Dupuis, Q. Huang, J. Q. Chen, C. Tang and C. Li, *Nat. Catal.*, 2018, **1**, 870–877.
139 J. Chen, Q. Ma, X. Zheng, Y. Fang, J. Wang and S. Dong, *Nat. Commun.*, 2022, **13**, 2808.
140 Y. Zhou, N. Jin, Y. Ma, Y. Cui, L. Wang, Y. Kwon, W.-K. Lee, W. Zhang, H. Ge and J. Zhang, *Adv. Mater.*, 2023, **35**, 2209500.
141 B. Ni, K. Wang, T. He, Y. Gong, L. Gu, J. Zhuang and X. Wang, *Adv. Energy Mater.*, 2018, **8**, 1702313.
142 X. Lin, S. Cao, X. Chen, H. Chen, Z. Wang, H. Liu, H. Xu, S. Liu, S. Wei and X. Lu, *Adv. Funct. Mater.*, 2022, **32**, 2202072.
143 C. Du, Y. Gao, H. Chen, P. Li, S. Zhu, J. Wang, Q. He and W. Chen, *J. Mater. Chem. A*, 2020, **8**, 16994–17001.
144 X. Cao, C. Zhu, Q. Hong, X. Chen, K. Wang, Y. Shen, S. Liu and Y. Zhang, *Angew. Chem.*, 2023, **135**, e202302463.
145 H. Zhang, L. Huang, J. Chen, L. Liu, X. Zhu, W. Wu and S. Dong, *Nano Energy*, 2021, **83**, 105798.
146 P. Ling, S. Cheng, N. Chen, C. Qian and F. Gao, *ACS Appl. Mater. Interfaces*, 2020, **12**, 17185–17192.
147 Z. Lu, G. Chen, S. Siahrostami, Z. Chen, K. Liu, J. Xie, L. Liao, T. Wu, D. Lin, Y. Liu, T. F. Jaramillo, J. K. Nørskov and Y. Cui, *Nat. Catal.*, 2018, **1**, 156–162.
148 R. Shen, W. Chen, Q. Peng, S. Lu, L. Zheng, X. Cao, Y. Wang, W. Zhu, J. Zhang, Z. Zhuang, C. Chen, D. Wang and Y. Li, *Chem*, 2019, **5**, 2099–2110.
149 C. H. Choi, M. Kim, H. C. Kwon, S. J. Cho, S. Yun, H.-T. Kim, K. J. Mayrhofer, H. Kim and M. Choi, *Nat. Commun.*, 2016, **7**, 10922.
150 L. A. Curtiss, K. Raghavachari, P. C. Redfern and J. A. Pople, *J. Chem. Phys.*, 1997, **106**, 1063–1079.
151 K. P. Kuhl, E. R. Cave, D. N. Abram and T. F. Jaramillo, *Energy Environ. Sci.*, 2012, **5**, 7050–7059.
152 X. Zhang, S.-X. Guo, K. A. Gandionco, A. M. Bond and J. Zhang, *Mater. Today Adv.*, 2020, **7**, 100074.
153 J. Greeley, *Annu. Rev. Chem. Biomol. Eng.*, 2016, **7**, 605–635.
154 A. Vasileff, C. Xu, Y. Jiao, Y. Zheng and S.-Z. Qiao, *Chem*, 2018, **4**, 1809–1831.
155 F. Franco, C. Rettenmaier, H. S. Jeon and B. R. Cuenya, *Chem. Soc. Rev.*, 2020, **49**, 6884–6946.
156 R. Reske, H. Mistry, F. Behafarid, B. R. Cuenya and P. Strasser, *J. Am. Chem. Soc.*, 2014, **136**, 6978–6986.
157 D. Gao, H. Zhou, J. Wang, S. Miao, F. Yang, G. Wang, J. Wang and X. Bao, *J. Am. Chem. Soc.*, 2015, **137**, 4288–4291.
158 J. Lee, H. Choi, J. Mun, E. Jin, S. Lee, J. Nam, M. Umer, J. Cho, G. Lee, Y. Kwon and W. Choe, *Small Struct.*, 2023, **4**, 2200087.
159 X. Cui, H. Bai, J. Zhang, R. Liu, H. Yu, Y. Wang, T. Kong, M.-Y. Gao, Z. Lu and Y. Xiong, *Nat. Commun.*, 2024, **15**, 9048.
160 S. Ni, W. Lyu, Z. Ji, L. Wang, M. Wang, C. He, K. Wang, Y. Guan, K. Wei and X. Pan, *J. Cleaner Prod.*, 2025, **501**, 145283.
161 H. Mistry, R. Reske, Z. Zeng, Z.-J. Zhao, J. Greeley, P. Strasser and B. R. Cuenya, *J. Am. Chem. Soc.*, 2014, **136**, 16473–16476.
162 X. Li, S. Shi, Y. Deng, M. Zu, H. Zhang and S. Ma, *ACS Sustainable Chem. Eng.*, 2025, 13219–13226.
163 J. Pascual-Colino, Q. J. S. Virpurwala, S. Mena-Gutiérrez, S. Pérez-Yáñez, A. Luque, G. Beobide, V. K. Velisoju, P. Castaño and O. Castillo, *Inorg. Chem.*, 2023, **62**, 17444–17453.
164 J. Chen, Q. Ma, M. Li, D. Chao, L. Huang, W. Wu, Y. Fang and S. Dong, *Nat. Commun.*, 2021, **12**, 3375.
165 L. Fan, D. Lou, H. Wu, X. Zhang, Y. Zhu, N. Gu and Y. Zhang, *Adv. Mater. Interfaces*, 2018, **5**, 1801070.
166 H. Y. Kim, J. Song, K. S. Park and H. G. Park, *Chem. Commun.*, 2020, **56**, 8912–8915.
167 X. Xiao, H.-q. Xia, R. Wu, L. Bai, L. Yan, E. Magner, S. Cosnier, E. Lojou, Z. Zhu and A. Liu, *Chem. Rev.*, 2019, **119**, 9509–9558.
168 T. Pirmohamed, J. M. Dowding, S. Singh, B. Wasserman, E. Heckert, A. S. Karakoti, J. E. King, S. Seal and W. T. Self, *Chem. Commun.*, 2010, **46**, 2736–2738.
169 T. N. Vo, T. D. Tran, H. K. Nguyen, D. Y. Kong, M. I. Kim and I. T. Kim, *Mater. Lett.*, 2020, **281**, 128662.
170 X. Xu, J. Wang, R. Huang, W. Qi, R. Su and Z. He, *Catal. Sci. Technol.*, 2021, **11**, 3402–3410.
171 H. Guo, H. Yin, X. Yan, S. Shi, Q. Yu, Z. Cao and J. Li, *Sci. Rep.*, 2016, **6**, 39162.
172 M. Zhiani, S. Barzi, M. Gholamian and A. Ahmadi, *Int. J. Hydrogen Energy*, 2020, **45**, 13496–13507.
173 X. Zhang, X. Chen and Y. Zhao, *Nano-Micro Lett.*, 2022, **14**, 95.
174 X. Wei, J. Guo, H. Lian, X. Sun and B. Liu, *Sens. Actuators, B*, 2021, **329**, 129205.

175 G. J. Soufi, P. Iravani, A. Hekmatnia, E. Mostafavi, M. Khatami and S. Iravani, *Comments Inorg. Chem.*, 2022, **42**, 174–207.
176 A. Thamilselvan and M. I. Kim, *TrAC, Trends Anal. Chem.*, 2024, 117815.
177 Y. Xiang, T. Liu, B. Jia, L. Zhang and X. Su, *Biosens. Bioelectron.*, 2023, **220**, 114895.
178 D. Hu, H. Chen, Q. Su, J.-R. Zhang, L. Wang and J.-J. Zhu, *J. Power Sources*, 2025, **643**, 237050.
179 Z. Li, M. Wang, Y. Zhang, Z. Bian, X. Liu, L. Bai and A. Liu, *Microchem. J.*, 2025, **216**, 114676.
180 Y. Li, X. Li, M. Yang, R. Wang, J. Li, G. Cui, Y. Zhao and H. Wang, *Electrochim. Acta*, 2024, **495**, 144491.
181 R. Franz, E. A. Uslamin and E. A. Pidko, *Mendeleev Commun.*, 2021, **31**, 584–592.
182 M. S. A. S. Shah, C. Oh, H. Park, Y. J. Hwang, M. Ma and J. H. Park, *Adv. Sci.*, 2020, **7**, 2001946.
183 A. R. Kulkarni, Z.-J. Zhao, S. Siahrostami, J. K. Nørskov and F. Studt, *Catal. Sci. Technol.*, 2018, **8**, 114–123.
184 Q. Zhang, J. Yu and A. Corma, *Adv. Mater.*, 2020, **32**, 2002927.
185 Y. Li and J. Yu, *Nat. Rev. Mater.*, 2021, **6**, 1156–1174.
186 G. Zhao, M. Drewery, J. Mackie, T. Oliver, E. M. Kennedy and M. Stockenhuber, *Energy Technol.*, 2020, **8**, 1900665.
187 N. J. Gunsalus, A. Koppaka, S. H. Park, S. M. Bischof, B. G. Hashiguchi and R. A. Periana, *Chem. Rev.*, 2017, **117**, 8521–8573.
188 N. F. Dummer, D. J. Willock, Q. He, M. J. Howard, R. J. Lewis, G. Qi, S. H. Taylor, J. Xu, D. Bethell, C. J. Kiely and G. J. Hutchings, *Chem. Rev.*, 2023, **123**, 6359–6411.
189 M. Ahlquist, R. J. Nielsen, R. A. Periana and W. A. Goddard III, *J. Am. Chem. Soc.*, 2009, **131**, 17110–17115.
190 K. Otsuka and Y. Wang, *Appl. Catal., A*, 2001, **222**, 145–161.
191 C. Hammond, M. M. Forde, M. H. A. Rahim, A. Thetford, Q. He, R. L. Jenkins, N. Dimitratos, J. A. Lopez-Sanchez, N. F. Dummer, D. M. Murphy, A. F. Carley, S. H. Taylor, D. J. Willock, E. E. Stangland, J. Kang, H. Hagen, C. J. Kiely and G. J. Hutchings, *Angew. Chem., Int. Ed.*, 2012, **51**, 5129–5133.
192 R. A. Periana, D. J. Taube, S. Gamble, H. Taube, T. Satoh and H. Fujii, *Science*, 1998, **280**, 560–564.
193 J. Colby, D. I. Stirling and H. Dalton, *Biochem. J.*, 1977, **165**, 395–402.
194 A. V. Marenich, S. V. Jerome, C. J. Cramer and D. G. Truhlar, *J. Chem. Theory Comput.*, 2012, **8**, 527–541.
195 A. A. Latimer, A. Kakekhani, A. R. Kulkarni and J. K. Nørskov, *ACS Catal.*, 2018, **8**, 6894–6907.
196 F. Sastre, V. Fornés, A. Corma and H. García, *J. Am. Chem. Soc.*, 2011, **133**, 17257–17261.
197 Y. Hu, L. Dai, D. Liu, W. Du and Y. Wang, *Renewable Sustainable Energy Rev.*, 2018, **91**, 793–801.
198 S. K. Kaiser, Z. Chen, D. F. Akl, S. Mitchell and J. Pérez-Ramírez, *Chem. Rev.*, 2020, **120**, 11703–11809.
199 R. J. White, R. Luque, V. L. Budarin, J. H. Clark and D. J. Macquarrie, *Chem. Soc. Rev.*, 2009, **38**, 481–494.
200 Q.-L. Zhu and Q. Xu, *Chem*, 2016, **1**, 220–245.
201 J. Baek, B. Rungtaweevoranit, X. Pei, M. Park, S. C. Fakra, Y.-S. Liu, R. Matheu, S. A. Alshmimri, S. Alshehri, C. A. Trickett, G. A. Somorjai and O. M. Yaghi, *J. Am. Chem. Soc.*, 2018, **140**, 18208–18216.
202 H. Lee, C. Kwon, C. Keum, H.-E. Kim, H. Lee, B. Han and S.-Y. Lee, *Chem. Eng. J.*, 2022, **450**, 138472.
203 M. Ren, Q. Shi, L. Mi, W. Liang, M. Yuan, L. Wang, Z. Gao, W. Huang, J. Huang and Z. Zuo, *Mater. Today Sustain.*, 2021, **11–12**, 100061.
204 M. Xia, L. Qiu, Y. Li, T. Shen, Z. Sui, L. Feng and Q. Chen, *Mater. Lett.*, 2022, **307**, 131078.
205 G. Xu, A. Yu, Y. Xu and C. Sun, *Catal. Commun.*, 2021, **158**, 106338.
206 T. Ikuno, J. Zheng, A. Vjunov, M. Sanchez-Sanchez, M. A. Ortuño, D. R. Pahls, J. L. Fulton, D. M. Camaioni, Z. Li, D. Ray, B. L. Mehdi, N. D. Browning, O. K. Farha, J. T. Hupp, C. J. Cramer, L. Gagliardi and J. A. Lercher, *J. Am. Chem. Soc.*, 2017, **139**, 10294–10301.
207 J. N. Hall and P. Bollini, *Chem. – Eur. J.*, 2020, **26**, 16639–16643.
208 T. Imyen, E. Znoutine, D. Suttipat, P. Iadrat, P. Kidkhunthod, S. Bureekaew and C. Wattanakit, *ACS Appl. Mater. Interfaces*, 2020, **12**, 23812–23821.
209 H. Zhou, T. Liu, X. Zhao, Y. Zhao, H. Lv, S. Fang, X. Wang, F. Zhou, Q. Xu, J. Xu, C. Xiong, Z. Xue, K. Wang, W.-C. Cheong, W. Xi, L. Gu, T. Yao, S. Wei, X. Hong, J. Luo, Y. Li and Y. Wu, *Angew. Chem., Int. Ed.*, 2019, **58**, 18388–18393.
210 B. Wu, R. Yang, L. Shi, T. Lin, X. Yu, M. Huang, K. Gong, F. Sun, Z. Jiang and S. Li, *Chem. Commun.*, 2020, **56**, 14677–14680.
211 P. Xie, J. Ding, Z. Yao, T. Pu, P. Zhang, Z. Huang, C. Wang, J. Zhang, N. Zecher-Freeman and H. Zong, *Nat. Commun.*, 2022, **13**, 1375.
212 M. Chauhan, B. Rana, P. Gupta, R. Kalita, C. Thadhani and K. Manna, *Nat. Commun.*, 2024, **15**, 9798.
213 P. Zhang, D. Sun, A. Cho, S. Weon, S. Lee, J. Lee, J. W. Han, D.-P. Kim and W. Choi, *Nat. Commun.*, 2019, **10**, 940.
214 L. Jiao, W. Ye, Y. Kang, Y. Zhang, W. Xu, Y. Wu, W. Gu, W. Song, Y. Xiong and C. Zhu, *Nano Res.*, 2022, **15**, 959–964.
215 J. Shen, J. Chen, Y. Qian, X. Wang, D. Wang, H. Pan and Y. Wang, *Adv. Mater.*, 2024, **36**, 2313406.
216 H. Wei and E. Wang, *Chem. Soc. Rev.*, 2013, **42**, 6060–6093.
217 E. Kuah, S. Toh, J. Yee, Q. Ma and Z. Gao, *Chem. – Eur. J.*, 2016, **22**, 8404–8430.
218 F. Mancin, L. J. Prins, P. Pengo, L. Pasquato, P. Tecilla and P. Scrimin, *Molecules*, 2016, **21**, 1014.
219 F. Yu, Y. Huang, A. J. Cole and V. C. Yang, *Biomaterials*, 2009, **30**, 4716–4722.

220 J. Sang, R. Wu, P. Guo, J. Du, S. Xu and J. Wang, *J. Appl. Polym. Sci.*, 2016, **133**, 43065.
221 B. Liu and J. Liu, *Nano Res.*, 2017, **10**, 1125–1148.
222 Y. Gao, Z. Wei, F. Li, Z. M. Yang, Y. M. Chen, M. Zrinyi and Y. Osada, *Green Chem.*, 2014, **16**, 1255–1261.
223 M. Huo, L. Wang, Y. Wang, Y. Chen and J. Shi, *ACS Nano*, 2019, **13**, 2643–2653.
224 G. Wu, X. Zheng, P. Cui, H. Jiang, X. Wang, Y. Qu, W. Chen, Y. Lin, H. Li and X. Han, *Nat. Commun.*, 2019, **10**, 4855.
225 J. He, F. Xu, J. Hu, S. Wang, X. Hou and Z. Long, *Microchem. J.*, 2017, **135**, 91–99.
226 Y. Zhou, Y. Wei, J. Ren and X. Qu, *Mater. Horiz.*, 2020, **7**, 3291–3297.
227 S. Li, X. Zhu, H. Liu and B. Sun, *Coord. Chem. Rev.*, 2024, **518**, 216046.
228 M. Feng, Q. Zhang, X. Chen, D. Deng, X. Xie and X. Yang, *Biosens. Bioelectron.*, 2022, **210**, 114294.
229 X. Wang, Q. Shi, Z. Zha, D. Zhu, L. Zheng, L. Shi, X. Wei, L. Lian, K. Wu and L. Cheng, *Bioact. Mater.*, 2021, **6**, 4389–4401.
230 H. Song, M. Zhang and W. Tong, *Molecules*, 2022, **27**, 5426.
231 H.-l. Liu, F. Nosheen and X. Wang, *Chem. Soc. Rev.*, 2015, **44**, 3056–3078.
232 A. Amiri, V. Yurkiv, A. H. Phakatkar, T. Shokuhfar and R. Shahbazian-Yassar, *Adv. Funct. Mater.*, 2024, **34**, 2304685.
233 H. Cheng, C. Wang, D. Qin and Y. Xia, *Acc. Chem. Res.*, 2023, **56**, 900–909.
234 R. Ferrando, J. Jellinek and R. L. Johnston, *Chem. Rev.*, 2008, **108**, 845–910.
235 S. Li, L. Shang, B. Xu, S. Wang, K. Gu, Q. Wu, Y. Sun, Q. Zhang, H. Yang and F. Zhang, *Angew. Chem.*, 2019, **131**, 12754–12761.
236 M. Zhou, C. Li and J. Fang, *Chem. Rev.*, 2020, **121**, 736–795.
237 X. Meng, H. Fan, L. Chen, J. He, C. Hong, J. Xie, Y. Hou, K. Wang, X. Gao and L. Gao, *Nat. Commun.*, 2024, **15**, 1626.
238 L. Kong, D. Chen, X. Zhang, L. Zhou, Y. Deng and S. Wei, *ACS Appl. Nano Mater.*, 2023, **6**, 3618–3626.
239 J. Liu, S. Dong, S. Gai, Y. Dong, B. Liu, Z. Zhao, Y. Xie, L. Feng, P. Yang and J. Lin, *ACS Nano*, 2023, **17**, 20402–20423.
240 D. Yan, L. Jiao, C. Chen, X. Jia, R. Li, L. Hu, X. Li, Y. Zhai, P. E. Strizhak and Z. Zhu, *Nano Lett.*, 2024, **24**, 2912–2920.
241 L. Zheng, L. Xu, P. Gu and Y. Chen, *Nanoscale*, 2024, **16**, 8672–8672.
242 Y. Zhu, R. Zhao, L. Feng, C. Wang, S. Dong, M. V. Zyuzin, A. Timin, N. Hu, B. Liu and P. Yang, *ACS Nano*, 2023, **17**, 6833–6848.
243 S. Xia, F. Wu, L. Cheng, H. Bao, W. Gao, J. Duan, W. Niu and G. Xu, *Small*, 2023, **19**, 2205997.
244 J. Liu, C. Lee, Y. Hu, Z. Liang, R. Ji, X. Y. D. Soo, Q. Zhu and Q. Yan, *SmartMat*, 2023, **4**, e1210.
245 H.-S. Chen, T. M. Benedetti, V. R. Gonçales, N. M. Bedford, R. W. Scott, R. F. Webster, S. Cheong, J. J. Gooding and R. D. Tilley, *J. Am. Chem. Soc.*, 2020, **142**, 3231–3239.
246 S. Han, C. He, Q. Yun, M. Li, W. Chen, W. Cao and Q. Lu, *Coord. Chem. Rev.*, 2021, **445**, 214085.
247 Y. Tang, Y. Chen, Y. Wu, W. Xu, Z. Luo, H.-R. Ye, W. Gu, W. Song, S. Guo and C. Zhu, *Nano Lett.*, 2022, **23**, 267–275.
248 Y. Zhu, X. Wang, L. Feng, R. Zhao, C. Yu, Y. Liu, Y. Xie, B. Liu, Y. Zhou and P. Yang, *Nat. Commun.*, 2024, **15**, 8696.
249 C. Zhan, Y. Xu, L. Bu, H. Zhu, Y. Feng, T. Yang, Y. Zhang, Z. Yang, B. Huang and Q. Shao, *Nat. Commun.*, 2021, **12**, 6261.
250 F. Lin, M. Li, L. Zeng, M. Luo and S. Guo, *Chem. Rev.*, 2023, **123**, 12507–12593.
251 J.-T. Ren, L. Chen, H.-Y. Wang and Z.-Y. Yuan, *Chem. Soc. Rev.*, 2023, **52**, 8319–8373.
252 X. Chang, M. Zeng, K. Liu and L. Fu, *Adv. Mater.*, 2020, **32**, 1907226.
253 Y. Zhang, D. Wang and S. Wang, *Small*, 2022, **18**, 2104339.
254 Y. Ai, M. Q. He, H. Sun, X. Jia, L. Wu, X. Zhang, H. b. Sun and Q. Liang, *Adv. Mater.*, 2023, **35**, 2302335.
255 R. Sheng, Y. Liu, T. Cai, R. Wang, G. Yang, T. Wen, F. Ning and H. Peng, *Chem. Eng. J.*, 2024, **485**, 149913.
256 J. Feng, X. Yang, T. Du, L. Zhang, P. Zhang, J. Zhuo, L. Luo, H. Sun, Y. Han and L. Liu, *Adv. Sci.*, 2023, **10**, 2303078.
257 X. Wang, C. Shu, G. Wang, P. Han, L. Zheng, L. Xu and Y. Chen, *Nanoscale*, 2025, 10557–10580.
258 J. Wan, W. Chen, C. Jia, L. Zheng, J. Dong, X. Zheng, Y. Wang, W. Yan, C. Chen and Q. Peng, *Adv. Mater.*, 2018, **30**, 1705369.
259 S. Kitagawa, R. Kitaura and S. i. Noro, *Angew. Chem., Int. Ed.*, 2004, **43**, 2334–2375.
260 J. H. Cavka, S. Jakobsen, U. Olsbye, N. Guillou, C. Lamberti, S. Bordiga and K. P. Lillerud, *J. Am. Chem. Soc.*, 2008, **130**, 13850–13851.
261 M. Taddei, *Coord. Chem. Rev.*, 2017, **343**, 1–24.
262 J. E. Mondloch, W. Bury, D. Fairen-Jimenez, S. Kwon, E. J. DeMarco, M. H. Weston, A. A. Sarjeant, S. T. Nguyen, P. C. Stair and R. Q. Snurr, *J. Am. Chem. Soc.*, 2013, **135**, 10294–10297.
263 N. C. Burtch, H. Jasuja and K. S. Walton, *Chem. Rev.*, 2014, **114**, 10575–10612.
264 C. L. Hobday, R. J. Marshall, C. F. Murphie, J. Sotelo, T. Richards, D. R. Allan, T. Düren, F. X. Coudert, R. S. Forgan and C. A. Morrison, *Angew. Chem.*, 2016, **128**, 2447–2451.
265 L. Valenzano, B. Civalleri, S. Chavan, S. Bordiga, M. H. Nilsen, S. Jakobsen, K. P. Lillerud and C. Lamberti, *Chem. Mater.*, 2011, **23**, 1700–1718.
266 H. Wu, Y. S. Chua, V. Krungleviciute, M. Tyagi, P. Chen, T. Yildirim and W. Zhou, *J. Am. Chem. Soc.*, 2013, **135**, 10525–10532.

267 Z. Fang, B. Bueken, D. E. De Vos and R. A. Fischer, *Angew. Chem., Int. Ed.*, 2015, **54**, 7234–7254.
268 W. Xiang, Y. Zhang, Y. Chen, C.-j. Liu and X. Tu, *J. Mater. Chem. A*, 2020, **8**, 21526–21546.
269 J. He, N. Li, Z. G. Li, M. Zhong, Z. X. Fu, M. Liu, J. C. Yin, Z. Shen, W. Li and J. Zhang, *Adv. Funct. Mater.*, 2021, **31**, 2103597.
270 T. Li, Y. Bao, H. Qiu and W. Tong, *Anal. Chim. Acta*, 2021, **1152**, 338299.
271 G. Ye, Y. Gu, W. Zhou, W. Xu and Y. Sun, *ACS Catal.*, 2020, **10**, 2384–2394.
272 J. Wang, L. Liu, C. Chen, X. Dong, Q. Wang, L. Alfilfil, M. R. AlAlouni, K. Yao, J. Huang and D. Zhang, *J. Mater. Chem. A*, 2020, **8**, 4464–4472.
273 Z. Xue, K. Liu, Q. Liu, Y. Li, M. Li, C.-Y. Su, N. Ogiwara, H. Kobayashi, H. Kitagawa and M. Liu, *Nat. Commun.*, 2019, **10**, 5048.
274 X. Zhang, Z. Zhang, J. Boissonnault and S. M. Cohen, *Chem. Commun.*, 2016, **52**, 8585–8588.
275 S. M. Cohen, *J. Am. Chem. Soc.*, 2017, **139**, 2855–2863.
276 P. Yang, F. Mao, Y. Li, Q. Zhuang and J. Gu, *Chem. – Eur. J.*, 2018, **24**, 2962–2970.
277 G. G. Chang, X. C. Ma, Y. X. Zhang, L. Y. Wang, G. Tian, J. W. Liu, J. Wu, Z. Y. Hu, X. Y. Yang and B. Chen, *Adv. Mater.*, 2019, **31**, 1904969.
278 X. Ma, L. Wang, Q. Zhang and H. L. Jiang, *Angew. Chem., Int. Ed.*, 2019, **58**, 12175–12179.
279 Y. Wang, L. Jin, C. Wang and Y. Du, *Colloids Surf., A*, 2020, **587**, 124257.
280 H. Kim, N. Kim and J. Ryu, *Inorg. Chem. Front.*, 2021, **8**, 4107–4148.
281 S. Wang, X. Xia and F. E. Chen, *Adv. Mater. Interfaces*, 2022, **9**, 2200874.
282 J. Gan, A. R. Bagheri, N. Aramesh, I. Gul, M. Franco, Y. Q. Almulaiky and M. Bilal, *Int. J. Biol. Macromol.*, 2021, **167**, 502–515.
283 L. Zhang, Z. Liu, Q. Deng, Y. Sang, K. Dong, J. Ren and X. Qu, *Angew. Chem., Int. Ed.*, 2021, **60**, 3469–3474.
284 X.-S. Wang, M. Chrzanowski, D. Yuan, B. S. Sweeting and S. Ma, *Chem. Mater.*, 2014, **26**, 1639–1644.
285 G. Li, W. Ma, Y. Yang, C. Zhong, H. Huang, D. Ouyang, Y. He, W. Tian, J. Lin and Z. Lin, *ACS Appl. Mater. Interfaces*, 2021, **13**, 49482–49489.
286 Y. Peng, M. Huang, L. Chen, C. Gong, N. Li, Y. Huang and C. Cheng, *Nano Res.*, 2022, **15**, 8783–8790.
287 D.-M. Liu and C. Dong, *Process Biochem.*, 2020, **92**, 464–475.
288 T. Jesionowski, J. Zdarta and B. Krajewska, *Adsorption*, 2014, **20**, 801–821.
289 H. Mo, J. Qiu, C. Yang, L. Zang and E. Sakai, *Cellulose*, 2020, **27**, 4963–4973.
290 C.-P. Zhao, S.-J. Yin, G.-Y. Chen, Y. Wang, H. Chen, J. Zhao and F.-Q. Yang, *J. Pharm. Biomed. Anal.*, 2021, **193**, 113743.
291 B. J. Kalita and N. Sit, *Food Sci. Biotechnol.*, 2024, **33**, 1163–1175.
292 N. Shi, M. Zheng, X. Wu, N. Chen, L. Jiang, B. Chang, F. Lu and F. Liu, *J. Agric. Food Chem.*, 2023, **71**, 13401–13408.
293 J. Ouyang, S. Pu, J. Wang, Y. Deng, C. Yang, S. Naseer and D. Li, *Process Biochem.*, 2020, **99**, 187–195.
294 F. L. Oliveira, A. de S. França, A. M. de Castro, R. O. A. de Souza, P. M. Esteves and R. S. B. Gonçalves, *ChemPlusChem*, 2020, **85**, 2051–2066.
295 P.-C. Kuo, Z.-X. Lin, T.-Y. Wu, C.-H. Hsu, H.-P. Lin and T.-S. Wu, *RSC Adv.*, 2021, **11**, 10010–10017.
296 J. S. Souza, F. T. Hirata and P. Corio, *J. Nanopart. Res.*, 2019, **21**, 35.
297 S. J. Lee, H. Jang and D. N. Lee, *Pharmaceutics*, 2022, **14**, 1887.
298 S. Sasidharan, S. Pc, N. Chaudhary and V. Ramakrishnan, *Sci. Rep.*, 2017, **7**, 17335.
299 S. Sasidharan, S. Ghosh, R. Sreedhar, K. Kumari, S. Thota and V. Ramakrishnan, *J. Phys. Chem. C*, 2022, **126**, 8511–8518.
300 J. Ge, J. Lei and R. N. Zare, *Nat. Nanotechnol.*, 2012, **7**, 428–432.
301 Z. Lei, C. Gao, L. Chen, Y. He, W. Ma and Z. Lin, *J. Mater. Chem. B*, 2018, **6**, 1581–1594.
302 C. Altinkaynak, S. Tavlasoglu and I. Ocsoy, *Enzyme Microb. Technol.*, 2016, **93**, 105–112.
303 M. B. Majewski, A. J. Howarth, P. Li, M. R. Wasielewski, J. T. Hupp and O. K. Farha, *CrystEngComm*, 2017, **19**, 4082–4091.
304 K. Liang, C. J. Coghlan, S. G. Bell, C. Doonan and P. Falcaro, *Chem. Commun.*, 2016, **52**, 473–476.
305 M. Bilal, M. Adeel, T. Rasheed and H. M. Iqbal, *J. Mater. Res. Technol.*, 2019, **8**, 2359–2371.
306 S. Liang, X.-L. Wu, J. Xiong, M.-H. Zong and W.-Y. Lou, *Coord. Chem. Rev.*, 2020, **406**, 213149.
307 S. Kempahanumakkagari, V. Kumar, P. Samaddar, P. Kumar, T. Ramakrishnappa and K.-H. Kim, *Biotechnol. Adv.*, 2018, **36**, 467–481.
308 C. Wang and K. Liao, *ACS Appl. Mater. Interfaces*, 2021, **13**, 56752–56776.
309 S. S. Nadar, L. Vaidya and V. K. Rathod, *Int. J. Biol. Macromol.*, 2020, **149**, 861–876.
310 Y. Ai, Z. N. Hu, X. Liang, H. b. Sun, H. Xin and Q. Liang, *Adv. Funct. Mater.*, 2022, **32**, 2110432.
311 C. Peng, R. Pang, J. Li and E. Wang, *Adv. Mater.*, 2024, **36**, 2211724.
312 S. Yadav and P. K. Maurya, in *Nanobioanalytical Approaches to Medical Diagnostics*, Elsevier, 2022, pp. 255–284.
313 L. Li, Y. Hu, Y. Shi, Y. Liu, T. Liu, H. Zhou, W. Niu, L. Zhang, J. Zhang and G. Xu, *Chem. Eng. J.*, 2023, **463**, 142494.
314 Z. Wang, Y. Zhang, E. Ju, Z. Liu, F. Cao, Z. Chen, J. Ren and X. Qu, *Nat. Commun.*, 2018, **9**, 3334.
315 J. Zhang, E. Ha, D. Li, S. He, L. Wang, S. Kuang and J. Hu, *J. Mater. Chem. B*, 2023, **11**, 4274–4286.
316 J. Ye, W. Lv, C. Li, S. Liu, X. Yang, J. Zhang, C. Wang, J. Xu, G. Jin and B. Li, *Adv. Funct. Mater.*, 2022, **32**, 2206157.

317 F. Gong, N. Yang, Y. Wang, M. Zhuo, Q. Zhao, S. Wang, Y. Li, Z. Liu, Q. Chen and L. Cheng, *Small*, 2020, **16**, 2003496.
318 Y. K. Jung, J. I. Kim and J.-K. Lee, *J. Am. Chem. Soc.*, 2010, **132**, 178–184.
319 D. Ito, S. Yokoyama, T. Zaikova, K. Masuko and J. E. Hutchison, *ACS Nano*, 2014, **8**, 64–75.
320 R. Zhao, Y. Zhu, J. Zhou, B. Liu, Y. Du, S. Gai, R. Shen, L. Feng and P. Yang, *ACS Nano*, 2022, **16**, 10904–10917.
321 D. Jana, D. Wang, A. K. Bindra, Y. Guo, J. Liu and Y. Zhao, *ACS Nano*, 2021, **15**, 7774–7782.
322 Y. Liu, X. Tian, Y.-C. Han, Y. Chen and W. Hu, *Chin. J. Catal.*, 2023, **48**, 66–89.
323 W. Shi, H. Liu, Z. Li, C. Li, J. Zhou, Y. Yuan, F. Jiang, K. Fu and Y. Yao, *SusMat*, 2022, **2**, 186–196.
324 C. Wu, Y. Fu, Y. Zeng, G. Chen, X. Pan, F. Lin, L. Xu, Q. Chen, D. Sun and Z. Hai, *Chem. Eng. J.*, 2023, **463**, 142518.
325 Y. Yao, Z. Huang, P. Xie, S. D. Lacey, R. J. Jacob, H. Xie, F. Chen, A. Nie, T. Pu and M. Rehwoldt, *Science*, 2018, **359**, 1489–1494.
326 M. Cui, C. Yang, S. Hwang, M. Yang, S. Overa, Q. Dong, Y. Yao, A. H. Brozena, D. A. Cullen and M. Chi, *Sci. Adv.*, 2022, **8**, eabm4322.
327 X. Wang, Z. Huang, Y. Yao, H. Qiao, G. Zhong, Y. Pei, C. Zheng, D. Kline, Q. Xia and Z. Lin, *Mater. Today*, 2020, **35**, 106–114.
328 H. Qiao, M. T. Saray, X. Wang, S. Xu, G. Chen, Z. Huang, C. Chen, G. Zhong, Q. Dong and M. Hong, *ACS Nano*, 2021, **15**, 14928–14937.
329 L. Yu, K. Zeng, C. Li, X. Lin, H. Liu, W. Shi, H. J. Qiu, Y. Yuan and Y. Yao, *Carbon Energy*, 2022, **4**, 731–761.
330 M. Cui, B. Xu and L. Wang, *BMEMat*, 2024, **2**, e12043.
331 Y. Wei, J. Wu, Y. Wu, H. Liu, F. Meng, Q. Liu, A. C. Midgley, X. Zhang, T. Qi and H. Kang, *Adv. Mater.*, 2022, **34**, 2201736.
332 C. D. Flynn and D. Chang, *Diagnostics*, 2024, **14**, 1100.
333 D. Xu, L. Wu, H. Yao and L. Zhao, *Small*, 2022, **18**, 2203400.
334 F. Sun, Y. Liang, L. Jin, J. Shi and L. Shang, *ACS Appl. Mater. Interfaces*, 2021, **13**, 58209–58219.
335 H. Lewandowska, K. Wojciuk and U. Karczmarczyk, *Appl. Sci.*, 2021, **11**, 9019.
336 M. B. Kulkarni, N. H. Ayachit and T. M. Aminabhavi, *Biosensors*, 2022, **12**, 892.
337 L. Zheng, M. Cao, Y. Du, Q. Liu, M. Y. Emran, A. Kotb, M. Sun, C.-B. Ma and M. Zhou, *Nanoscale*, 2024, **16**, 44–60.
338 C. Cao, N. Yang, X. Wang, J. Shao, X. Song, C. Liang, W. Wang and X. Dong, *Coord. Chem. Rev.*, 2023, **491**, 215245.
339 D. P. Cormode, L. Gao and H. Koo, *Trends Biotechnol.*, 2018, **36**, 15–29.
340 L. Gabrielli, L. J. Prins, F. Rastrelli, F. Mancin and P. Scrimin, *Eur. J. Org. Chem.*, 2020, **2020**, 5044–5055.
341 N. E. T. Castillo, E. M. Melchor-Martínez, J. S. O. Sierra, N. M. Ramírez-Torres, J. E. Sosa-Hernández, H. M. Iqbal and R. Parra-Saldívar, *Int. J. Biol. Macromol.*, 2021, **179**, 80–89.
342 Z. Wang, K. Dong, Z. Liu, Y. Zhang, Z. Chen, H. Sun, J. Ren and X. Qu, *Biomaterials*, 2017, **113**, 145–157.
343 Q. Wang, X. Zhang, L. Huang, Z. Zhang and S. Dong, *ACS Appl. Mater. Interfaces*, 2017, **9**, 7465–7471.
344 G. Bystrzejewska-Piotrowska, J. Golimowski and P. L. Urban, *Waste Manage.*, 2009, **29**, 2587–2595.
345 M. Munoz, Z. M. de Pedro, J. A. Casas and J. J. Rodriguez, *Appl. Catal., B*, 2015, **176**, 249–265.
346 Y. Hu, H. Cheng, X. Zhao, J. Wu, F. Muhammad, S. Lin, J. He, L. Zhou, C. Zhang and Y. Deng, *ACS Nano*, 2017, **11**, 5558–5566.
347 G. Song, Y. Chen, C. Liang, X. Yi, J. Liu, X. Sun, S. Shen, K. Yang and Z. Liu, *Adv. Biomater.*, 2016, **28**, 7143–7148.
348 N. J. Lang, B. Liu and J. Liu, *J. Colloid Interface Sci.*, 2014, **428**, 78–83.
349 A. Asati, S. Santra, C. Kaittanis, S. Nath and J. M. Perez, *Angew. Chem.*, 2009, **121**, 2344–2348.
350 Y. Zhou, B. Liu, R. Yang and J. Liu, *Bioconjugate Chem.*, 2017, **28**, 2903–2909.
351 K. E. Sapsford, W. R. Algar, L. Berti, K. B. Gemmill, B. J. Casey, E. Oh, M. H. Stewart and I. L. Medintz, *Chem. Rev.*, 2013, **113**, 1904–2074.
352 G. Y. Tonga, Y. Jeong, B. Duncan, T. Mizuhara, R. Mout, R. Das, S. T. Kim, Y.-C. Yeh, B. Yan and S. Hou, *Nat. Chem.*, 2015, **7**, 597–603.
353 F. Wang, Y. Zhang, Z. Du, J. Ren and X. Qu, *Nat. Commun.*, 2018, **9**, 1209.
354 A. Gupta, R. Das, G. Y. Tonga, T. Mizuhara and V. M. Rotello, *ACS Nano*, 2018, **12**, 89–94.
355 A. M. Ashrafi, Z. Bytesnikova, J. Barek, L. Richtera and V. Adam, *Biosens. Bioelectron.*, 2021, **192**, 113494.
356 S. Sahoo, K. Y. Wickramathilaka, E. Njeri, D. Silva and S. L. Suib, *Front. Chem.*, 2024, 12, 2024.
357 X. Xiao, L. Yang, W. Sun, Y. Chen, H. Yu, K. Li, B. Jia, L. Zhang and T. Ma, *Small*, 2022, **18**, 2105830.
358 L. Gao, J. Zhuang, L. Nie, J. Zhang, Y. Zhang, N. Gu, T. Wang, J. Feng, D. Yang, S. Perrett and X. Yan, *Nat. Nanotechnol.*, 2007, **2**, 577–583.
359 R. Z. Harris, P. A. Liddell, K. M. Smith and P. R. Ortiz de Montellano, *Biochemistry*, 1993, **32**, 3658–3663.
360 H. M. Abdel-Mageed, A. Z. Barakat, R. I. Bassuiny, A. M. Elsayed, H. A. Salah, A. M. Abdel-Aty and S. A. Mohamed, *Folia Microbiol.*, 2022, 1–12.
361 A. N. U. Haq, A. Nadhman, I. Ullah, G. Mustafa, M. Yasinzai and I. Khan, *J. Nanomater.*, 2017, **2017**, 8510342.
362 S. Kalathil, K. P. Katuri, A. S. Alazmi, S. Pedireddy, N. Kornienko, P. M. Costa and P. E. Saikaly, *Chem. Mater.*, 2019, **31**, 3686–3693.
363 I. H. Park, Y. H. Heo, P. Kim and K. S. Nahm, *RSC Adv.*, 2013, **3**, 16665–16671.

364 A. Mehdinia, E. Ziaei and A. Jabbari, *Int. J. Hydrogen Energy*, 2014, **39**, 10724–10730.
365 L. Singh, S. Rana, S. Thakur and D. Pant, *Trends Biotechnol.*, 2020, **38**, 469–473.
366 F. S. Roberts, K. P. Kuhl and A. Nilsson, *Angew. Chem.*, 2015, **127**, 5268–5271.
367 Y. Zhou, F. Che, M. Liu, C. Zou, Z. Liang, P. De Luna, H. Yuan, J. Li, Z. Wang and H. Xie, *Nat. Chem.*, 2018, **10**, 974–980.
368 C. G. Morales-Guio, E. R. Cave, S. A. Nitopi, J. T. Feaster, L. Wang, K. P. Kuhl, A. Jackson, N. C. Johnson, D. N. Abram and T. Hatsukade, *Nat. Catal.*, 2018, **1**, 764–771.
369 Z. Zhang, X. Zhang, B. Liu and J. Liu, *J. Am. Chem. Soc.*, 2017, **139**, 5412–5419.
370 Z. Zhang, B. Liu and J. Liu, *Small*, 2017, **13**, 1602730.
371 R. M. Yusop, A. Unciti-Broceta, E. M. Johansson, R. M. Sánchez-Martín and M. Bradley, *Nat. Chem.*, 2011, **3**, 239–243.
372 J. T. Weiss, J. C. Dawson, C. Fraser, W. Rybski, C. Torres-Sánchez, M. Bradley, E. E. Patton, N. O. Carragher and A. Unciti-Broceta, *J. Med. Chem.*, 2014, **57**, 5395–5404.
373 H. Mistry, A. S. Varela, S. Kühl, P. Strasser and B. R. Cuenya, *Nat. Rev. Mater.*, 2016, **1**, 1–14.
374 Y. Huang, A. D. Handoko, P. Hirunsit and B. S. Yeo, *ACS Catal.*, 2017, **7**, 1749–1756.
375 Y. Peng, X. Chen, G. Yi and Z. Gao, *Chem. Commun.*, 2011, **47**, 2916–2918.
376 J.-D. Cafun, K. O. Kvashnina, E. Casals, V. F. Puntes and P. Glatzel, *ACS Nano*, 2013, **7**, 10726–10732.
377 R. Cao-Milán, L. D. He, S. Shorkey, G. Y. Tonga, L.-S. Wang, X. Zhang, I. Uddin, R. Das, M. Sulak and V. M. Rotello, *Mol. Syst. Des. Eng.*, 2017, **2**, 624–628.
378 S. Singh, *Front. Chem.*, 2019, **7**, 46.
379 M. Lowe, R. Qin and X. Mao, *Water*, 2022, **14**, 1384.
380 E. H. Jang, Y. S. Park, M. S. Kim and D. H. Choi, *Pharmaceutics*, 2020, **12**(5), 453.
381 H.-J. Jeon, H. S. Kim, E. Chung and D. Y. Lee, *Theranostics*, 2022, **12**, 6308.
382 H.-J. Jeon, S. Kim, S. Park, I.-K. Jeong, J. Kang, Y. R. Kim, D. Y. Lee and E. Chung, *Nano Lett.*, 2021, **21**, 8933–8940.
383 S. Park, D. Y. Nam, H.-J. Jeon, J. H. Han, D. Jang, J. Hwang, Y.-S. Park, Y.-G. Han, Y. B. Choy and D. Y. Lee, *Biomater. Res.*, 2023, **27**, 135.
384 Z. Wang, R. Zhang, X. Yan and K. Fan, *Mater. Today*, 2020, **41**, 81–119.
385 Y. Wang, X. He, K. Huang and N. Cheng, *J. Nanobiotechnol.*, 2024, **22**, 226.
386 Revolutionizing Biocatalysis: The Promise of Organic Nanozymes, https://scienceemerge.com/?s=Revolutionizing+Biocatalysis%3A+The+Promise+of+Organic+Nanozymes, (accessed July, 2025).
387 Harnessing the Power of Industrial Enzymes: A comprehensive Cost Model, https://www.imarcgroup.com/insight/harnessing-the-power-of-industrial-enzymes-a-comprehensive-cost-model#:~:text=Harnessing%20the%20Power%20of%20Industrial%20Enzymes%3A%20A%20Comprehensive%20Cost%20Model,%2C%20biofuel%2C%20and%20detergent%20industries, (accessed July 2025).
388 H. M. Abdel-Mageed, N. Z. AbuelEzz, R. A. Radwan and S. A. Mohamed, *J. Microencapsulation*, 2021, **38**, 414–436.
389 H. M. Abdel-Mageed, A. E. A. E. Aziz, S. A. Mohamed and N. Z. AbuelEzz, *J. Microencapsulation*, 2022, **39**, 72–94.
390 C. Purcarea, R. Ruginescu, R. M. Banciu and A. Vasilescu, *Biosensors*, 2024, **14**, 143.
391 Y. Gao, Z. Zhu, Z. Chen, M. Guo, Y. Zhang, L. Wang and Z. Zhu, *Biomater. Sci.*, 2024, **12**, 2229–2243.
392 S. Pandey, Y. Xiang, D. V. W. Kankanamalage, J. Jayawickramarajah, Y. Leng and H. Mao, *J. Phys. Chem. B*, 2021, **125**, 11112–11121.
393 J.-H. Shin, M.-J. Lee, J.-H. Choi, J.-a. Song, T.-H. Kim and B.-K. Oh, *Nano Convergence*, 2020, **7**, 1–8.
394 R. A. Sheldon and S. van Pelt, *Chem. Soc. Rev.*, 2013, **42**, 6223–6235.
395 M. Razzaghi, A. Homaei, F. Vianello, T. Azad, T. Sharma, A. K. Nadda, R. Stevanato, M. Bilal and H. M. Iqbal, *Bioprocess Biosyst. Eng.*, 2022, 1–20.
396 M. Bilal, T. Rasheed, Y. Zhao, H. M. Iqbal and J. Cui, *Int. J. Biol. Macromol.*, 2018, **119**, 278–290.
397 S. Chakraborty, H. Rusli, A. Nath, J. Sikder, C. Bhattacharjee, S. Curcio and E. Drioli, *Crit. Rev. Biotechnol.*, 2016, **36**, 43–58.
398 D. Eixenberger, A. Kumar, S. Klinger, N. Scharnagl, A. W. Dawood and A. Liese, *Catalysts*, 2023, **13**, 1130.
399 J. Shen, S. Zhang, X. Fang and S. Salmon, *Gels*, 2022, **8**, 460.
400 W. Jianping, P. Lei, X. Xiaojing and Z. Zhiyong, *Eng. Life Sci.*, 2003, **3**, 271–275.
401 C. Fernandes, M. Jathar, B. K. S. Sawant and T. Warde, in *Pharmaceutical Process Engineering and Scale-up Principles*, Springer, 2023, pp. 173–203.
402 M. Bilal, S. A. Qamar, D. Carballares, Á. Berenguer-Murcia and R. Fernandez-Lafuente, *Biotechnol. Adv.*, 2024, **70**, 108304.
403 H. M. Abdel-Mageed, *Micro Nano Syst. Lett.*, 2025, **13**, 1–28.